PRE-ANALYTICAL SAMPLE PROCESS MODIFICATIONS TO DECREASE TIME TO DETECTION OF *SALMONELLA* SER. NEWPORT AND *LISTERIA MONOCYTOGENES* FROM DIVERSE FOOD MATRICES

By

Meaghan Glowacki

A DISSERTATION

Submitted to
Michigan State University
in partial fulfillment of the requirements
for the degree of

Comparative Medicine and Integrative Biology – Doctor of Philosophy

2025

ABSTRACT

Foodborne illnesses continue to negatively affect public health. Current strategies to detect and prevent illnesses rely on prolonged enrichment protocols of 24-48 hours. While rapid methods are constantly being developed, these methods do not consider preanalytical sample processing, which is a critical first step for reliable and reproducible results. Additionally, the time to detection for an assay does not include the preparation and enrichment steps that must be completed to arrive at optimal pathogen numbers to enable detection. To address this gap, the author evaluated and refined the use of a proprietary magnetic nanoparticle functionalized with chitosan (F#1 MNPs) as a preanalytical sample processing tool to capture and concentrate foodborne pathogens from complex food matrices.

Two foodborne pathogens, *Listeria monocytogenes* (gram-positive) and *Salmonella* ser. Newport (gram-negative) were used to evaluate the F#1 MNPs in strawberries, romaine lettuce, and cotto salami, representing diverse food matrices. These pathogens were chosen for this proof-of-concept study based on their significant public health impact. Chitosan electrostatically binds to the cell-surface structure of bacteria. Therefore, it is hypothesized that the F#1 MNPs also bind to the exterior of pathogens. However, the exact binding mechanism remains unknown. Due to this, all testing used cold-stressed pathogens to simulate their physiological state after food processing.

First, statistical design of experiments (DOE) was used to optimize protocols for extracting ≤ 3 CFU/g of bacterial contamination in diverse matrices with only minor protocol adjustments. This study highlights the potential to standardize protocols and

the ability to rapidly adjust them based on regulatory requirements for different pathogens and food matrices.

Next, using the same strains and food matrices, the effect of the F#1 MNPs on pathogen enrichment was evaluated. Modifications reduced broth enrichment times to 4-12 hours without inhibiting target pathogen growth on selective agars, expediting the overall time to single-colony isolation. This is especially important for regulatory enforcement that still relies on the isolation of pathogens for downstream testing and outbreak surveillance and investigation.

Finally, the use of shotgun metagenomics revealed potential applications beyond bacterial pathogens. The F#1 MNPs can also capture non-pathogenic bacteria, viruses, and fungi, which may have applications such as environmental bioindicators. This further shows the versatility of the F#1 MNPs as a preanalytical sample processing tool in a wide range of detection pipelines, such as multi-organism detection with multiplex assays, pathogen-agnostic testing, and identifying pathogens in emerging food vehicles. By streamlining pathogen extraction and concentration, F#1 MNPs offer significant potential to improve surveillance, outbreak detection and prevention, and overall food safety.

ACKNOWLEDGEMENTS

Foremost, thank you to Stephen for being overly supportive and enabling me to finish this degree. To Monk, Panda, and Catalina you were/are my soundboards and never judge me, if you get treats. I thank my parents and brother for instilling a sense of grit and determination to accomplish my goals. Dr. Krista La Perle, you earned a spot in the 'family paragraph!' You have given me more guidance than I could have ever imagined. From getting me through vet school to the first half of my Army career, and now a PhD, I appreciate you more than you will ever know.

To my Army mentors, MG Paula Lodi, COL Manuel Menendez, COL(R) Shannon Shaw, and COL(R) Chad Weddell – you all set my career on an unbelievable trajectory. I will be forever grateful that you provided me with unique opportunities so that I could grow and develop as a leader. I will not let you down and I will pay it forward.

Drs. Teresa Bergholz and Shawn Zimmerman, and Margaret ("Margie") Krueger thank you for helping me through the long days of growth curves, letting me bounce ideas off you – especially when some experiments did not go as expected, and listening to me think aloud. I could not have stayed sane without your invaluable feedback and support!

Last, but not least, thank you to Dr. Srinand Sreevatsan for your mentorship and letting me focus on my areas of interest. I would like to thank Dr. Evangelyn Alocilja for helping me craft my dissertation around the use of magnetic nanoparticles and providing large quantities of them! And Dr. Rinosh Mani for providing me unique perspectives and making me step out of my comfort zone to improve my experimental design.

TABLE OF CONTENTS

CHAPTER 1: INTRODUCTION AND BACKGROUND

Public Health Burden of Foodborne Diseases

Annually, 31 major foodborne pathogens cause approximately nine million illnesses, 56,000 hospitalizations, and 1,300 deaths in the United States (1). A recent Centers for Disease Control and Prevention (CDC) study highlighted that in 2019, seven major pathogens caused 9.9 million illnesses, 53,500 hospitalizations, and 931 deaths (2). Norovirus, *Campylobacter* spp., and *Salmonella* (nontyphoidal) were the leading causes of illnesses, while the case fatality rates are highest with *Salmonella, Campylobacter* spp., norovirus, and invasive *Listeria*. Despite prevention and controls measures, the incidence of these pathogens did not significantly change from 2016-2018 to 2023 (3).

Symptoms of foodborne illnesses are typically associated with vomiting and diarrhea; however, vulnerable populations such as children under five, adults over 65, pregnant women, and immunocompromised individuals may suffer more severe forms of disease and/or long-term health consequences (4). For example, hemolytic uremic syndrome, which is characterized by low red blood cells and platelets and acute renal failure, develops in some children after consuming products contaminated with Shiga toxin-producing *Escherichia coli* strains, such as *E. coli* O157:H7 (5, 6). Similarly, Guillain-Barré syndrome, a disease characterized by acute ascending paralysis, is associated with *Campylobacter* infection (7, 8). Severe sequela from *Listeria monocytogenes* and *Salmonella* spp. are discussed later. These examples highlight the increased risks and potential long-term consequences of foodborne illnesses in vulnerable populations.

Impact of *Listeria monocytogenes*

Of the 17 species of *Listeria*, *L. monocytogenes* and *L. ivanovii* are the only known pathogens in humans and animals, of which, *L. monocytogenes* causes the majority of illnesses in humans (1, 9, 10). *L. monocytogenes* causes approximately 1,600 illnesses, 1,200 hospitalizations, and 250 deaths per year, leading to an economic burden of ~$3.2 billion annually (11, 12). While the number of infections is relatively low compared to other foodborne pathogens, it is one of the leading causes of death, with a case-fatality rate of 20-30% despite antimicrobial treatments (10, 13). These statistics highlight the significant public health impact of this pathogen.

The infectious dose of *L. monocytogenes* is not well characterized, but it likely depends on the strain, host susceptibility, and the food matrix (14–16). Notably, the 1998 frankfurter outbreak of listeriosis involved concentrations as low as ≤ 0.3 most probable number/gram (17). In an ice-cream associated outbreak, it is estimated that 1,200 (95% credible interval 760-4,200) *L. monocytogenes* colony-forming units (CFUs) were unlikely to cause illness in healthy individuals; however, this dose did cause illness in susceptible populations (18). This groups model further predicted that the probability of infection after ingestion of 1 CFU was 2.6×10^{-9} in healthy individuals and 1.2×10^{-7} to 5.5×10^{-7} in a susceptible population, which is similar to a Food and Agriculture Organization of World Health Organization study that estimated the probability to be 3.2×10^{-7} (18, 19). These studies highlight the ability for *L. monocytogenes* to cause illnesses at low doses.

Infections caused by *L. monocytogenes* typically range from asymptomatic to flu-like or mild-gastrointestinal illnesses in young, healthy individuals (10, 20). However, pregnant women, children less than five, the elderly (over 65), and people with weakened immune systems are at increased risk from severe forms of illness, such as miscarriage, septicemia, meningitis, and death (10, 20). This is due to the unique pathogenesis of *L. monocytogenes*, which allows it to evade the immune system by replicating intracellularly within epithelial cells and macrophages, facilitating its systemic spread (21).

L. monocytogenes is a highly adaptable saprotroph that prefers decaying, moist vegetation (22). As a gram-positive facultative anaerobic rod-shaped bacterium, it is a psychrophile capable of growth at high salt concentrations (10%), and a broad pH range (4.7-9.2) (10, 23, 24). It routinely forms biofilms on equipment and other food and non-food contact surfaces that then lead to cross-contamination (25). Its survivability mechanisms and growth conditions make it highly resistant and able to persist in food production and processing environments (10, 25). Consequently, the majority of *L. monocytogenes* illnesses (77.2% of cases) are most often attributed to dairy products, vegetable row crops, and fruits (26). This environmental persistence and source attribution to ready-to-eat foods has led to several documented outbreaks. For example, in 2023 there was an outbreak linked to leafy greens that resulted in 18/19 cases requiring hospitalization (27). While the source attribution data from recent reports (published through 2022) does not include ready-to-eat meat products as a major source of outbreaks, the year 2024 saw two substantial outbreaks leading to 80 cases, 77 hospitalizations, and 12 deaths despite the U.S. having a zero-tolerance policy for *L. monocytogenes* in these products (28–30).

L. monocytogenes continues to be a significant public health threat due to its high case fatality rate and adaptability to diverse environments. Its ability to survive and grow in food processing environments, coupled with its source attribution to ready-to-eat products and ongoing outbreaks highlights the need for faster detection mechanisms to improve monitoring and prevention.

Impact of *Salmonella*, nontyphoidal

Salmonella is a highly diverse, facultative anaerobic, gram-negative rod-shaped bacterium. The genus consists of two species, *enterica* and *bongori*, with *enterica* being the primary public health concern. This species is divided into six subspecies, with *S. enterica* subsp. *enterica* responsible for most human illnesses. This subspecies is further divided into typhoidal and non-typhoidal based on syndromes, with more than 2,500 serotypes described. Nontyphoidal salmonellosis is the most common bacterial foodborne disease in the U.S., resulting in one million illnesses, 20,000 hospitalizations, 400 deaths, and an annual economic burden of ~$4.1 billion (11, 12).

While the theoretical infectious dose can be as low as a single CFU, variations among serotypes, food matrices, and the host's immune status influence the infectious dose (31–35). Symptoms generally include nausea, vomiting, diarrhea, abdominal cramps, fever, and headache (2). In 1.6-9.1% of cases, long-term complications such as reactive arthritis and Reiter's syndrome have been observed 3-4 weeks after initial symptoms (36, 37). Other serotypes, such as *Salmonella* ser. Dublin, can also cause severe infections, such as septicemia (38).

Some serotypes are host adapted, but can still occasionally cause disease in humans, such as *Salmonella* ser. Choleraesuis in swine or *Salmonella* ser. Dublin in cattle while other serotypes are more ubiquitous and found in many reservoirs (35, 38, 39). From 2004-2021, the most common serotypes in the U.S. were Enteritidis, Typhimurium, and Newport (40–42). Enteritidis is commonly associated with eggs but is found ubiquitously and causes a disproportionate number of outbreaks in poultry products, sprouts, and seeds and nuts (42–44). Typhimurium is commonly reported in outbreaks associated with beef, dairy, pork, and vegetable row crops, whereas Newport is commonly associated with fruits and seeded vegetables (42). While these three serotypes are consistently among the top three causes, other serotypes fluctuate more often (42). For example, a *Salmonella* ser. Reading clonal group is considered an emerging strain and caused two outbreaks in turkey products from 2017-2019 (45). However, in the last 75 years there were only sporadic outbreaks reported (46).

Salmonella serotypes can survive and grow in a wide range of hosts and environments due to its adaptability. Cheng et al. provide a comprehensive overview of *Salmonella's* adaptive abilities (35). Briefly, *Salmonella* possesses a range of virulence factors such as *Salmonella* pathogenicity islands, toxins, flagella antigens, fimbriae, and plasmids that allow it to host adapt, be ubiquitous, cause a wide range of symptoms, evade the hosts immune defenses, and withstand environmental challenges to persist in the food supply. While *Salmonella* is less likely than *L. monocytogenes* to be isolated and persist in the environment, it can still form biofilms and likely lead to environmental contamination of foods (47–49). This adaptability also allows it to survive in low-moisture foods (water activity below 0.8), once thought to be a low risk for human infections. From 2008-2009, peanut butter was found to cause 714 human illnesses in 46 states prompting one of the largest food recalls in U.S. history (50). *Salmonella* has also been implicated in outbreaks associated with wheat and cereals (51, 52). Another challenge in the control of *Salmonella* is that current control strategies often target a specific serotype but as illnesses attributed to that serotype decrease there is an increase in other serotypes detected (35).

The adaptability of *Salmonella* allows it to thrive in diverse host and ecological niches, including environments once thought to be low risk. These unique traits underscore the importance of detecting and monitoring *Salmonella* throughout the food supply.

The U.S. Food Supply Chain: Regulatory Framework and Challenges

Food safety in the United States relies on a “farm-to-fork” or “farm-to-table” continuum, which involves multiple stages, including production, transportation, processing, packaging, and retail distribution. The U.S. is also a major importer and exporter of foods that require oversight. The U.S. Department of Agriculture (USDA) and The Food and Drug Administration (FDA) are tasked with regulating food safety under Titles 9 and 21 of the Code of Federal Regulations, respectively (53, 54). The USDA regulates meat, poultry, processed egg products, and Siluriformes (catfish), while the FDA regulates all other foods. The main regulatory framework for the USDA consists of the Federal Meat Inspection Act, Poultry Products Inspection Act, Egg Products Inspection Act, and Humane Methods of Slaughter Act (54). Whereas the FDA regulatory framework relies mostly on the Food, Drug and Cosmetic Act (FD&C) of 1938 and the Food Safety Modernization Act (FSMA) of 2011 (53, 55). Together, this framework helps safeguard public health and maintain consumer confidence in the food supply.

The USDA has implemented several control strategies to militate salmonellosis risks associated with poultry. While the prevalence in poultry has decreased, there has not been a reduction in human salmonellosis associated with poultry (56). In response, the USDA is shifting to a risk-based approach to concentrate their efforts on products most likely to contain highly virulent *Salmonella* serotypes in sufficient quantities to cause illness (43, 44, 57, 58). It is expected that further risk-based assessments and control efforts will be developed with other pathogen and food combinations.

Similarly, FSMA was enacted to expand the FDA's authority to prevent foodborne illnesses, but its implementation introduced significant challenges (55). FSMA consists of 10 main rules, some of which are still being phased in 14 years after its passage. For instance, the Final Rule on Pre-Harvest Agricultural Water, signed in July 2024, has compliance deadlines extending through 2027 (59). This rule aims to reduce produce contamination through improvement of water management practices. However, it took nine years of feedback and revisions to establish a practical and enforceable rule.

To enforce these regulations and maintain a safe food supply, the USDA and FDA developed protocols for pathogen testing. The USDA's Microbiology Laboratory Guidebook (MLG) and FDA's Bacteriological Analytical Manual (BAM) outline procedures for detecting and identifying foodborne pathogens (60, 61). While these guidelines support the use of rapid detection assays, they still require verification based on time-consuming enrichment and culturing of microbes. The time-intensive process allows for genotyping and tracking of isolates, enabling these agencies to conduct risk-based assessments and implement targeted control measures. Additionally, this process allows the Centers for Disease Control and Prevention (CDC) to monitor and detect outbreaks.

Outbreak Surveillance

Despite the efforts by the USDA and FDA, foodborne-related disease outbreaks remain a challenge. Outbreak surveillance is an important aspect of food safety through the focus on identifying, tracking, and mitigating illnesses. The CDC works with local health departments to monitor foodborne outbreaks through surveillance systems like PulseNet, the Foodborne Diseases Active Surveillance Network (FoodNet), the System for Enteric Disease Response, Investigation, and Coordination (SEDRIC), and the Foodborne Disease Outbreak Surveillance System, among others. When an outbreak is detected, the CDC works with the USDA and FDA to conduct trace-back and trace-forward investigations to determine the cause of contamination and prevent its propagation. Outbreak surveillance and investigation relies on whole genome sequencing to identify similarities between strains. This requires the isolation of single colonies to reach the required resolution (62). While these systems help uncover patterns, such as source attributing most solved multistate outbreaks to fruits and vegetable row crops, particularly romaine lettuce (63), the reliance on the time-intensive process to recover and isolate microbes causes delays. This underscores the need for faster methods to isolate pathogens.

Impact of Food Matrix Characteristics on Pathogen Growth and Detection

Growth of microorganisms in foods is reliant on several key factors that influence their survival and growth. These critical factors include nutrient availability, temperature, pH level, oxygen levels, and available water (water activity - a_w). Different bacterial species have unique requirements for optimal growth, which can further vary between strains. Additionally, food matrices are inherently diverse and complex. For the purposes of foodborne outbreaks, the Interagency Food Safety Analytics Collaboration (IFSAC) categorizes foods into five main categories with 234 subcategories based on distinguishing features, highlighting the diversity of foods (64). These different categories are often combined, such as in a salad, further adding diversity and complexity. Foods are complex; they are comprised of macronutrients, micronutrients, and other bioactive compounds and are structurally heterogenous consisting of solids, liquids, and/or gases (65, 66). This diversity and complexity complicate the development of standardized methods for removing foodborne pathogens from food matrices.

Bacteria undergo physiological changes when exposed to the suboptimal environments often present in food matrices and imposed on the bacteria during food production and processing (67–69). For example, in acidic environments like strawberries, which are high in citric and malic acids, bacteria undergo cellular adaptations such as altering their cell membranes, affecting both the structural integrity and functional properties (69–71). Likewise, refrigeration induces a cold stress response causing cell membranes to lose fluidity (69, 72). Bacteria respond to heat stresses leading to protein and cell membrane modifications (69, 70). Bacteria can also activate a general stress response to a wide range of stresses, which also leads to multiple adaptations to the cell membrane and cellular components for survival (67–69, 73). These physiological responses allow bacteria to persist in challenging conditions and complicates bacterial extraction method development due to these cell membrane alterations.

Factors such as food components, processing methods, and competing microbes can affect the sensitivity and specificity of detection assays. The complex composition of foods introduces multiple potential interference mechanisms that can influence detection accuracy. Physical interference when bacteria attach to food matrix components can limit their detectability (74, 75). Chemical components, such as fats and polyphenols can inhibit detection techniques such as PCR (76–78). Biological interferences from competing microflora can cause an outgrowth of non-target microbes during enrichment processes, which can lead to false- positive or negative results. Mitigating these interferences is critical for improving the reliability of microbial detection assays in complex food matrices.

This study examines strawberries, romaine lettuce, and cotto salami, representing the diversity and complexity of food matrices. Strawberries are acidic with a pH of approximately 4, making them a lower risk food for pathogen contamination. However, they are usually field packed and not processed prior to reaching the consumer; therefore, pathogens such as *Salmonella* can attach to them and infect consumers (79–81). As previously mentioned, romaine lettuce and other row crop vegetables are at a high risk for contamination (63). This is due to their proximity to soil and irrigation systems and their favorable bacterial growth conditions (82). The cotto salami used in this study consisted of chicken, beef, and pork. Unlike traditional salamis, cotto salami is cooked instead of fermented and must be refrigerated. Cotto salami supports the growth of *L. monocytogenes* and other microbes due to its neutral pH (6.4) and relatively high a_w (0.96) (83). These differences highlight the need for preanalytical sample processing methods to improve sensitivity and accuracy of identification of bacterial pathogens across diverse food matrices.

Pre-Analytical Sample Processing for Foodborne Pathogen Detection

Current research in foodborne pathogen detection focuses primarily on the speed, accuracy, and affordability of detection assays with little attention to the pre-analytical processing of the samples needed to improve assay sensitivity and specificity (84–86). For a detection assay to accurately determine a pathogen's presence, absence, or quantity, the food sample must: 1) include an "analytical portion" representative of the entire sample, 2) undergo separation and enrichment of the target microbe from the matrix, 3) reduce the load of competing microbes, and 4) depending on the assay, the volume must be reduced or concentrated before detection (87). These requirements pose many challenges because foodborne pathogens are often heterogeneously dispersed within food matrices and present in low concentrations. Additionally, food matrices are highly diverse and complex, presenting unique challenges for developing universally applicable pre-analytical processing techniques. As a result, various sample preparation methods are used to improve assay sensitivity and specificity. However, one must also carefully consider the downstream detection method, particularly if cell viability is required. Addressing these challenges requires a pre-analytical sample processing method that accounts for the complexity of food matrices and is compatible with a wide range of downstream detection assays.

The following section emphasizes the separation and concentration of intact, viable bacteria, which can be achieved through selective or non-selective techniques, or more commonly, a combination of both. Selective techniques target a specific target pathogen, usually via its cell surface structures; however, there are techniques that target internal components, such as DNA or RNA. Examples of selective techniques include antibody-based techniques, such as immunomagnetic separation (IMS), and aptamer-based techniques. Each technique has distinct advantages and disadvantages that must be considered.

Immunomagnetic separation (IMS) relies on an antibody bound to a magnetic bead to bind bacteria-specific antigens. The antigen-antibody-bead complexes can then be magnetically separated and used in detection assays. For example, Fan et al. used IMS to extract *Salmonella* spp., *E. coli* O157:H7, and *L. monocytogenes* from meat samples, achieving specificity and simultaneous pathogen capture that was then detected using a multiplex real-time polymerase chain reaction (PCR). However, the capture efficiency ranged from 74-84% in the various meat matrices, necessitating the need for pre-enrichment for reliable detection (88). Another important consideration for antibody-based separation of bacteria is the antigen of interest. For instance, Eser et al. used IMS coupled with a cell-based assay that relied on the presence of flagella (89). However, this target may prove to be problematic if processing steps lead to flagella loss.

Aptamers are single stranded DNA or RNA oligonucleotides that can bind to nucleic or non-nucleic acid targets with high affinity and specificity (90). Aptamers can be attached to various surfaces, such as micro- or nanoparticles or fibers to bind to targets of interest. Joshi et al. detected *Salmonella* ser. Typhimurium in spiked fecal and chicken rinsate samples and naturally contaminated chicken litter samples with aptamers attached to magnetic beads (91). Tests with *E. coli* extracts showed no cross-reactivity but they did not test other bacteria or pathogens. Another group used aptamer-bound magnetic nanoparticles to separate *L. monocytogenes* from artificially contaminated raw milk, cream cheese, chicken meat, chicken liver, minced meat, and fresh lettuce and cabbage (92). Their technique relied on culture for manual plate counting, and they recovered 82.5-91.8% of the spiked bacteria. Their work showed low-level cross-reactivity with different bacterial species.

In contrast, non-selective techniques capture and/or concentrate microbes and food matrix particles indiscriminately and usually aid in separating inhibitors from those substrates. These methods are designed to ensure the comprehensive removal of microbes, which is essential in pathogen-agnostic testing. Some non-selective techniques rely on physical methods, for example centrifugation and filtration. While other methods target shared cell surface structures, such as lipopolysaccharides (LPS) in gram-negative bacteria or teichoic acids in gram-positive bacteria through bioaffinity-based approaches like glycans.

Physical separation methods, such as centrifugation and filtration separate materials based on size. Buoyant density centrifugation protocols are used to separate bacterial cells from food particles based on their densities in gradient medium. Centrifugation can be used with a range of food matrices and is often done with liquid matrices, such as milk or suspensions that were previously blended or stomached. Filtration removes microbes from food matrices based on size by using various filter pore sizes. However, the filters may become clogged with fatty matrices or other matrix material.

Glycan-coated magnetic nanoparticles are a notable non-selective tool to remove bacteria from food matrices, as reviewed by Dester and Alocilja (93). Additionally, glycan can be coated on other materials (94). Glycans' ability to bind microbial surfaces stems from their interaction with lectins (proteins), which is one way that bacteria attach to host cells to initiate infection (95). Glycans, such as chitosan, carry a net positive charge, which forms electrostatic bonds with the negative surfaces found in LPS and teichoic acid, key components of the cell walls in gram-negative and gram-positive bacteria, respectively (96). Therefore, glycan-coated materials can effectively separate microbes from food matrices. However, like IMS, these protocols rely on magnetic extraction, which poses challenges in viscous solutions, reducing efficiency (97–99). These considerations emphasize the need for optimization when applying non-selective methods in diverse food matrices.

Integrating selective and non-selective preparation techniques can further enhance pathogen detection. For instance, Solovchuk et al. combined sucrose gradient centrifugation with anti-*E. coli* antibody coated-carbon nanoparticles to isolate *E. coli* in milk samples within six minutes (100). In another study, a Syringe Enzymatic Filter-based assay was used to detect *Salmonella* in lettuce extracts. This method combined *Salmonella* DNA aptamers with filtration resulting in colorimetric detection (101).

Although separation techniques can play a vital role in pathogen isolation, many detection protocols rely on enrichment, either after separation or in the presence of food matrices. Federal guidelines, such as the FDA BAM and USDA MLG, rely on enrichment and culture as the gold standard (60, 61). Briefly, these protocols typically involve an initial incubation in a non-selective broth formulated to recover sublethally injured cells, followed by a secondary incubation with selective agents (e.g., antimicrobials, bile acids, dyes, etc.) to allow for the pathogen of interest to outcompete other microbes (60, 61). Enrichment remains a cornerstone for reliable pathogen recovery and detection, particularly in low-level contamination that may be localized on the matrix.

In conclusion, rapid identification of foodborne pathogens at low, yet biologically relevant, concentrations is crucial for public health and minimizing economic impacts on the food industry. To achieve this, improvements to pre-analytical sample processing techniques are paramount. Optimizing these protocols and pairing them with the appropriate down-stream pathogen-specific detection assay is critical to advancing food safety.

Chitosan-Functionalized Magnetic Nanoparticles

Chitosan is a cationic biopolymer derived from the deacetylation of chitin, found in the exoskeletons of crustaceans, insects, and fungal cell walls (102). It consists of repeating units of glucosamine and N-acetylglucosamine, providing an abundance of amino ($-NH_2$) and hydroxyl (-OH) groups (102–104). In acidic pH conditions ($pH < 6.5$), such as those commonly found in foods, the amino groups are protonated, giving chitosan a positively charged surface that can electrostatically bind to negatively charged surfaces such as LPS on gram-negative bacteria cell-walls or teichoic acids on gram-positive bacteria (105–111). This ability, combined with the antimicrobial effects of chitosan lends itself to being widely used in pharmaceutical development and drug delivery (107, 112, 113). Reviews by Yu et al. and Chicea et al. extensively cover its biomedical applications, while Chicea et al. also highlights its uses in the food industry

(112, 113). Additionally, reviews by Cheba and Flórez et al. provide in-depth analyses of chitosan's specific applications in food safety, such as its incorporation into food packaging to act as a food quality indicator and an antimicrobial barrier, as well as water purification and shelf-life extension (114, 115).

Magnetic nanoparticles (MNPs) are characterized by their large surface area-to-volume ratio and superparamagnetic properties (116, 117). The large surface area lends itself to functionalization, or surface modifications, using micro-emulsion, cross-linking, or covalent bonding (118). The surface can be functionalized with antibodies, aptamers, or carbohydrates to facilitate the binding to biological targets of interest, including pathogens. This enables MNPs to be used in a vast array of fields such as biomedical imaging, drug delivery, and pathogen detection (93, 99, 119–130). The superparamagnetic properties of MNPs allow them to remain suspended in liquids without aggregation until exposed to an external magnet, enabling the separation of biological targets from complex matrices with only the use of a magnet. MNPs are compatible with a wide range of detection assays, such as cyclic voltammetry, chemiluminescence, PCR and immunoassays (93, 99, 119–128). The specificity and cross-reactivity of the MNPs is dependent on the functionalization; therefore, MNPs can be used as either selective or non-selective modalities (131, 132). These properties make them an efficient tool for isolating pathogens from food samples.

By combining the properties of chitosan and MNPs, the Alocilja Nano-Biosensors Laboratory at Michigan State University developed a chitosan-coated iron oxide magnetic nanoparticle (F#1 MNP) (133). The F#1 MNPs are synthesized by coating an iron oxide core with chitosan through an electrostatic process. Transmission electron microscopy studies show these MNPs preferentially bind to the flagella and cell membranes of gram-negative and gram-positive bacteria (99, 127). Once bound, the bacteria-MNP complexes can be magnetically separated from food matrices, streamlining detection processes.

The Nano-Biosensors Laboratory demonstrated that F#1 MNPs can capture log-phase *Salmonella*, *E. coli*, and *Bacillus cereus* inoculated at concentrations of 2.9-4.5 $\log_{10}$ CFU/mL, with capture efficiencies ranging from 75-90% in fat-free, 2%, and whole (3.25%) pasteurized milk, and 85-97% in phosphate buffered saline (PBS) (99). Similar studies showed successful capture of log-phase *B. cereus, E. coli* O157:H7, *L. monocytogenes, Salmonella* ser. Enteritidis, and *Staphylococcus aureus* from a variety of spiked food matrices, such as deli ham, romaine lettuce, chicken salad, and flour and fecal samples (123, 125, 127, 134). Similarly to the milk study, they did not achieve 100% capture, largely due to the F#1 MNPs binding non-selectively to other microbes and food matrix interference. This matrix interference and cross-reactivity with non-target microbes remain significant obstacles to using F#1 MNPs to improve the sensitivity and specificity of detection assays. Complex food matrices, such as those with high fat, protein, or polysaccharide contents may interfere with the binding and magnetic separation (97–99). These findings stress the potential of F#1 MNPs, while also highlighting the challenges related to cross-reactivity and matrix effects. Further research is needed to optimize capture protocols and test whether the antimicrobial effects of chitosan negatively impact the target pathogen's ability to multiply and be detected at low levels of contamination.

Conclusion and Purpose

Foodborne diseases remain a significant public health concern. Outbreaks attributed to diseases such as listeriosis and salmonellosis continue despite established prevention, control, and monitoring measures. A key challenge is the slow pace of pathogen detection and source attribution, particularly in developing truly rapid techniques that can also provide isolates for further typing and analysis. Addressing these limitations requires a concerted effort to improve pre-analytical sample processing, such as through the use chitosan-functionalized MNPs. Improving this critical step will enhance the speed and accuracy of pathogen detection to respond to food safety challenges and protect public health.

The purpose of this dissertation is to evaluate the use of chitosan-functionalized magnetic nanoparticles (F#1 MNPs) for the rapid and sensitive detection of *Salmonella* ser. Newport and *L. monocytogenes* in various food matrices. The first objective of the research is optimization of the F#1 MNP capture protocol targeting *Salmonella* ser. Newport in strawberries and romaine lettuce and *L. monocytogenes* in romaine lettuce and cotto salami. Next, the research investigates the effect of F#1 MNPs on the growth of target pathogens and aims to reduce current enrichment protocol times to detection in the selected food matrices. Lastly, the broad-spectrum capture capability of F#1 MNPs is assessed in romaine lettuce using shotgun metagenomics to identify the range of microbes that can be captured. Refining and evaluating the use of the F#1 MNPs as a preanalytical sampling processing tool for the detection of foodborne pathogens in food matrices contributes to improving the speed of detecting and isolating low-level pathogen contamination in foods, which ultimately effects public health.

CHAPTER 2: CAPTURE PROTOCOL OPTIMIZATION OF CHITOSAN-FUNCTIONALIZED MAGNETIC NANOPARTICLES AGAINST *SALMONELLA* SER. NEWPORT AND *LISTERIA MONOCYTOGENES* IN VARIOUS FOOD MATRICES

Abstract

Foodborne pathogens such as *Listeria monocytogenes* and *Salmonella* spp. continue to cause illnesses and impose significant economic burdens. A key challenge in detecting these pathogens is the inability to reliably extract them from food matrices. In this study, statistical design of experiments (DOE) were used to optimize the extraction protocol for chitosan-functionalized magnetic nanoparticles (F#1 MNP) to extract stationary-phase *Salmonella* ser. Newport and *L. monocytogenes* from strawberries, romaine lettuce, and cotto salami after 24 hours of refrigeration. The most significant variables influencing extraction were the MNP concentration (0.20mg/mL) and the contact time between the MNP's, food matrices, and pathogens (10-15 min). The optimized protocol achieved a lower limit of capture of 0.28 CFU/g for *Salmonella* ser. Newport in strawberries and 2-3 CFU/g in romaine lettuce. For *L. monocytogenes*, the lower limits of capture were 0.36 CFU/g in romaine lettuce and 0.5 CFU/g in cotto salami. By using stationary-phase bacteria at low concentrations under simulated natural contamination conditions, this study demonstrates the effectiveness of DOE for rapidly optimizing extraction protocols across a range of pathogens and foods. The results support the integration of F#1 MNPs into analytical methods for detecting foodborne pathogens with improved sensitivity.

Introduction

Foodborne illnesses are responsible for approximately 1,351 deaths, 9.4 million illnesses, and $75 billion worth of damages each year in the U.S. (1, 135). Two bacterial foodborne pathogens of particular concern are *Listeria monocytogenes* and *Salmonella* spp. (135). While there have been improvements in the rapid detection of pathogens, the limit of detection of these methods and low levels of contamination often necessitates the use of enrichment prior to detection. Additionally, little to no attention is given to the sample preparation method that influences the sensitivity and specificity of the detection assays. This is because foodborne pathogens are not homogenously dispersed in food samples, often present in low concentrations, and food matrices are highly diverse and complex. To overcome these challenges several pre-analytical sample processing techniques have been developed, but challenges remain in their widespread applicability.

One area of considerable research in improving pre-analytical sample processing techniques is the use of functionalized magnetic nanoparticles (MNPs). MNPs can be functionalized with a range of biorecognition reagents, such as antibodies, aptamers, bacteriophages, antibiotics, lectins, and polymers (136). Mao et al. coated MNPs with monoclonal antibodies to extract various *Listeria* spp. from lettuce for use in a multiplex PCR, resulting in a limit of detection of 10 CFU/g (137). However, their procedure was limited to 1 gram of lettuce spiked with log-phase bacteria that were not further stressed. Huang et al. used a bacteriophage functionalized MNP to bind *Salmonella* spp. combined with real-time PCR to detect < 30 CFU/mL in milk and lettuce; however, this study was also completed with log-phase bacteria without further stress (138). These studies represent the lack of readily available, naturally contaminated foods to validate methods. Simulating natural infection is critical because bacteria face environmental stresses, challenges, and selective pressures during food processing that induce adaptive responses and varying degrees of injury to bacteria (i.e., sublethal injury) (70, 139). Therefore, the physiological state of bacteria must be considered when developing pathogen detection methods.

The Alocilja Nano-Biosensor Laboratory at Michigan State University developed a chitosan-functionalized magnetic nanoparticle (F#1 MNP) (133). Their previous work showed the successful capture of several foodborne pathogens in various matrices as reviewed in chapter 1 (93, 99, 123–127). However, like the previously mentioned studies, their current protocol is limited by the use of log-phase bacteria. Their protocol has also not been optimized and is used on samples containing 2-5 log CFU of pathogens.

For these reasons, the objective of this proof-of-concept study was to optimize the preanalytical pathogen concentration protocol of chitosan-functionalized magnetic nanoparticles using simulated contamination across a diverse group of matrices. This was done by using the gram-negative bacteria, *Salmonella* ser. Newport in strawberries and romaine lettuce and the gram-positive bacteria, *L. monocytogenes* in cotto salami and romaine lettuce. The bacteria were cold stressed and refrigerated on the appropriate matrix to simulate natural infection (139–141). Statistical design of experiments were used as a proof-of-concept approach, laying the foundation for future refinement and adaptation to other strains, pathogens, and food matrices.

Materials and Methods

<u>Inoculum Preparation</u>

Salmonella ser. Newport, strain MDD314, originally recovered from tomato fields during a multistate outbreak, and *L. monocytogenes*, CC1, originally isolated from the

1981 coleslaw-associated outbreak, were obtained from the Bergholz Laboratory (Michigan State University; East Lansing, MI) (142, 143). The bacteria were rejuvenated from 25% glycerol stocks stored at -20°C by streaking them on tryptic soy agar (TSA – Sigma Aldrich; St. Louis, MO) and incubating at 35 ± 2°C for 24 ± 2 hours. A single colony was transferred to 5 mL of tryptic soy broth (TSB – Sigma Aldrich; St. Louis, MO) in a 15 mL conical tube and incubated at 35 ± 2°C for 20 ± 2 hours at 250 rpm. Subsequently, 20 µL of overnight culture was transferred to 20 mL of TSB in a 50 mL conical tube and incubated at 35 ± 2°C for 20 ± 2 hours or 24 ± 2 hours at 250 rpm for *L. monocytogenes* and *Salmonella* ser. Newport, respectively. Ten-fold serial dilutions of the stock culture were prepared using phosphate buffered saline (PBS - Fisher BioReagents; Pittsburgh, PA) for manual aerobic plate count on TSA. The dilutions were refrigerated at 4 ± 2°C for 24 ± 2 hours then additional dilutions of the first original serial dilution were completed to accomplish the desired inoculum (144, 145). The inoculum amount was confirmed by plating 100 µL of the inoculum with three to five replicates for manual aerobic plate counts on TSA.

Food Sample Preparation

Strawberries, romaine lettuce ("lettuce"), and cotto salami were purchased from a local supermarket and stored in the original packaging at 4 ± 2°C until use. Both conventional and organic batches of strawberries (grade no. 1) and romaine lettuce were used (146). All romaine lettuce and cotto salami batches were used prior to their "best by" dates and any brown-discolored or damaged pieces of lettuce excluded. For unprocessed romaine lettuce, all samples were used within 12 days of their "pack date." All foods were screened for natural contamination using the culture-dependent methods outlined in the Food and Drug Administration's Bacteriological Analytical Manual (FDA BAM) or U.S. Department of Agriculture Microbiology Laboratory Guidebook (USDA MLG) (147–149). Rappaport-Vassiliadis broth (RV) and Tetrathionate broth (TT) samples were incubated in a noncirculating water bath. All samples screened negative.

All ready-to-eat lettuce batches were pre-chopped, as defined by commercial standards (150). Unprocessed samples had the three outermost leaves removed then were manually chopped with a sterilized knife to the same commercial standards. Lettuce and strawberry samples of 25 ± 1 g were weighed and placed in a 250mL reagent bottle with the lids tightened then loosened approximately one turn, unless otherwise described. When multiple strawberries were required to reach the desired weight, only one calyx was included in each sample and 3-6 cut surfaces were included. One piece of cotto salami 28 ± 1 g, cut into approximately eight equal slices was used for each sample. Foods were inoculated in a drop-wise fashion using 100 µL of inoculum, samples were then lightly shaken to disperse the inoculum prior to refrigeration (4 ± 2°C) for 24 ± 1 hours, unless otherwise stated (139–141).

FDA Bacteriological Analytical Manual (BAM) and USDA Microbiology Laboratory Guidebook (MLG) Media Preparation

For *Salmonella* ser. Newport, Rappaport-Vassiliadis broth (RV) was prepared using tryptone, magnesium chloride, and potassium dihydrogen phosphate (Sigma Aldrich; St. Louis, MO), sodium chloride (Honeywell Fluka), and malachite green (ThermoScientific Chemicals). Tetrathionate Broth base (Neogen Corps; Lansing, MI) was combined with Iodine-Potassium Iodide solution (Fisher Scientific and Sigma-Aldrich, respectively) and 0.1% Brilliant Green Solution (Sigma Aldrich) (TT). The agars used were Xylose Lysine Deoxycholate (XLD) (Sigma Aldrich), Hektoen Enteric (HE), and Bismuth Sulphite (BS) (Neogen Corps).

For *L. monocytogenes* testing in lettuce, GranuCult® Buffered *Listeria* Enrichment Broth and *Listeria* selective enrichment supplement (Sigma Aldrich) were paired with *Listeria monocytogenes* Differential Agar according to Ottaviani & Agosti Base (Sigma-Aldrich) supplemented with L-α-phosphatidylinositol (Sigma Aldrich) and *Listeria* Chromogenic Selective Supplement (Neogen Corps) - Agar *Listeria* Ottavani and Agosti (ALOA). In lieu of ALOA for the preliminary work, Oxford *Listeria* Agar with supplement was used (OXA; Neogen Corps, Lansing MI). For *L. monocytogenes* in cotto salami, GranuCult® Modified UVM (UVM) broth base (Sigma Aldrich) was paired with modified oxford agar (MOX) consisting of Oxford *Listeria* Agar (Neogen Corps) supplemented with colistin and 1% moxalactam solution (Sigma Aldrich). All media were prepared according to the manufacturers' instructions.

<u>Chitosan-functionalized Magnetic Nanoparticles</u>

Chitosan-functionalized magnetic nanoparticles (F#1 MNPs) (100-200 nm) were received from the Alocilja Nano-Biosensors Laboratory at Michigan State University. They were aseptically resuspended with molecular grade water (Sigma Life Science; United Kingdom) to the appropriate concentration and vortexed at maximum speed for 5-10 minutes. F#1 MNP solutions (100 μL) were plated on TSA and incubated at 35 ± 2°C for 48 ± 2 hours at the conclusion of each experimental day to confirm sterility and the absence of cross-contamination.

Phosphate Buffered Saline pH Preparation

Phosphate buffered saline (PBS) (Fisher BioReagents; Pittsburgh, PA) was diluted to 1x strength using distilled water. The pH of the PBS was adjusted with 1.0 N or 0.1 N hydrochloric acid (Fisher Scientific; Canada) or 1 N sodium hydroxide (Fisher Scientific; Canada), as appropriate. The pH was confirmed with a calibrated SevenCompact pH meter S220 (Mettler-Toledo; Switzerland) then 0.22 µm filter sterilized.

Sample Preparation Preliminary Testing

Analytical portions (25 ± 1 g) of romaine lettuce were aseptically weighed into a Whirl-Pak™ [Nasco Whirl-Pak™ Write-On Homogenizer Blender Filter Bag (710 mL)] or 250 mL round media storage bottle and inoculated with 100 µL of 4 $\log_{10}$ CFU/mL *L. monocytogenes* as previously described. Samples were refrigerated for 30 ± 2 hours before processing via one of four methods.

For the first method, six samples were processed using hand homogenization, divided into two variations (three samples each). In both, 100 mL of PBS was added to each sample and hand homogenized for 1 minute. In the first variation, the liquid portion was transferred to a sterile 250 mL reagent bottle, 1 mL of 5 mg/mL F#1 MNPs was added, and the samples were incubated for 5 minutes. In the second variation, F#1 MNPs (1 mL of 5 mg/mL) were added directly to the homogenized samples, incubated for 5 minutes, and then the liquid portion was transferred to a sterile 250 mL reagent bottle. The second method involved soaking. Three samples were soaked in 100 mL of PBS for 5 minutes, followed by the addition of 1 mL of 5 mg/mL F#1 MNPs and incubation for 5 minutes. The liquid portion was then transferred to a sterile 250 mL reagent bottle. The third method used stomaching. Three samples were combined with 100 mL of PBS and stomached for 30 seconds at 230 rpm using a Seward Stomacher® 400 Circulator. F#1 MNPs (1mL of 5mg/mL) were then added to the Whirl-Pak™ opposite the food portion, and the samples were incubated for 5 minutes. For all methods, all MNP incubation steps were done on a Corning LSE Nutating Mixer. The reagent bottles or Whirl-Paks™ were attached to a Spherotech® Fleximag Separator FMS-1000 Magnet (Lake Forest, IL) using three rubber bands for 5 minutes (Figure S1.1). The supernatant was removed, the MNPs were resuspended in 1 mL of PBS, and the samples were serial diluted with PBS and spread on OXA and incubated at 35 ± 2°C for 24 ± 2 hours for manual aerobic plate count. The resulting plate counts from all methods were compared using a one-way ANOVA with $\alpha \leq 0.05$ as the level of significance.

Definitive Screening Design (DSD)

The current process map described by the Nano-Biosensors Laboratory formed the basis for determining the independent and dependent variables (123). The definitive screening design used three levels for each factor (low, middle, high). JMP® Pro 17.2.0 was used to create a randomized definitive screening design matrix with two blocks representing two batches (e.g., container/bag) of the food matrix to account for variation between samples and four extra center points to estimate quadratic effects (Tables S1.1-S1.3). Factors included were: bacterial concentration (levels: 2, 4, and 6 $\log_{10}$ CFU/25 g), PBS volume (levels: 25, 125, 225 mL), pH of PBS (for strawberries and lettuce only) (levels: 3.5, 5.75, 8), soaking time in PBS (levels: 1, 3, 5 minutes), final concentration of F#1 MNPs (levels: 0.025, 0.1375, 0.25 mg/mL), incubation time of

MNPs with the matrix and pathogens (levels: 1, 10.5, 20 minutes), and magnetic separation time (levels: 5, 12.5, 20 minutes).

The inoculum (*Salmonella* ser. Newport) and food samples (strawberries and romaine lettuce) were prepared as previously described, except various size reagent bottles were used based on the required PBS volume (25-, 125-, or 225-mL were placed in a 100-, 250-, or 500-mL reagent bottle, respectively) to maintain consistent contact between the container/liquid level and magnet height. For testing in PBS, 25 mL of PBS (pH 7.4 ± 0.02) was inoculated in 50 mL conical tubes and vortexed at maximum speed for 5 seconds prior to refrigeration. An additional 25 g or mL portion was artificially spiked with 100 µL of 4 $\log_{10}$ CFU bacteria to serve as a positive control. *L. monocytogenes* was not tested using a DSD.

Samples were removed from the refrigerator 45-60 minutes prior to extraction and verified to be at room temperature (19-22°C) by an infrared thermometer (Etekcity LaserGrip1080). Next, the appropriate volume of PBS at the specified pH was added to the sample, the sample swirled to remove the food matrix from the bottom/side of the reagent bottle and put on a Corning® LSE™ Nutating Mixer for the specified amount of time. Then 1 mL of the appropriate concentration of F#1 MNPs was added to the sample and placed back onto the mixer for the designated amount of time. The liquid was then removed from the lettuce samples using a 25 mL serological pipette and put into a new, sterile reagent bottle. This step was not done with the strawberry samples as these samples floated and the supernatant could be removed in the presence of the strawberries in the bottle attached to the magnet. The bottles were then attached to Spherotech® Fleximag Separator FMS-1000 Magnet (Lake Forest, IL) using three rubber bands for the specified period of time. For testing in PBS, the conical tubes were attached to the magnet with the provided 50 mL conical tube holder. The supernatant was then removed using a 25 mL serological pipette and the MNPs resuspended with 1mL of PBS. The MNPs from food samples were plated on XLD agar and the samples from PBS were plated on TSA, both were incubated at 35 ± 2°C for 24 ± 2 hours.

Capture efficiency was calculated as the recovered bacteria ($\log_{10}$ CFU/mL) divided by the starting number of bacteria ($\log_{10}$ CFU/mL). The number of starting bacteria were estimated using ten-fold serial dilutions plated on TSA for PBS samples, or XLD for food matrix samples.

<u>Central Composite Design (CCD)</u>

For *Salmonella* ser. Newport testing in PBS, JMP® Pro 17.2.0 was used to create a custom design, which returned a face-centered central composite design (Table S1.4). This design was run in triplicate using four center points resulting in 36 runs. For *L. monocytogenes* in PBS, JMP® Pro 17.2.0 was used to create a custom design, with response surface modeling run in duplicate, resulting in a modified face-centered central composite design with 22 runs (Table S1.5). For both pathogens, initial testing was completed in 25 mL of PBS with bacterial inoculations prepared as before. Factors included were concentration of MNPs (levels: 0.025, 0.1375, 0.25 mg/mL) and incubation time of MNPs with the matrix and pathogens (levels: 1, 10.5, 20 minutes). Magnet separation time was standardized to 5 minutes and the same Spherotech® Magnet as the DSDs was used. The resuspended MNPs were plated on TSA and incubated at 35 ± 2°C for 24 ± 2 hours for manual plate count. The supernatant was placed in a new 50 mL conical tube and centrifuged at 3,000 g for 30 minutes at 4°C.

The supernatant was removed to 0.5 mL, the liquid was then pipetted up and down to resuspend any bacteria and was plated on TSA for manual plate count. This number of CFUs was added to the number of CFUs recovered by F#1 MNPs to estimate the starting CFUs. The resultant capture efficiency (CFUs extracted by F#1 MNPs divided by starting CFUs) was also transformed to nominal data (presence/absence) for evaluation. The average inoculum for testing in PBS was 3.6 ± 2.3 CFU for *Salmonella* ser. Newport and 7.8 ± 4.8 CFU for *L. monocytogenes.*

Next, for *Salmonella* ser. Newport testing in strawberries, JMP® Pro 17.2.0 was again used to create a custom design, which resulted in a face-centered central composite design (Table S1.6). For the first replicate, the factors included were pH of PBS (levels: 3.5, 5.75, 8), concentration of MNPs (levels: 0.025, 0.1375, 0.25 mg/mL), and incubation time of MNPs with the matrix and pathogens (levels: 1, 10.5, 20 minutes). The second replicate eliminated the use of pH. There was a total of 28 runs. The average inoculum was 8.7 ± 3.4 CFU. Magnet separation time was standardized to 20 minutes and the same Spherotech® Magnet and supernatant removal protocol as the DSDs was used. The resuspended MNPs were incubated in 100 mL of Universal Pre-enrichment Broth (UPB) at 35 ± 2°C for 24 ± 2 hours. Then 1,000 µL or 100 µL were added to TT or RV, respectively and incubated at 43 ± 0.2°C or 42 ± 0.2°C, respectively, for 24 ± 2 hours. Streak plates (10 µL loop) were then made on XLD, HE, and BS.

For *Salmonella* ser. Newport testing in lettuce, JMP® Pro 17.2.0 was used to design a face-centered central composite design (Table S1.7). The factors were the same as those used for strawberries, excluding pH, resulting in a total of 20 runs. The magnet protocol followed the same steps as the DSD. The MNPs were incubated in

UPB and RV/TT, followed by streaking on XLD, HE, and BS agars as described for the strawberry testing. The average inoculum was 10.9 ± 4.0 CFU. For *L. monocytogenes*, the same protocol was applied to romaine lettuce (Table S1.8) and cotto salami (Table S1.9) with the following exceptions: BLEB with supplement or UVM incubated at 30 ± 2°C for 24 ± 2 hours replaced UPB, RV, and TT as the enrichment media for lettuce and cotto salami, respectively. Instead of XLD/HE/BS, ALOA was used for romaine lettuce, and MOX for cotto salami. The average inoculum for romaine lettuce was 9.2 ± 3.6 CFU and cotto salami was 13.4 ± 3.5 CFU.

<u>Optimized Protocol Comparison in PBS</u>

The capture efficiency of the optimized protocol was compared to the original protocol in 25 mL PBS. Capture efficiency was calculated as the recovered bacteria (CFU) divided by the starting number of bacteria (CFU). The starting number of bacteria was calculated as the number of CFU in the MNP capture plus the number of CFU in the supernatant. The supernatant was placed in a 50 mL conical tube and centrifuged at 3,000 g for 30 minutes at 4°C, all liquid except 0.5mL was removed, the pellet resuspended and then spread on TSA. Results were analyzed with a two-sample *t*-test.

<u>Lower Limit of Capture Estimation</u>

For *Salmonella* ser. Newport in strawberries, five replicates from three batches were tested using the optimized F#1 MNP extraction protocol. The original three batches for strawberry testing were for validation of the model; however, since the positivity rate was lower than expected, these results were repurposed to estimate the lower limit of capture (see discussion). The subsequent testing for *L. monocytogenes* in romaine lettuce and cotto salami used 10 replicates from one batch.

The positivity rate was compared to the Poisson distribution for the inoculum amount to estimate the lower limit of capture. Using the Poisson distribution, the inoculum amount was adjusted to ensure that the probability of inoculating below the estimated lower limit of capture was ≤ 0.5%. All calculations were completed using the "POISSON.DIST" function in Microsoft® Excel. For *Salmonella* ser. Newport in lettuce, various inoculum levels were tested in triplicate to estimate the lower limit of capture.

Protocol Validation Testing

Using the estimated inoculum needed to minimize false negatives, three batches of five replicates were used to verify the F#1 MNP capture protocol for *Salmonella* ser. Newport in strawberries and *L. monocytogenes* in romaine lettuce and cotto salami. The goal sensitivity, according to the USDA, was 90% (151).

Aerobic Plate Count of Matrices

Aerobic plate counts (APCs) were conducted on all batches for all food matrices in duplicate. Food samples were prepared as previously described except the samples were placed in a Nasco Whirl-Pak™ Write-On Homogenizer Blender Filter Bag (710 mL) with 100 μL of PBS in lieu of bacteria inoculation. After 24 ± 1 hours of refrigeration at 4 ± 2°C, the matrices were removed from the refrigerator and brought to room temperature (19-22°C), verified by an infrared thermometer (Etekcity LaserGrip1080). For sample processing, a total of 225 mL of PBS was added to strawberry and romaine lettuce samples and 252 mL of PBS added to cotto salami to create a 1:9 dilution. During the preliminary and definitive screening steps, samples were homogenized using a Seward Stomacher® model 400 Circulator set at 230 rpm for 2 minutes with approximately 125 mL of the PBS added, after which the remainder was added and the bag vigorously shaken. All aerobic plate counts conducted after the definitive screening design steps used a Stomacher Lab Blender 400 (Tekmar Company; Cincinnati, OH), which homogenized the samples for 2 minutes. Ten-fold serial dilutions of the supernatant were prepared using PBS, spread onto TSA, and incubated at 35 ± 2°C for 48 ± 2 hours for manual aerobic plate count.

Data Analysis

Experimental designs and data analyses for the DSDs and CCDs were conducted using JMP® Pro 17.2.0 statistical software. For DSDs, “Fit Definitive Screening” model with standard least squares was used. CCDs were analyzed using either standard least squares for capture efficiency or nominal logistic regression for presence/absence. Across all models, backward elimination was used. All other analyses were completed using data analysis functions in Microsoft® Excel. Unless otherwise noted the significance level was $\alpha \leq 0.05$.

Results

Sample Preparation Preliminary Testing

Lower numbers of bacteria than expected were extracted with the previous, unoptimized F#1 MNP capture protocol, using stationary-phase bacteria plated directly on selective agar without a recovery incubation (Table 1.1). The results ranged from a mean of 0.92 - 1.34 $\log_{10}$ CFU/mL. However, there was no significant difference in bacterial recovery among the methods ($p = 0.1154$).

Definitive Screening Design (DSD)

The only variable of significance that was consistent in all models was bacterial concentration ($p < 0.0001$) (Table 1.2). In the PBS model, the MNP concentration was also significant (p = 0.0011). Next, the individual variables were evaluated for inclusion in the central composite design (CCD). Even though the bacterial concentration was significant in the DSD, this variable was standardized (~10 CFU per sample) to optimize the CCD at low concentrations of bacteria. PBS volume was standardized to 100 mL since this amount was deemed sufficient to cover most of the matrix present. The magnet separation time was standardized to 20 minutes, as the time required for the liquid to appear clear (the F#1 MNPs have a brown tint) was 12-17 minutes depending on the matrix. Sample preparation (or soak time) was standardized to 1 minute. The starting pH of PBS was 3.5, 5.75, and 8 and when added to the strawberry and lettuce matrices resulted in a pH of 3.56-7.76. MNP concentration, MNP incubation time, and pH were included in the CCD model for further examination.

<u>Central Composite Design</u>

The variable pH remained non-significant (p = 0.4097) in the first iteration of the strawberry model and was excluded from further analysis for all models. The remaining variables were MNP concentration and MNP incubation time.

A least fit squares model was used for *Salmonella* ser Newport (SSN) and *L. monocytogenes* (*Lm*) testing in PBS with capture efficiency as the dependent variable (Table 1.3). The use of variable*variable denotes an interaction term in the model. For SSN, the significant variables were MNP concentration (p = 0.0071), incubation time*incubation time (p = 0.0507), and MNP concentration*incubation time (p = 0.0121). Incubation time (p = 0.2132) remained in the model due to the presence in significant effects. This model predicted a maximum desirability with an MNP concentration of 0.25 mg/mL and MNP incubation time of 20 minutes. For *Lm,* the significant variables were

MNP concentration ($p = 0.0092$), MNP concentration*MNP concentration ($p = 0.0176$), MNP concentration*incubation time ($p = 0.0612$), and incubation time ($p = 0.0187$). This model predicted a maximum desirability with an MNP concentration of 0.14 mg/mL and MNP incubation time of 20 minutes. While MNP concentration*incubation time had $p > 0.05$, it remained in the model for comparison testing due to it resulting in a lower MNP concentration than if it were eliminated (0.14 mg/mL compared to 0.17 mg/mL).

Nominal logistic models were run for all pathogen/matrix combinations with presence/absence as the dependent variable (Table 1.4). First, the SSN in PBS data was transformed to presence or absence. The significant variable was MNP concentration*incubation time ($p = 0.0011$). The variables MNP concentration ($p = 0.0599$) and incubation time ($p = 0.8655$) remained in the model due to the presence in the significant effect. This model predicted a maximum desirability with an MNP concentration of 0.25 mg/mL and MNP incubation time of 20 minutes. When the parameters were set to an MNP concentration of 0.20 mg/mL and time of 10 or 20 minutes, the predicted value of presence were 0.983 and 1 and predicted value of absence were 0.017 and 0.001, respectively. Transformation of the *Lm* in PBS data resulted in a nonsignificant model due to 21/22 (95.5%) of the samples being positive and was excluded.

For SSN in strawberries, the significant variables were MNP concentration ($p = 0.0027$), MNP concentration*MNP concentration ($p = 0.0442$), incubation time ($p = 0.0072$), and MNP concentration*incubation time ($p = 0.0052$). This model predicted a maximum desirability with an MNP concentration of 0.24 mg/mL and MNP incubation time of 17.35 minutes. When the parameters were set to an MNP concentration of 0.20

mg/mL and time of 10 minutes, the predicted value of presence was 1 and predicted value of absence was 3×10^{-7}.

For SSN in lettuce, only 4/20 (20%) samples in the CCD were positive and therefore did not produce a reliable model.

The significant variables for *Lm* in cotto salami were MNP concentration (p = 0.0022), MNP concentration*MNP concentration (p = 0.0120), and incubation time*incubation time (p = 0.0132). The variable incubation time (p = 0.1889) remained in the model due to the presence in significant effects. This model predicted a maximum desirability with an MNP concentration of 0.19 mg/mL and MNP incubation time of 19.8 minutes. With a MNP concentration of 0.20 mg/mL and time of 10 or 15 minutes, the predicted value of presence was 0.989 and 1 and predicted value of absence was 0.011 and 6×10^{-7}, respectively.

For *Lm* in romaine lettuce, the significant variables were MNP concentration (p = 0.0028), MNP concentration*MNP concentration (p = 0.0339), incubation time*incubation time (p = 0.0097), MNP concentration*incubation time (p = 0.0005). Incubation time (p = 0.1889) remained in the model due to the presence in significant effects. This model predicted a maximum desirability with an MNP concentration of 0.22 mg/mL and MNP incubation time of 3.52 minutes. When the parameters were set to an MNP concentration of 0.20 mg/mL and time of 10 minutes the predicted value of presence was 1 and predicted value of absence was 0.

Optimized Protocol Comparison in PBS

The optimized protocols in PBS (*Salmonella* ser. Newport – MNP concentration: 0.20 mg/mL, MNP incubation time 20 min; *L. monocytogenes* – MNP concentration:

0.14 mg/mL, MNP incubation time 20 min) were compared to the current protocol (MNP concentration: 0.05 mg/mL, MNP incubation time 5 min). Both protocols used 5 minutes for magnetization. The optimized *Salmonella* protocol showed a capture efficiency of 0.9028 ± 0.1335 compared to the original protocol of 0.2435 ± 0.2529 ($p < 0.0001$). The optimized *L. monocytogenes* protocol capture efficiency of 0.9640 ± 0.0568 was significantly different ($p = 0.0009$) compared to the original protocol of 0.6321 ± 0.1663.

<u>Lower Limit of Capture Estimation</u>

The lower limit of capture was estimated by using an inoculum that provided fractional positive results for the protocol. The percentage of positive samples was then compared to the Poisson distribution to estimate the lower limit of capture. This lower limit of capture was then used to estimate the inoculum needed, according to the Poisson distribution, to not have false negative results (Table 1.5) (140, 152, 153). This approximate inoculum amount was used in future testing. However, due to the higher-than-expected lower limit of capture of *Salmonella* ser. Newport in romaine lettuce, use of the central composite design did not create an accurate model. Therefore, several inoculations were used to estimate the range of the lower limit of capture using the MNP concentration and incubation times that were successful for the other matrix-pathogen combinations.

For *Salmonella* ser. Newport in strawberries, five samples from three batches were tested using an average inoculum of 7.7 ± 1.5 CFU. This resulted in 10/15 (66.7%) samples testing positive. When this observed percentage (66.7%) was compared to the Poisson distribution with $\lambda = 7.7$, the probability $P(X \geq x)$ was calculated for x resulting in a value between 6 and 7. Based on this comparison, the estimated lower limit of capture was determined to be 7. Next, using the Poisson distribution and $\lambda = 7$, x must be 18 for $P(X \leq x)$ to be <0.5%. Therefore, the goal inoculation for future testing was 18 CFU. The same methodology was applied to *L. monocytogenes* in romaine lettuce and cotto salami and resulted in an approximate limit of capture of 9 and 14, respectively with a goal of 20 and 27 CFU for future inoculations.

As previously discussed, the lower limit of capture for *Salmonella* ser. Newport in lettuce was estimated using various inoculations with the parameters MNP concentration: 0.20 mg/mL, MNP incubation time: 15 min. Inoculations ranging from 10-197 CFU/25g sample were tested in batches of ready-to-eat (pre-cut) and unprocessed lettuce samples (Table 1.6). The lower limit of capture was estimated at < 56.0 ± 12.1 CFU/25 g; therefore, future inoculations were targeted at 75 CFU.

<u>Protocol Validation Testing</u>

Using the target minimal inoculations estimated in the lower limit of capture testing, the protocols were validated (Table 1.7). *Salmonella* ser. Newport in strawberries [average inoculum (CFU/sample): 21.6 ± 4.9] and *L. monocytogenes* in romaine lettuce [average inoculum (CFU/sample): 21.0 ± 3.7] had 15/15 (100%) positive results. *L. monocytogenes* in cotto salami [average inoculum (CFU/sample): 26.5 ± 5.7] had 14/15 (93.3%) positive results. The negative result was in the batch with an inoculum less than that required by the previous calculations [inoculum (CFU/sample): 22.0 ± 3.8 versus target of 27 CFU/sample].

<u>Aerobic Plate Count of Matrices</u>

Aerobic plate counts were conducted to assess the competing microbial background of the food matrices. Strawberries had an average aerobic plate count of

4.91 ± 0.54 log_{10} CFU/g. While ready-to-eat (pre-cut) lettuce had a higher microbial load, averaging 6.95 ± 0.69 log_{10} CFU/g. Unprocessed lettuce, with the three most outer leaves removed then aseptically chopped, showed slightly lower counts at 5.18 ± 0.44 log_{10} CFU/g. Cotto salami samples showed a wide range from the occasional CFU to 4.22 log_{10} CFU/g, including one sample too numerous to count (> 3 log_{10} CFU/g).

Discussion

This proof-of-concept study highlights the use of statistical design of experiments (DOE), specifically the definitive screening design (DSD) and central composite design (CCD), to optimize the extraction of pathogens from various food matrices using chitosan-functionalized magnetic nanoparticles (F#1 MNP). The pathogens *Salmonella* ser. Newport and *L. monocytogenes* were chosen as representative pathogens to examine the extraction protocol's performance under simulated conditions.

The original extraction protocol had several shortcomings. There was a lack of prior optimization with the standardized use of 5 mg of MNPs incubated for 5 minutes followed by 5 minutes of magnetization, reliance on moderate to high initial bacterial concentrations (2-5 log_{10} CFU), and use of log-phase bacteria, which do not represent real-world food contamination (139–141). This study used stationary-phase bacteria at low concentrations (< 2 log_{10} CFU) that were further stressed under refrigerated conditions. Additionally, the original method used stomaching and Whirl-Pak™ bags, which caused issues with sample handling and led to suboptimal MNP removal due to the MNPs being trapped by food particles and the bag filter. This was replaced with a soaking preparation method, which simplified the procedure and reduced the amount of interfering matrix components during pathogen extraction. While this method aligns with recommendations for food surface-level contamination, it may be inadequate for internalized or strongly attached pathogens to food matrices (145, 154–156).

The variable “bacterial concentration” was a dominant variable in the DSD, which the author believes affected the model outcomes, leading to the use of a CCD to further optimize variables of interest. Higher starting *Salmonella* ser. Newport concentrations were associated with increased capture efficiency (Table S1.1-S1.3). This observation aligned with findings by Matta et al (99). This variable was excluded from further analysis to focus on optimizing low-concentration scenarios. This led the author to evaluate the inclusion/exclusion of the non-significant variables from the DSD in the CCD, as explained in the results section.

The effect of PBS pH was not significant in either the DSD or initial CCD iteration with strawberries. This is likely due to the buffering capacity of the PBS and food matrices tested, where the resultant pH fell within the range 3.56-7.76. To the authors’ knowledge, there are no studies examining the pKa of *Salmonella* or *L. monocytogenes* when bound to the F#1 MNPs, or the binding strength of these pathogens to the F#1 MNPs. The pKa of chitosan (~6.5) suggests that its protonation state remained relatively consistent within this range, corroborating findings by Boodoo et al., who observed successful pathogen extraction across a pH of 5-10 (127). Alternatively, the low pH would lead to a bacterial stress response whereby this change in cell physiology may affect the MNPs ability to bind (67, 68). This suggests the F#1 MNPs are capable of extracting pathogens in moderate pH variations, making them adaptable to a range of food matrices. However, the study did not evaluate matrices leading to a resultant pH outside this range.

When evaluating the parameters of maximum desirability outcomes for the models, the models produced an average MNP concentration in the food matrices of 0.22 ± 0.03 mg/mL; therefore, the MNP concentration was standardized to 0.20 mg/mL for consistency. Next, the incubation time was evaluated and times chosen for practicality of maintaining consistency throughout the testing protocol while maintaining a near optimal predicted value for presence and absence. While standardizing the MNP concentration and determining the time needed to maximize the odds of obtaining a positive sample has the benefit of consistency, maintaining accuracy throughout subsequent testing, and user friendliness it may lead to false negatives.

Distinct lower limits of capture estimations were observed for SSN and *Lm* across food matrices, suggesting that matrix composition and pathogen adherence properties influence capture efficiency. However, these initial estimations were based on a limited number of replicates and batches. The conservative Poisson distribution adjustment for the inoculum likely minimized the risk of over- or underestimating the lower limit of capture. Since validation testing using additional replicates and batches yielded > 90% positive rates, further refinement of the lower limit of capture was not completed for this proof-of-concept study. For future studies aiming to more accurately estimate the lower limit of capture, a more comprehensive approach can be used. For example, serial dilutions of the target pathogen can be spiked into the food matrix of interest. The probability of a positive result can then be plotted against the bacterial concentration to more accurately determine the estimated limit of capture. Initial sample sizes for each dilution can be determined using a probability model to ensure sufficient statistical confidence.

The lower limit of capture for SSN was estimated at 0.28 CFU/g in strawberries and 2-3 CFU/g in romaine lettuce. Whereas *Lm* showed a lower limit of capture of 0.36 CFU/g and 0.5 CFU/g in romaine lettuce and cotto salami, respectively. The differences in the lower limits of capture may be attributed to differences in competing microbial populations, food matrix composition, and/or bacterial adherence properties.

Aerobic plate counts were performed to examine the influence of competing microbes. The counts were comparable to previous studies, showing these samples were representative in these regards for representing competing microbe effects on the MNPs (157–163). Given the ability for the F#1 MNPs to capture SSN in strawberries and *Lm* in lettuce, the author attributes the lower limit of capture that was higher for SSN in lettuce to how SSN attaches to lettuce. This hypothesis is supported by previous studies using various species of lettuce and leafy greens showing that the attachment of *Salmonella* is dependent on the serotype, *Salmonella* inoculum growth conditions, and leafy green storage conditions (164, 165). Patel and Sharma's study showed SSN's attachment to cabbage, iceberg lettuce, and romaine lettuce happened within five minutes and strengthened over time (1, 4, and 24h post-inoculation) (164). Among the tested matrices, the strongest bacterial attachment was observed in romaine lettuce. Takeuchi et al. observed similar results and further showed there was no difference in adherence between cut and intact lettuce surfaces, though their study used *Salmonella* ser. Typhimurium (165).

In contrast, there are less studies on the attachment of *Salmonella* to strawberries. Pérez-Lavalle et al. demonstrated the formation of biofilms but did not study if the bacteria physically attach to the surface or integrate within the fruit (166).

Another study by Yin et al. showed *Salmonella* attach to strawberries to a lesser extent than *L. monocytogenes* and hypothesized this was due to the effects of competing microbes (167). Taken together, these findings suggest that *Salmonella* attachment varies by matrix, with stronger adherence observed in romaine lettuce than strawberries, which is hypothesized to have influenced the lower limit of capture.

The starkest difference in matrix composition is the presence of animal protein and fat in the cotto salami. Previous studies established that *L. monocytogenes* readily binds to meat and fat surfaces and the surface charge of the *L. monocytogenes* was correlated with the cell physiology, which influenced how tightly adhered the bacteria were to the meat product surface (168–171). *L. monocytogenes* also attaches to cabbage, as shown by Ells and Hansen, but is dependent on the strain, growth temperature, incubation time, and surface (cut vs whole) (172). Takeuchi et al. also showed *Lm* attaches preferentially to cut edges rather than the surface of romaine lettuce (165). However, to the author's knowledge, there are no studies comparing the attachment strength of *Lm* in cotto salami to romaine lettuce; however, this difference may account for the slightly decreased extraction of *Lm* from cotto salami as compared to romaine lettuce. Further studies are needed to determine the F#1 MNP attraction strength to bacteria for comparisons to the attraction strength to food matrices to improve their utility. Additionally, it is suggested that future studies include alternative pretreatments such as stomaching and matrix lysis to release pathogens prior to MNP extraction.

Conclusion

This proof-of-concept study demonstrated the use of DSD and CCD to optimize extraction of low levels of contamination of *Salmonella* ser. Newport and *L. monocytogenes* on diverse food matrices using chitosan-functionalized magnetic nanoparticles. By addressing the key limitations of the original protocol - reliance on unoptimized conditions, high initial bacterial concentrations, and use of log-phase bacteria - this study provides a framework for establishing standardized extraction protocols optimized to specific pathogens and food matrices under simulated environmental challenges, stresses, and selective pressures faced by foodborne pathogens.

Tables

Method Tested				Bacteria Count ($\log_{10}$ CFU/mL) Mean ± Standard Deviation		
Hand Homogenization with Liquid Removed Prior to MNP Addition				0.95 ± 0.20		
Hand Homogenization with MNPs Incubated with Lettuce				1.03 ± 0.27		
Soaking				0.92 ± 0.14		
Stomaching				1.34 ± 0.17		
ANOVA - Sample Preparation Preliminary Testing Comparison						
Source of Variation	*SS*	*df*	*MS*	*F*	*p-value*	*F crit*
Between Groups	0.3307	3	0.1102	2.7097	0.1154	4.0662
Within Groups	0.3254	8	0.0407			
Total	0.6561	11				

Table 1.1: Summary of sample preparation preliminary testing. There was no significant difference (p-value = 0.1154) among sample preparation methods tested.

DSD Reduced Model Statistics			
	PBS	Strawberry	Romaine Lettuce
Effect Summary			
Source	p-value		
Bacterial Concentration	< 0.0001	< 0.0001	< 0.0001
MNP Concentration	0.0011	NS	NS
Model Statistics			
Root Mean Squared Error (RMSE)	0.1138	0.1152	0.0926
Coefficient of Determination (R^2)	0.83	0.73	0.89
P-value	< 0.0001	< 0.0001	< 0.0001

Table 1.2: Summary of definitive screening design (DSD) regression analysis for *Salmonella* ser. Newport in PBS, strawberries, and romaine lettuce. Significant variables (source) are listed, other sources and source interactions were not significant (NS) and were eliminated in the final model. Sources with a p-value ≤ 0.05 are statistically significant.

CCD Reduced Model Statistics - PBS Capture Efficiency		
	SSN	*Lm*
Effect Summary		
Source	p-value	
MNP Concentration	0.0071	0.0092
MNP Concentration*MNP Concentration	NS	0.0176
Incubation Time	0.2132^	0.0187
Incubation Time*Incubation Time	0.0507	NS
MNP Concentration*Incubation Time	0.0121	0.0612
Model Statistics		
Root Mean Squared Error (RMSE)	0.283	0.1976
Coefficient of Determination (R^2)	0.44	0.61
P-value	0.0018	0.0022
Lack of Fit F Ratio	1.0279	0.8724
Lack of Fit p-value	0.4123	0.5064
Maximum Desirability		
MNP Concentration (mg/mL)	0.25	0.14
Incubation Time (min)	20	20

Table 1.3: Summary of central composite design (CCD) regression analysis evaluating capture efficiency for *Salmonella* ser. Newport (SSN) and *L. monocytogenes* (*Lm*) in PBS. Significant variables (source) are listed, other sources and source interactions were not significant (NS) and were eliminated in the final model. To maximize the capture efficiency, 25 mg or 14 mg per 100 mL of PBS incubated for 20 minutes is optimal for SSN and *Lm*, respectively. Sources with a p-value ≤ 0.1 are statistically significant.

CCD Reduced Model Statistics				
	PBS - SSN	Strawberry - SSN	Cotto Salami - *Lm*	Romaine Lettuce - *Lm*
Effect Summary				
Source	p-value			
MNP Concentration	0.0599^	0.0027	0.0022	0.0028
MNP Concentration*MNP Concentration	NS	0.0442	0.0120	0.0339
Incubation Time	0.8655^	0.0072	0.1889^	0.1889^
Incubation Time*Incubation Time	NS	NS	0.0132	0.0097
MNP Concentration*Incubation Time	0.0011	0.0052	NS	0.0005
Model Statistics				
Whole Model Test Chi Square	16.2868	11.9375	15.8549	17.5801
Whole Model Test P-value	0.0010	0.0178	0.0032	0.0035
Coefficient of Determination (R^2)	0.5140	0.3395	0.6122	0.6788
Lack of Fit Chi Square	1.0610	7.6382	6.08×10^{-7}	8.20×10^{-7}
Lack of Fit p-value	0.9575	0.3656	1	1
Prediction Profiler				
Maximum Desirability				
MNP Concentration (mg/mL)	0.25	0.24	0.19	0.22
Incubation Time (min)	20.00	17.35	19.80	3.52
Predicted Value of Presence	1	1	1	1
Predicted Value of Absence	5.00×10^{-5}	0	0	0
MNP Concentration 0.20 mg/mL and Incubation Time 10 min				
Predicted Value of Presence	0.983	1	0.989	1
Predicted Value of Absence	0.017	3.00×10^{-7}	0.011	0
MNP Concentration 0.20 mg/mL and Incubation Time 15 (cotto salami) or 20 (PBS) min				
Predicted Value of Presence	1		1	
Predicted Value of Absence	0.001		6.00×10^{-7}	
Note: ^ denotes effects contained in significant source				

Table 1.4: Summary of central composite design (CCD) regression analysis evaluating presence/absence for *Salmonella* ser. Newport (SSN) in PBS and strawberries and *L. monocytogenes* (*Lm*) in cotto salami and romaine lettuce. Significant variables (source) are listed, other sources and source interactions were not significant (NS) and were eliminated in the final model unless they were contained in a significant source (^). Use of 20 mg/100 mL at an incubation time of 10-20 minutes maximizes capture of bacteria. Sources with a p-value ≤ 0.05 are statistically significant.

Lower Limit of Capture Estimation					
Matrix	Pathogen	Average Inoculum (CFU)	Results	Poisson Distribution Estimation of LOC x [P(X ≥ x)] (CFU)	Inoculum (λ) Needed to have <0.5% Probability of Inoculating At or Below LOC [P(X ≤ x)] (CFU)
Strawberry	SSN	7.7 ± 1.5	10/15 (66.7%)	7 (64.9%)	18 (0.29%)
Romaine Lettuce	*Lm*	11.2 ± 1.6	8/10 (80%)	9 (78.5%)	20 (0.50%)
Cotto Salami	*Lm*	12.6 ± 3.2	4/10 (40%)	14 (38.3%)	27 (0.46%)

Table 1.5: Lower limit of capture (LOC) estimation for *Salmonella* ser. Newport (SSN) in strawberries and *L. monocytogenes* (*Lm*) in cotto salami and romaine lettuce. LOCs were calculated using the Poisson distribution based on positive sample percentages for the given average inoculum (mean ± standard deviation). Target inoculations for future testing were adjusted to minimize false negatives. For SSN in strawberries the LOC was 7 CFU/sample with a target of 18 CFU/sample. For *Lm* in romaine lettuce and cotto salami the LOC was 9 and 14 CFU/sample, respectively, with targets of 20 and 27 CFU.

Lower Limit of Capture Estimation of *Salmonella* ser. Newport in Romaine Lettuce		
Average Inoculum (CFU)	Results	Ready-to-Eat (RTE) or Unprocessed
10.0 ± 3.7	1/3 (33.3%)	RTE
18.2 ± 6.0	1/3 (33.3%)	RTE
33.2 ± 7.5	2/3 (66.7%)	RTE
56.0 ± 12.1	3/3 (100%)	RTE
	2/3 (66.7%)	Unprocessed
95.8 ± 10.8	3/3 (100%)	RTE
125.0 ± 7.6	3/3 (100%)	RTE
	3/3 (100%)	Unprocessed
196.7 ± 27.4	3/3 (100%)	RTE
	3/3 (100%)	Unprocessed

Table 1.6: Lower limit of capture (LOC) estimation for *Salmonella* ser. Newport (SSN) in romaine lettuce. LOCs were compared between RTE and unprocessed samples at various inoculum amounts (mean ± standard deviation). The LOC in RTE lettuce was estimated at 56 ± 12 CFU/sample; therefore, a target inoculation of 75 CFU was used for future testing.

Chitosan-Functionalized Magnetic Nanoparticle Extraction Protocol Validation				
Matrix	Pathogen	Incubation Time (min)	Average Inoculum (CFU)	Results
Strawberry	SSN	10	21.8 ± 4.3	5/5 (100%)
			21.4 ± 6.0*	5/5 (100%)
			21.4 ± 6.0*	5/5 (100%)
Cotto Salami	*Lm*	15	30.2 ± 5.4	5/5 (100%)
			27.2 ± 5.1	5/5 (100%)
			22.0 ± 3.8	4/5 (80%)
Romaine Lettuce	*Lm*	10	18.8 ± 3.6**	5/5 (100%)
			18.8 ± 3.6**	5/5 (100%)
			23.2 ± 2.1	5/5 (100%)
F#1 MNP Amount: 20 mg/sample for all testing *Batches B & C for *SSN* testing in strawberries used the same inoculum preparation **Batches A & B for *Lm* testing in romaine lettuce used the same inoculum preparation				

Table 1.7: Chitosan-functionalized magnetic nanoparticle (F#1 MNP) extraction protocol validation for *Salmonella* ser. Newport (SSN) in strawberries and *L. monocytogenes* (*Lm*) in cotto salami and romaine lettuce. Positive detection rates are presented, with average inoculum levels and standard deviations. The single negative result for *Lm* in cotto salami occurred in the batch below the calculated target inoculum (27 CFU/sample).

CHAPTER 3: ENRICHMENT OF *SALMONELLA* SER. NEWPORT AND *LISTERIA MONOCYTOGENES* WITH CHITOSAN-FUNCTIONALIZED MAGNETIC NANOPARTICLES

Abstract

Foodborne pathogens remain a significant public health challenge, requiring rapid detection to prevent outbreaks, ensure food safety, and maintain regulatory compliance. Traditional enrichment-based pathogen detection methods for isolating single colonies are time consuming, often requiring 48-96 hours. This study evaluated the integration of chitosan-functionalized magnetic nanoparticles (F#1 MNPs) into enrichment protocols to reduce the incubation time and broth volume. The F#1 MNPs captured foodborne pathogens without inhibiting microbial growth and resulted in enrichment times of 4 or 8 hours (plus plating) for *Salmonella* ser. Newport in romaine lettuce and strawberries, respectively, and 8 and 12 hours for *L. monocytogenes* in romaine lettuce and cotto salami. These MNPs are a promising technology for accelerating pathogen isolation and detection, which will benefit food safety and public health.

Introduction

Foodborne illnesses continue to be a public health burden. Timely detection of foodborne pathogens is crucial for preventing and detecting outbreaks, improving food safety practices and regulations, and ensuring regulatory guidance. Current standard protocols outlined in the FDA's Bacteriological Analytical Manual (BAM) and USDA Microbiology Laboratory Guidebook (MLG), rely on enrichment and plating methods that require 24-48 hours of enrichment in broth followed by 24-48 hours of enrichment on selective agars to produce an isolate (60, 61).

Obtaining viable pathogen isolates is critical for downstream applications, such as whole-genome sequencing for surveillance, epidemiological investigations (e.g., outbreak investigations and trace-back and trace-forward investigations), and ensuring regulatory compliance. The ability to quickly isolate viable pathogens is critical to addressing foodborne illness threats. Recent advancements in pathogen isolation focus on optimizing enrichment broths and agars, fine-tuning incubation conditions, and employing advanced imaging techniques to monitor and assess microbial colony development.

Daquigan et al., combined various nonselective enrichment broths such as lactose broth, tryptic soy broth, and Universal Preenrichment broth with a modified tetrathionate broth (without brilliant green dye and reduced iodine-potassium iodide) to shorten the time of *Salmonella* colony isolation by one day in samples spiked with low levels of inoculum (~28 CFU) in cilantro, peanut butter, liquid whole eggs, and raw chicken thighs (173). Similarly, Silk et al. compared the growth kinetics of *L. monocytogenes* in eight broths to determine the lag-phase duration and generation time; however, this study was completed with pure cultures (174). Temperature modifications based on competing microbial loads further optimized the performance of Tetrathionate broth and Rappaport-Vassiliadis broth in the detection of *Salmonella* spp. (175, 176).

Advanced imaging techniques further accelerate colony detection. Balmages et al. used an optical contactless laser speckle imaging technique to reduce the time to detect *Vibrio natriegens* colonies from 8-13 hours with white light illumination to 3 hours (177). Likewise, Jung and Lee used an on-chip microscopy platform to detect log-phase

Staphylococcus epidermidis colony formation within 6 hours of plating compared to the conventional 24-hour colony counting method (178).

Despite advancements in rapid pathogen isolation and detection, progress in preanalytical sample processing techniques remains limited due to the diverse and complex nature of food matrices (64–66, 84–86). Magnetic nanoparticles (MNPs) have emerged as a valuable tool in foodborne pathogen detection as a pre-analytical sample processing tool in combination with culture independent detection assays as a means for rapid detection. For instance, MNPs with various functionalizations have been paired with biosensors, nucleic acid-based detection methods [polymerase chain reaction (PCR), loop-mediated isothermal amplification (LAMP), and strand displacement amplification], lateral flow assays, and microfluidic chips (136). While previous studies with chitosan-functionalized magnetic nanoparticles (F#1 MNPs) have involved plating samples for culture confirmation, no studies have integrated F#1 MNPs with the aim of decreasing enrichment protocol time requirements. Of particular importance, chitosan possesses antimicrobial properties that could affect microbial growth and requires further investigation for integration into enrichment protocols (105, 110, 111).

This study evaluated the use of F#1 MNPs in enrichment protocols to decrease the time needed to obtain an isolate. The author hypothesizes that integrating F#1 MNPs into the enrichment workflow will shorten the time required to obtain an isolate and decrease the volume of broth needed. This approach is expected to significantly improve the speed of foodborne pathogen isolation and detection, with important implications for public health and food safety practices.

Materials and Methods

Inoculum Preparation

The inoculums were prepared as in chapter 2. The inoculations for each experiment and batch are summarized in Tables 2.1 and 2.2.

Food Sample Preparation

Food samples were prepared as before (see chapter 2). One cotto salami sample screened as presumptive positive; this batch (Batch C of growth curve analysis) was excluded from analysis and is described further in the results section. The batches used in the romaine lettuce (‘lettuce”) sample testing consisted of both chopped and shredded ready-to-eat varieties, whereas only chopped was used in chapter 2 (150).

FDA Bacteriological Analytical Manual (BAM) and USDA Microbiology Laboratory Guidebook (MLG) Media Preparation

All media was procured and made as described in chapter 2 with the following exceptions: the phosphate buffered saline (PBS) was from VWR Life Science (Solon, OH) and xylose lysine deoxycholate (XLD) for the modified *Salmonella* protocols was from Neogen Corps (Lansing, MI).

Chitosan-Functionalized Magnetic Nanoparticles

The F#1 MNPs were obtained and resuspended as previously described in chapter 2.

Magnetic Nanoparticle Capture Protocol

Samples were removed from the refrigerator 45-60 minutes prior to extraction and verified to be at room temperature (19-22°C) by an infrared thermometer (Etekcity LaserGrip1080). Next, 100 mL of PBS was added to the sample, the lid secured, and the sample swirled twice to free the food matrix from the side of the reagent bottle. The samples were placed on a rocker (Bellco Glass Inc. Rocker Platform 7740-20020, Vinland, N.J.) set at "8" for one minute. The samples were then removed from the rocker and 1 mL of MNPs added (20 mg/mL). The samples were then swirled twice and placed back on the rocker for 10 minutes for strawberries and lettuce or 15 minutes for cotto salami. After this incubation, the bottle was removed from the rocker and the liquid portion removed from the lettuce and cotto salami and placed in a new, sterile 250 mL reagent bottle using a 25 mL serological pipette and 1000 µL pipette. All samples were then applied to a Spherotech® Fleximag Separator FMS-1000 Magnet (Lake Forest, IL) using three rubber bands for 20 minutes. The supernatant was removed using a 25 mL serological pipette and 1000µL pipette. For strawberry samples, the MNPs were resuspended with 1 mL of PBS and transferred to 100 mL of Universal Preenrichment Broth (UPB) in a sterile 250 mL reagent bottle. For lettuce and cotto salami, the broth [(Buffered Listeria Enrichment Broth (BLEB) or modified University of Vermont (UVM)] was added to the reagent bottle and swirled to resuspend the MNPs prior to incubation as described below. F#1 MNP solutions (100 µL) were plated on TSA and incubated at 35 ± 2°C for 48 ± 2 hours at the conclusion of each experimental day to confirm sterility and the absence of cross-contamination. All samples requiring incubation, with the exception of those in Rappaport-Vassiliadis (RV) and Tetrathionate (TT) broth, were incubated on a shaking incubator set to 150 rpm. RV and TT samples were incubated in a noncirculating water bath. Specific incubation times and temperatures are further described in the respective methods sections. For all samples with MNPs incubated in an enrichment broth, the sample was either inverted (in the case of RV and TT) or swirled three times to resuspend the MNPs that settled prior to spread or streak plating. All agar plates were incubated at 35 ± 2°C and evaluated for growth at 24 ± 2 hours unless otherwise described.

Bacterial Growth in Presence of Magnetic Nanoparticles

L. monocytogenes in cotto salami

L. monocytogenes was inoculated with an average of 29.2 ± 1.2 CFU onto cotto salami (Table 2.1) and refrigerated (4 ± 2°C) for 28 ± 1 hours. Samples were either processed for MNP extraction or the USDA MLG. Once MNP extraction was complete, either 25 or 100 mL of UVM was added. Samples processed via the USDA MLG were stomached [Stomacher Lab Blender 400 (Tekmar Company; Cincinnati, OH)] for 2 minutes with 25, 100, or 225 mL of UVM. In the case of 225 mL, approximately 125 mL was added to the sample, stomached for 2 minutes, then the remaining 100 mL was added to the sample and mixed. All samples were incubated at 30 ± 2°C. For Batch A, timepoint samples were collected every 90 minutes from hours 12-18, with an additional sample at hour 24. For Batch B, samples were collected every 90 minutes from hours 18-24. Batches C-F were sampled at hours 20, 23, and 26. For all batches at all timepoints, two spread plating (100 µL) and ten-fold serial dilutions were performed on Modified Oxford Agar (MOX) using the “drop-plate” technique with five replicates of 10µL drops (179, 180).

L. monocytogenes in romaine lettuce

L. monocytogenes was inoculated onto lettuce with an average inoculum of 23.8 ± 1.9 CFU (Table 2.1) and refrigerated (4 ± 2°C) for 30 ± 1 hours. Samples were either processed for MNP extraction or the FDA BAM with various broth amounts. Once MNP extraction was complete, either 25 or 100 mL of BLEB was added. Samples processed via the FDA BAM had 25, 100, or 225 mL of BLEB added. Samples were incubated at 30 ± 2°C, with BLEB supplement added at hour 4. For Batch A, sampling occurred every 90 minutes from hours 12-18 and at hour 24. Batches B-D were sampled at hours 14, 19, and 24. At each timepoint, two spread plating (100 µL) and ten-fold serial dilutions (using 10 µL drop plates with five replicates) were performed on Agar *Listeria* Ottavani and Agosti (ALOA).

Salmonella ser. Newport in strawberries and romaine lettuce

First, *Salmonella* ser. Newport was inoculated with 28.8 ± 6.7 CFU (Table 2.1) then refrigerated at 4 ± 2°C for 32 ± 1 hour. Samples were processed as with *L. monocytogenes* testing in romaine lettuce with the exception of UPB instead of BLEB with supplement. Next, the samples were incubated at 35 ± 2°C. Samples were taken every 60 minutes starting at hour 12 until hour 15; hour 13 was excluded due to a sampling error. At each time point, 100 µL spread plates and ten-fold serial dilutions using 10 µL drop plates were incubated on XLD.

Next, *Salmonella* ser. Newport was inoculated with 28.4 ± 5.6 CFU, 24.0 ± 4.2 CFU, and 19.0 ± 3.1 CFU (Table 2.1), for samples B-D, respectively. The inoculum for sample “D” was significantly different than samples A and B ($p = 0.0254$). The same refrigeration and broth amounts were used as above with timepoint sampling at hours 11, 13, and 15. At each time point, 100 µL spread plates and ten-fold serial dilutions using 10 µL drop plates were done on XLD.

Due to the issues encountered with accurate plate counts with *Salmonella* ser. Newport in strawberries (see results), growth curve comparisons were not completed in lettuce.

Modified Federal Protocol (USDA MLG and FDA BAM)

L. monocytogenes in cotto salami

For the first protocol, *L. monocytogenes* was inoculated on cotto salami at an average of 31.0 ± 0.3 CFU (Table 2.2) and refrigerated at 4 ± 2°C for 24 ± 1 hour. Pre-warmed UVM (25 mL at 30 ± 2°C) was added and incubated for 4 hours at 30 ± 2°C before undergoing MNP extraction (20 mg of MNP incubated for 15 minutes). After the MNPs were added to the UVM/cotto salami mixture, the supernatant containing UVM and MNPs was removed from the cotto salami and placed into a 50 mL conical tube. Next, two 100 µL samples were spread on MOX. The sample was then applied to the magnet for 5 minutes. The supernatant was removed using a 25 mL serological pipette with 500 µL added back and the sample vortexed to resuspend the MNPs. A 10 µL loop was used to make a streak plate on MOX. Afterwards the supernatant was returned to the sample and incubated for an additional 6 hours, with samples taken every 2 hours (sampling times: hours 4, 6, 8, and 10). Testing was completed on three batches with each batch analyzed in duplicate for a total of 6 samples.

For protocol 2, the samples were prepared as before with an average inoculum of 27.5 ± 2.1 CFU (Table 2.2) but prior to adding UVM, the samples underwent MNP extraction. Next, 25 mL of pre-warmed UVM was added to the MNPs, the samples were incubated at 30 ± 2°C and measurements taken at hours 6, 8, 10, 12, and 14 using the same plating method as protocol 1. The same batches of cotto salami (i.e., container) as before were used. All samples were reclosed and stored in a refrigerator at 4 ± 2°C between experiments. Each batch was analyzed in duplicate for a total of 6 samples.

L. monocytogenes and romaine lettuce

First, an average of 25.1 ± 3.1 CFU of *L. monocytogenes* was inoculated on lettuce (Table 2.2) and refrigerated at 4 ± 2°C for 24 ± 1 hour. Pre-warmed BLEB (100 mL at 30 ± 2°C) was added and incubated for 4 hours at 30 ± 2°C. MNP extraction was performed using 20 mg of MNP incubated for 10 minutes. The supernatant was then removed from the lettuce and placed into a 250 mL reagent bottle. Next two 100 µL samples were spread on ALOA, before the sample was applied to the magnet for 20 minutes. The supernatant was removed using a 25 mL serological pipette with 500 µL added back to the sample and mixed to resuspend the MNPs. A 10 µL loop was used to make a streak plate on ALOA then 25 mL of fresh BLEB with supplement was added to the sample. The sample was placed in a 50 mL conical tube and incubated for an additional 6 hours, with samples taken every 2 hours (sampling times: hours 4, 6, 8, and 10). Testing was completed on three batches with each batch run in duplicate for a total of 6 samples.

For the second protocol, the samples were prepared as before with an average inoculum of 23.1 ± 2.5 CFU (Table 2.2), but prior to adding BLEB, the samples underwent MNP extraction. Following the addition of 25 mL of pre-warmed BLEB, the samples were incubated at 30 ± 2°C and samples taken at hours 4 (prior to BLEB supplement), 8, 10, 12, and 14. Each batch was run in duplicate for a total of 6 samples. Different batches of lettuce were used for protocol 1 than protocol 2.

Salmonella ser. Newport and strawberries and romaine lettuce

Salmonella ser. Newport was inoculated on strawberries or lettuce and refrigerated at 4 ± 2°C for 24 ± 1 hour. The average inoculums were 22.6 ± 4.5 CFU and 79.1 ± 6.6 CFU for strawberries and lettuce, respectively (Table 2.2). Next, 25 or 100 mL of UPB prewarmed to 35 ± 2°C was added to the strawberries and lettuce, respectively, then the samples were incubated at 35 ± 2°C for 2 hours. MNP extraction was performed using 20 mg of MNP incubated for 10 minutes. The supernatant was then removed from the strawberries and placed into a 50 mL conical tube before the sample was applied to a magnet for 10 minutes and the supernatant removed. The liquid portion of the lettuce sample was removed and put into a new 250 mL reagent bottle and attached to the magnet for 20 minutes. Subsequently, half the samples had 10 mL of TT added and the other half had 10 mL of RV added. The samples were then transferred to a 15 mL conical tube and incubated in a water bath at 43 ± 0.2°C or 42 ± 0.2°C for TT or RV, respectively. At hours 2, 4, and 6 post-TT/RV (hours 4, 6, 8 total) the samples were removed from the water bath, inverted 3 times to resuspend the MNPs, and two 100 µL samples were spread on XLD. Next the sample was applied to a magnet for 3 minutes; supernatant was removed with a 5 mL serological pipette and 500 µL was added back to the sample and pulse vortexed at maximum speed for 3-5 seconds to resuspend the MNPs. A 10 µL loop was used to make a streak plate on XLD, after which the supernatant was returned to the sample and incubated. XLD was the only agar used based on current standards and given the preliminary work to develop the protocol (chapter 2) resulted in 100% agreement between the broth and plate combinations. Testing was completed on three batches with each batch analyzed in duplicate for a total of 6 samples.

Data Analysis

Inoculum comparisons among batches for growth curves were evaluated using a one-way ANOVA followed by Tukey's Honestly Significant Difference test, as needed. For the comparison of inoculations between the two *L. monocytogenes* testing protocols, a two-tailed *t*-test was performed. To assess the difference in doubling time between the FDA BAM and F#1 MNP protocols and broth amounts for *L. monocytogenes* in romaine lettuce, a nested ANOVA was conducted. All statistical analyses were completed using data analysis functions in Microsoft® Excel, with a significance level of $\alpha \leq 0.05$.

Results

Bacterial Growth in Presence of Magnetic Nanoparticles

L. monocytogenes in cotto salami

A total of six growth curves were produced (Figure 2.1). Batch C was excluded due to a presumptive false positive for the negative control, which was replated on ALOA and incubated for 48 hours. The Batch C MOX plates were incubated an additional 24 hours. At 48 hours, the incubated MOX plate colonies had an irregular shape and the patched colonies from MOX to ALOA showed no growth. Of the five remaining batches, the inoculations were not significantly different ($p = 0.8737$); the average inoculation was 29.2 ± 1.2 CFU.

Batch A was completed first, with timepoints included every 90 minutes from hours 12-18 and then at hour 24. Based on the results of Batch A, extended timepoints of every 90 minutes from hours 18-24 were used for Batch B. It was decided to sample during the recommended timepoints of the USDA MLG (hours 20-26) for comparisons among Batches C-F. There was batch-to-batch variation among the growth curves. Batches A, B, and D visually had similar growth curves which differed from Batches E and F. Doubling times were calculated for each protocol/broth combination (Table 2.3); however, some combinations did not yield a valid doubling time due to either a decline in CFUs or no CFUs present. A timepoint summary for Batches D-F are presented in Table 2.4. After autoclaving the samples (cotto salami in PBS), there was a subjective difference in turbidity that was not appreciated between these groups prior to autoclaving (Figure 2.2).

L. monocytogenes in romaine lettuce

The resultant growth curves (Figure 2.3) were used to calculate doubling times. A nested ANOVA revealed no significant difference in doubling times between the protocol used (FDA BAM and F#1 MNP) ($p = 0.1611$) or between the broth volumes (25 mL or 100 mL) ($p = 0.0914$). The 225 mL broth volume in the FDA BAM protocol was not included in this analysis as it was not tested with the F#1 MNPs (Table 2.5).

Salmonella ser. Newport in strawberries and lettuce

An initial growth curve for *Salmonella* ser. Newport in strawberries was completed; however, when repeated in triplicate, the plate counts were inconsistent due to the presence of competing microbes, with some samples having no distinguishable *Salmonella* colonies at various timepoints.

Modified Federal Protocol (USDA MLG and FDA BAM)

L. monocytogenes in cotto salami

The same batches of cotto salami were used for both experimental protocols with the second protocol taking place six days after the first. The cotto salami was appropriately refrigerated and used within the seven days recommended by the manufacturer. Inoculations between protocol 1 (31.0 ± 0.3 CFU) and 2 (27.5 ± 2.1 CFU) were significantly different ($p = 0.0476$).

The first experiment completed an initial 4 hours of enrichment in UVM followed by MNP extraction to remove the cotto salami matrix. The second protocol completed MNP extraction followed by enrichment in UVM. In the first protocol, 4/6 (66.7%) samples were positive at hour 10, which decreased to 2/6 (33.3%) at hour 24. This is in contrast to the second protocol where all samples were positive by hour 12 and remained positive at hour 24. Spread plates for both extraction protocols had a higher percentage of positive results than streak plates. However, no single technique was 100% positive (Table 2.6).

L. monocytogenes in romaine lettuce

Two modifications to the FDA BAM protocol were completed, one which involved MNP extraction after the initial 4-hour incubation in BLEB (prior to supplementation) and one that incorporated MNPs prior to any enrichment (Table 2.7). The average inoculum of the first protocol was 25.1 ± 3.1 CFU, compared to 23.1 ± 2.5 CFU of the second protocol was not significantly different ($p = 0.4153$).

When MNP extraction was completed after an initial 4-hour incubation (protocol 1), 5/6 (83.3%) samples were positive via either streak or spread plate. However, when

MNP extraction was done prior to enrichment in BLEB (protocol 2), only 1/6 (16.7%) samples were positive at 4 hours. By hour 8, protocol 1 had 4/6 (66.7%) positive samples by either plating method, compared to 5/6 (83.3%) samples via the second protocol. All samples in protocol 1 tested positive at hour 24. It is important to note that one sample in the second protocol was negative when replated at hours 24 and 48. When comparing streak plates to spread plates, the spread plates were positive more often throughout the duration of the experiment for both protocols, except at hour 14 in protocol 2 when both methods had 83.3% samples positive.

Salmonella ser. Newport in strawberries

The average initial inoculation of strawberry samples was 22.6 ± 4.5 CFU. Samples were incubated for 2 hours in UPB prior to MNP extraction then incubation in either RV or TT. The samples added to RV broth had 3/6 (50%), 5/6 (83.3%), and 6/6 (100%) samples positive at hours 4, 6, and 8, respectively. In contrast, samples added to TT broth only had 1/6 (16.7%) samples positive at hours 6 and 8 (the same sample) with all samples negative at hour 4. After 24 hours of incubation, the TT samples were replated, resulting in 5/6 positive samples. The remaining negative sample was positive when following the FDA BAM protocol (24-hour incubation in UPB followed by 24-hour incubation in RV and TT).

When evaluating the percentage of positive streak plates versus spread plates for the RV samples, more streak plates were positive at hours 4 and 6 than spread plates. However, all samples via either method were positive by hour 8. This data is summarized in Table 2.8.

Salmonella ser. Newport in romaine lettuce

Using the streak plate method, all samples (6/6) were positive in RV by hour 4 compared to 8 hours in TT (Table 2.9). The spread plate technique resulted in all (12/12) samples being positive by hour 6 in RV but only 11/12 (91.7%) samples positive in TT by hour 8. This remaining sample was positive at hour 24.

Discussion

This study evaluated the effect of chitosan-functionalized magnetic nanoparticles (F#1 MNPs) in regulatory enrichment protocols. Results demonstrated that the MNPs do not adversely affect the growth of *L. monocytogenes* in cotto salami or romaine lettuce or *Salmonella* ser. Newport in strawberries or romaine lettuce despite the antimicrobial properties of chitosan (105, 110, 111). Additionally, low volume enrichment showed no significant difference to current guidelines for the enrichment of *L. monocytogenes* in lettuce. This contrasts with cotto salami, where the primary factor to improving detection was likely the removal of the bulk of the matrix prior to incubation. However, due to the inability to calculate a doubling time for all protocol and broth volume combinations, a statistical comparison was not performed. Volume comparison testing in *Salmonella* ser. Newport was inconclusive due to the presence of competing microbes; however, all enrichment protocol modifications were completed with low volume (25 mL) enrichment resulting in positive samples. This agrees with Bosilevac as well as Koohmaraie and Samadpour who showed that using 1:0.1 to 1:3 (wt./vol.) broth volumes resulted in detection of pathogens such as *E. coli* and *Salmonella* spp. in various food matrices (181, 182).

Modifying the FDA BAM protocol by using MNPs to extract and remove *L. monocytogenes* from the romaine lettuce prior to enrichment in BLEB resulted in colony growth on ALOA after 8 hours of enrichment. By hour eight, 5/6 (83.3%) samples tested positive when using a 3-plate technique (two 100 µL spread plates and one 10 µL streak plate). However, 1/6 samples remained negative after 24 and 48 hours of enrichment, potentially due to either a lower-than-expected inoculum or differences in sample preparation, as this batch used shredded lettuce rather than chopped lettuce. *Lm* is relatively slow-growing and at low levels can be outcompeted by other microbes. The preliminary work to establish the lower limit of capture was done solely in chopped lettuce; however, as discussed in Chapter 2, *Lm* preferentially binds to cut edges of lettuce and shredded lettuce has an increased surface area of cut edges as compared to chopped lettuce, which may have led to a decrease in the available *Lm* for the MNPs to capture.

Performing the MNP extraction step prior to enrichment in cotto salami improved detection. This protocol resulted in all samples testing positive in 25 mL of UVM using a 3-plate technique by hour 12 compared to only 4/6 (66.7%) samples testing positive at hour 10, which decreased to 2/6 (33.3%) positive at hour 24 when MNP extraction was incorporated after enrichment began. These results highlight batch-to-batch variation, which is likely due to competing microbes and matrix composition. As was seen in Chapter 2 and the literature previously discussed, deli meats often show a wide range of microbial loads and are inconsistent between batches (158–160). Additionally, the matrix appearance was different between batches; given the high heat and pressure of autoclaving, the difference in appearance is likely attributed to different fat or protein contents. Further investigation is warranted to confirm the matrix composition effects on bacterial enrichment. Batches A and B had increased turbidity much like Batches A, B, and D in the growth curve analysis therefore they likely required a higher matrix-to-broth ratio (1:9) for optimal growth, which likely accounts for the false-negative results and decrease in positivity from hour 10 to 24 seen with the first protocol, which evaluated only 25 mL of UVM.

A shortcoming of UVM in the enrichment of stationary-phase *Lm* is false-negative results. A study by Sheth et al. compared BLEB, UVM, and Fraser Broth enrichment protocols for low levels of desiccation-stressed *Listeria* spp. from environmental surfaces and showed the recommended 23-26 hour enrichment in UVM was insufficient to consistently detect low levels of stationary-phase *Listeria* (183). Similarly, Ryser et al. reported false-negative results with the use of UVM in naturally contaminated raw refrigerated meats and poultry products (184). While these studies mainly attributed the false-negative results to the presence of competing microbes and strain-types, the presence of matrix components can also affect enrichment of bacteria (75). Also, in comparing multiple broths, Silk et al. showed UVM had a lag-phase duration of 10.29 ± 6.45 hours in injured *L. monocytogenes* (174). Therefore, the false-negative results observed in this study and the previously mentioned studies may be due to prolonged lag-phase and insufficient numbers of *L. monocytogenes* for detection.

Enrichment dynamic studies illustrate how the microbial diversity changes over time during enrichment (185–187). In the case of selective enrichment, microbial population diversity decreases, as was observed (Figure S2.1). However, with non-selective media, target pathogens can be outcompeted. In this study, competing microbes and batch-to-batch variation in strawberry samples precluded replication of growth curves for *Salmonella* ser. Newport when incubated in Universal Preenrichment Broth, a non-selective medium. Regardless, protocol modifications successfully shortened incubation periods, demonstrating the MNPs do not significantly impair the growth of *Salmonella* ser. Newport in these matrices.

In both the strawberry and lettuce modified protocol results, RV outperformed TT. This is consistent with previous reports of RV outperforming TT broth for the recovery of *Salmonella* spp. in foods with high microbial loads (175, 176, 188–190). Comparisons by Hammack et al. and June et al. showed a difference in broth efficiency based on incubation temperatures for low vs high microbial load foods; TT performed better than RV when incubated at 35°C in low microbial load foods, RV outperformed TT in high microbial load foods, and TT performed better at 43°C than 35°C (175, 176). Although TT in this study was incubated at 43°C, earlier research (chapter 2) indicated that MNPs do not capture all microbes present, which aligns with what was observed in the Alocilja Nano-Biosensor lab (99, 123, 124, 126, 127). This variability may alter the microbial load classification (e.g., low versus high), suggesting further testing at 35°C could provide valuable insights. Additionally, further investigation is needed to determine whether the components of the F#1 MNP react with any components in the enrichment broths, especially TT, due to the prolonged time to detection. For example, chitosan is studied as a means to remove iodine and iodide from wastewater and ferric oxide (the core of the MNPs) can also bind to iodine (191–194). Therefore, it is possible the F#1 MNPs had an adverse effect on the media, which subsequently effected bacterial growth kinetics in TT. Further study comparing the growth of *Salmonella* ser. Newport in the presence and absence of the F#1 MNP and/or the MNP components are needed to determine if any such reactions exist.

In the FDA BAM, RV and TT are also inoculated at different amounts (0.1 mL for RV versus 1.0 mL for TT) due to studies showing the benefit of different inoculation levels on isolation rates (195, 196). The lag-phase duration for competitors and *Salmonella* in TT also likely plays a significant effect in enrichment dynamics (196). In this study all MNPs were added to both broths and optimal broth amount was not evaluated. Further optimization of incubation temperature and ratio of MNP to broth volume is warranted.

The reasons for differences between the streak and spread plate techniques between *L. monocytogenes* and *Salmonella* ser. Newport and the matrices are complex and not fully explained by sample concentration alone. For streak plating, the samples were magnetized then reduced to a volume of 500 µL (a 20-fold reduction). A 10 µL loop was used leading to a plating of ~0.4x the original sample compared to 0.01x the original sample with the spread plate technique. Therefore, the streak plate theoretically contained 40 times more pathogen than the spread plate. Despite this, several factors may have contributed to the results. After magnetization and extraction, the samples were briefly vortexed; however, there may have been uneven distribution of the target prior to insertion of the loop. Alternatively, during incubation, the MNPs settled to the bottom of the conical tubes and while the tubes were inverted three times, this may have been insufficient in reforming MNP-pathogen complexes, requiring further optimization if streak plates are desired. Plating the entire 500uL and comparing the recovered target amount to that in the supernatant would identify if there was an issue with sample homogenization prior to streaking or if further MNP extraction optimization is needed to concentrate the pathogens to the theoretical amount during enrichment to effectively use a one-streak plate technique. Nevertheless, at low starting inoculations, single colonies were easily identifiable at all timepoints.

Conclusion

This study demonstrated the integration of MNPs into foodborne pathogen enrichment protocols to reduce incubation times and resources needed to obtain an isolate. The results indicate the MNPs do not negatively affect the growth of *Salmonella* ser. Newport or *L. monocytogenes* in romaine lettuce, strawberries, or cotto salami. By modifying enrichment protocols with the addition of MNPs, time to pathogen isolation and broth volume needed was reduced. This is essential since regulatory bodies continue to rely on culture-based testing for regulatory enforcement. Health protection agencies also continue to rely on the isolation of single- colonies for surveillance and trace-back and trace-forward requirements of outbreaks. Adding F#1 MNPs to already established protocols is promising for enhancing the speed of pathogen detection, thereby improving food safety and public health.

Tables

	L. monocytogenes		*Salmonella* ser. Newport	
Batch	Cotto Salami	Romaine Lettuce	Strawberries	Romaine Lettuce
A	29.4 ± 2.4	22.8 ± 4.0	28.8 ± 6.7^{AC}	100.0 ± 12.8
B	29.6 ± 4.8	21.6 ± 1.9	28.4 ± 5.6^{AC}	-
C	Excluded	25.4 ± 5.3	24.0 ± 4.2^{BC}	-
D	30.8 ± 7.0	25.2 ± 5.8	19.0 ± 3.1^{B}	-
E	27.6 ± 4.3	-	-	-
F	28.6 ± 4.6	-	-	-
Average	29.2 ± 1.2	23.8 ± 1.9	25.1 ± 4.6	-
ANOVA p-value	0.8737	0.4909	0.0254	-

Table 2.1: Growth curve inoculum amounts. The average inoculums (CFU/sample) ± standard deviation are presented by pathogen and matrix. Batch C for cotto salami was excluded from analysis due to a false-positive result on the negative control screening. For *Salmonella* ser. Newport in strawberries, Batch D is significantly different (p-value ≤ 0.05) than Batches A and B but not C (Tukey's Honestly Significant Difference Test).

	L. monocytogenes		*Salmonella* ser. Newport	
Batch	Cotto Salami	Romaine Lettuce	Strawberries	Romaine Lettuce
A	30.8 ± 6.2	27.0 ± 8.7	23.8 ± 3.4	86.7 ± 15.3
B	31.4 ± 6.3	26.8 ± 2.0	26.4 ± 10.3	75.7 ± 4.0
C	30.8 ± 2.9	21.6 ± 2.1	17.6 ± 3.6	75.0 ± 4.4
D	25.0 ± 7.4	20.2 ± 5.4	-	-
E	28.8 ± 5.7	24.6 ± 4.0	-	-
F	28.6 ± 5.3	24.4 ± 5.8	-	-
Average Protocol 1	31.0 ± 0.3	25.1 ± 3.1	22.6 ± 4.5	79.1 ± 6.6
Average Protocol 2	27.5 ± 2.1	23.1 ± 2.5	-	-
t-test p-value	0.0476	0.4153	-	-

Table 2.2: Protocol modification inoculum amounts. The average inoculums (CFU/sample) ± standard deviation are presented by pathogen and matrix. For *L. monocytogenes*, two protocols were tested. Protocol 1 consisted of Batches A-C and protocol 2 consisted of Batches D-F. For cotto salami, the same package of cotto salami was used for samples A and D, B and E, and C and F. There was a significant difference (p-value ≤ 0.05) between the inoculums for protocols 1 and 2 for cotto salami.

Doubling Time (min) of *L. monocytogenes* in Cotto Salami					
	USDA MLG			F#1 MNP	
	25 mL	100 mL	225 mL	25 mL	100 mL
Batch A	37.88	123.78	88.87	60.27	66.65
Batch B	-	-	-	50.97	60.27
Batch D	-	-	-	330.07	61.34
Batch E	-	198.04	53.32	50.59	54.58
Batch F	57.28	49.87	55.45	54.15	60.27

Table 2.3: Doubling time (minutes) of *L. monocytogenes* in cotto salami. Dashes (-) indicate the doubling time could not be calculated due to the growth curve output. The USDA Microbiology Laboratory Guidebook (MLG) protocol was tested using 25, 100, and 225 mL of modified University of Vermont media (UVM) whereas the chitosan-functionalized magnetic nanoparticles (F#1 MNPs) were only incubated in 25 or 100 mL of UVM. Batch C was eliminated from the study due to a presumptive positive result on the negative control.

Timepoint Growth Summary of *L. monocytogenes* in Cotto Salami (Log_{10} CFU/mL)						
	USDA MLG			F#1 MNP		
	25 mL	100 mL	225 mL	25 mL	100 mL	
Batch D	-	-	1.81	2.84	4.36	Hr 20
Batch E	6.83	4.92	5.42	5.73	4.26	
Batch F	4.97	5.24	4.91	5.01	3.41	
Batch D	1.00	1.18	2.34	2.83	5.21	Hr 23
Batch E	4.54	5.18	6.53	6.72	5.19	
Batch F	5.93	6.31	6.10	5.93	4.30	
Batch D	-	1.18	2.32	3.17	6.13	Hr 26
Batch E	4.58	5.48	7.45	7.87	6.25	
Batch F	6.86	7.41	6.87	7.02	5.21	

Table 2.4: Timepoint growth summary of *L. monocytogenes* in cotto salami. The log_{10} CFU/mL were calculated for each batch and protocol-broth combination at hours 20, 23, and 26. Dashes (-) indicate no visible growth. USDA MLG: USDA Microbiology Laboratory Guidebook. F#1 MNP: Chitosan-functionalized Magnetic Nanoparticles.

Doubling Time (min) of *L. monocytogenes* in Romaine Lettuce					
	FDA BAM			F#1 MNP	
	25 mL	100 mL	225 mL	25 mL	100 mL
Batch A	58.10	49.16	73.74	55.01	64.42
Batch B	71.46	58.74	65.39	61.89	64.78
Batch C	119.51	69.31	71.46	63.01	67.96
Batch D	96.27	70.73	64.18	60.80	67.96

Nested ANOVA (25 and 100 mL) - *L. monocytogenes* in Romaine Lettuce						
Source of Variation	*SS*	*df*	*MS*	*F*	*P-value*	*F crit*
Protocol	478.05	1	478.05	2.23	0.1611	4.7472
Broth Amount	1260.08	2	630.038	2.9392	0.0914	3.8852

Table 2.5: Doubling time (minutes) of *L. monocytogenes* in romaine. The FDA Bacteriological Analytical Manual (BAM) protocol was tested using 25, 100, and 225 mL of Buffered *Listeria* Enrichment Broth (BLEB) whereas the chitosan-functionalized magnetic nanoparticles (F#1 MNPs) were only incubated in 25 or 100 mL of BLEB. Both protocols received BLEB supplementation at hour 4. A nested ANOVA comparing the protocols (BAM and F#1 MNP) and broth amounts (25 and 100 mL only) showed no significant differences based on protocol or broth amount (p-value ≤ 0.05).

USDA MLG Protocol Modification - *L. monocytogenes* in Cotto Salami								
Time (hrs)	4	6	8	10	12	14	24	Protocol
Number of Positive Samples (n = 6)	0	0	3	4	N/A	N/A	2	1: UVM incubation then MNP extraction
Streak Plates Positive (n = 6)	0	0	0	2	N/A	N/A	2	
Spread Plates Positive (n = 12)	0	0	4	5	N/A	N/A	N/A	
Number of Positive Samples (n = 6)	N/A	1	2	5	6	6	6	2: MNP extraction then UVM incubation
Streak Plates Positive (n = 6)	N/A	0	0	3	3	5	6	
Spread Plates Positive (n = 12)	N/A	1	2	8	10	11	N/A	

Table 2.6: USDA Microbiology Laboratory Guidebook (MLG) protocol modification comparison for *L. monocytogenes* in cotto salami. In protocol 1, cotto salami was incubated in 25 mL of prewarmed modified University of Vermont Media (UVM) and then magnetic nanoparticle (MNP) extraction was performed at hour 4. In protocol 2, MNP extraction was completed and then the MNP-bacteria complexes were incubated in 25 mL prewarmed UVM. At each timepoint three samples were plated. First, 2x spread plates using 100 µL were plated onto Modified Oxford Agar (MOX). Next, a magnet was applied to the sample and the supernatant removed, with 500 µL added to resuspend the MNPs then 1x 10 µL loop was streaked onto MOX prior to returning the remaining supernatant for continued incubation. Not applicable (N/A) denotes timepoints not tested for the protocol.

FDA BAM Protocol Modification - *L. monocytogenes* in Romaine Lettuce								
Time (hrs)	4	6	8	10	12	14	24	Protocol
Number of Positive Samples (n = 6)	5	0	4	4	N/A	N/A	6	1: BLEB incubation then MNP extraction
Streak Plates Positive (n = 6)	1	0	1	0	N/A	N/A	6	
Spread Plates Positive (n = 12)	4	0	3	7	N/A	N/A	N/A	
Number of Positive Samples (n = 6)	1	N/A	5	5	5	5	5	2: MNP extraction then BLEB incubation
Streak Plates Positive (n = 6)	0	N/A	2	4	4	5	5	
Spread Plates Positive (n = 12)	1	N/A	9	10	10	10	N/A	

Table 2.7: FDA Bacteriological Analytical Manual (BAM) protocol modification comparison for *L. monocytogenes* in romaine lettuce. In protocol 1, romaine lettuce was incubated in 100 mL of prewarmed Buffered *Listeria* Enrichment Broth (BLEB), and then magnetic nanoparticle (MNP) extraction was performed at hour 4 then the MNP-bacteria complexes were added to 25 mL of prewarmed BLEB with supplement. In protocol 2, MNP extraction was completed and then the MNP-bacteria complexes were incubated in 25 mL prewarmed BLEB with supplementation at hour 4. At each timepoint, three samples were plated. First, 2x spread plates using 100 μL were plated onto Agar *Listeria* Ottaviani and Agosti (ALOA). Next, a magnet was applied to the sample and the supernatant removed, with 500 μL added to resuspend the MNPs then 1x 10 μL loop was streaked onto ALOA prior to returning the remaining supernatant for continued incubation. One sample in protocol 2 remained negative when plated at 24 and 48 hours. Not applicable (N/A) denotes timepoints not tested for the protocol.

FDA BAM Protocol Modification – *Salmonella* ser. Newport in Strawberries				
Time (hrs)	4	6	8	Broth
Number of Positive Samples (n = 6)	3	5	6	Rappaport Vassiliadis
Streak Plates Positive (n = 6)	3	4	6	
Spread Plates Positive (n = 12)	1	7	12	
Number of Samples Positive (n = 6)	0	1	1	Tetrathionate with 0.1% brilliant green
Streak Plates Positive (n = 6)	0	1	1	
Spread Plates Positive (n = 12)	0	0	0	

Table 2.8: FDA Bacteriological Analytical Manual (BAM) protocol modification comparison for *Salmonella* ser. Newport in strawberries. Samples were incubated in 25 mL of prewarmed Universal Preenrichment Broth (UPB) for 2 hours, then magnetic nanoparticle (MNP) extraction was performed. The sample was then either added to Rappaport Vassiliadis Broth (RV) or Tetrathionate Broth with 0.1% brilliant green (TT) and incubated. At hours 2, 4, and 6 post-TT/RV (hours 4, 6, 8 total) two 100 µL samples were spread on xylose lysine deoxycholate agar (XLD), then the sample was applied to a magnet for 3 minutes, supernatant removed with a 5 mL serological pipette with 500 µL added back with the sample vortexed to resuspend the MNPs. A 10 µL loop was used to make a streak plate on XLD. The supernatant was then returned to the sample and incubated.

FDA BAM Protocol Modification – *Salmonella* ser. Newport in Romaine Lettuce				
Time (hrs)	4	6	8	Broth
Number of Positive Samples (n = 6)	6	6	6	Rappaport Vassiliadis
Streak Plates Positive (n = 6)	6	6	6	
Spread Plates Positive (n = 12)	6	12	12	
Number of Samples Positive (n = 6)	3	5	6	Tetrathionate with 0.1% brilliant green
Streak Plates Positive (n = 6)	2	4	6	
Spread Plates Positive (n = 12)	5	9	11	

Table 2.9: FDA Bacteriological Analytical Manual (BAM) protocol modification comparison for *Salmonella* ser. Newport in romaine lettuce. Samples were incubated in 100 mL of prewarmed Universal Preenrichment Broth (UPB) for 2 hours, then MNP extraction was performed. The sample was then either added to Rappaport Vassiliadis Broth (RV) or Tetrathionate Broth with 0.1% brilliant green (TT) and incubated. At hours 2, 4, and 6 post-TT/RV (hours 4, 6, 8 total) two 100 μL samples were spread on xylose lysine deoxycholate agar (XLD), then the sample was applied to a magnet for 3 minutes, supernatant removed with a 5 mL serological pipette with 500 μL added back with the sample vortexed to resuspend the MNPs. A 10 μL loop was used to make a streak plate on XLD. The supernatant was then returned to the sample and incubated.

Figures

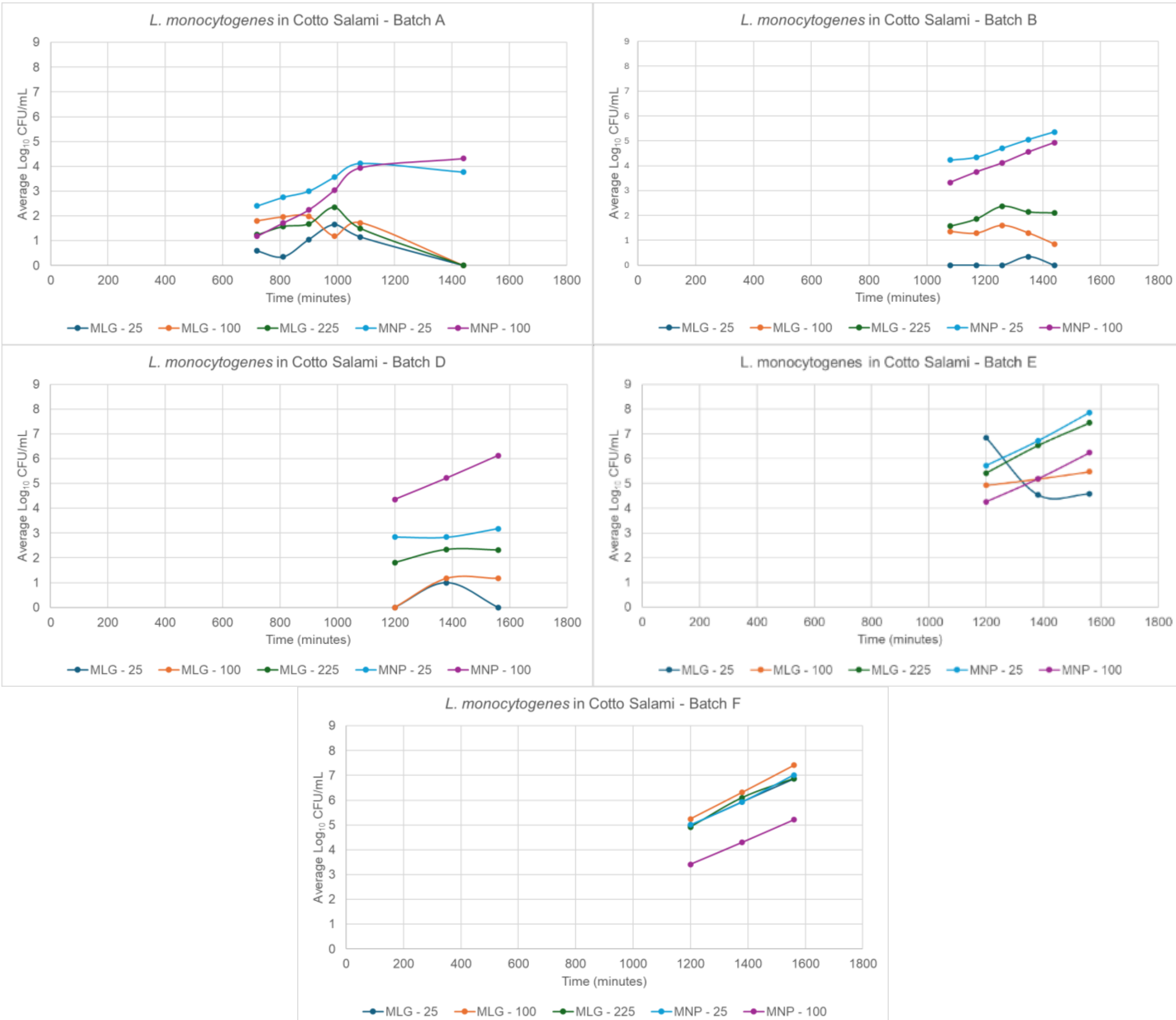

Figure 2.1: Growth curves of *L. monocytogenes* in cotto salami. Batches A, B, and D-F are represented; Batch C was eliminated due to a presumptive positive result on the negative control. Batch A was tested every 90 minutes from hours 12-18 and then hour 24. Batch B was tested every 90 minutes from hours 18-24. Batches D-F were tested at hours 20, 23, and 26. Each batch consisted of one sample tested for each protocol [USDA Microbiology Laboratory Guidebook (MLG) or Magnetic Nanoparticle (MNP) extraction] and volume combination (25, 100, or 225 mL).

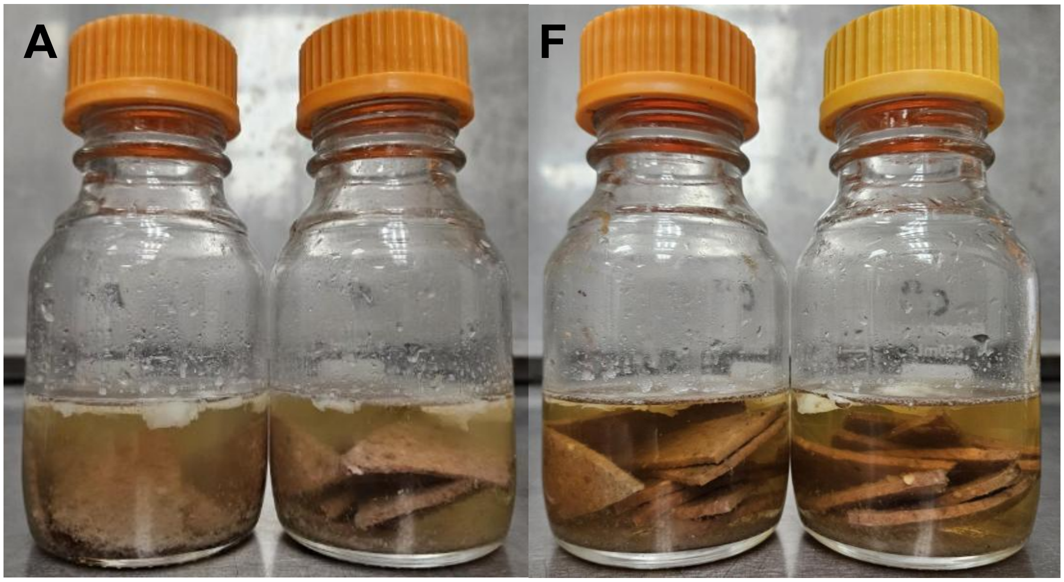

Figure 2.2: Comparison of samples post-autoclave. Batch A (left) shows an increase in turbidity and fat content within the liquid portion after autoclaving whereas Batch F had subjectively less turbidity and fat globules.

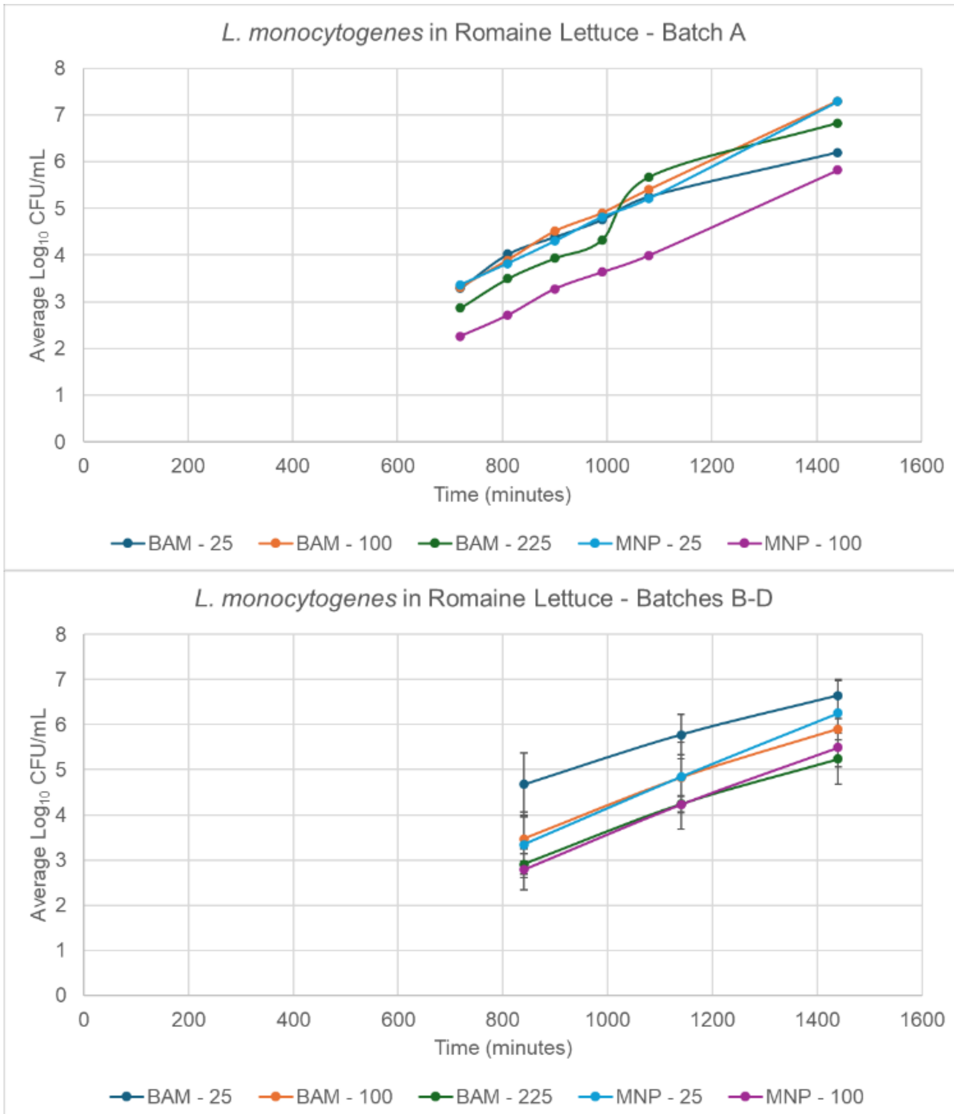

Figure 2.3: Growth curves of *L. monocytogenes* in romaine lettuce. Batch A was tested every 90 minutes from hours 12-18 and then hour 24. Batches B-D were tested at hours 14, 19, and 24. Each batch consisted of one sample tested for each protocol [FDA Bacteriological Analytical Manual (BAM) or Magnetic Nanoparticle (MNP) extraction] and volume combination (25, 100, or 225 mL).

CHAPTER 4: CAPTURE SPECIFICITY OF CHITOSAN-FUNCTIONALIZED MAGNETIC NANOPARTICLES IN ROMAINE LETTUCE

Abstract

The rapid detection of foodborne pathogens in complex food matrices remains a critical challenge in food safety. This study evaluated the broad-spectrum microbial capture capabilities of chitosan-functionalized magnetic nanoparticles (F#1 MNPs), which are hypothesized to non-selectively bind to bacteria, archaea, fungi, and viruses. Shallow shotgun metagenomic sequencing using the F#1 MNPs and romaine lettuce as a representative food matrix demonstrated the ability of the F#1 MNPs to capture gram-positive, gram-negative, and cell wall-less bacteria; archaea; fungi; and RNA and DNA viruses. This study highlights the potential of the F#1 MNPs as a preanalytical sample processing tool for pathogen-agnostic and multi-pathogen detection in food safety.

Introduction

The prevention of foodborne pathogen outbreaks relies on the ability to detect a wide spectrum of microorganisms in complex samples. The CDC recognizes 31 major foodborne pathogens (1). These include 21 bacterial species (both gram-positive and gram-negative), five non-enveloped RNA viruses, and five parasites. While viruses account for 59% of foodborne illnesses (predominantly norovirus), bacteria are responsible for 64% of foodborne related deaths, followed by parasites (25%) and viruses (12%) (1). The detection and prevention of foodborne pathogens presents unique challenges due to the diversity of causative agents and food matrix complexity. The rapid and comprehensive detection of foodborne pathogens remains a critical challenge in food safety.

Magnetic nanoparticles (MNPs) are emerging as tools for microbial capture and concentration in various fields, such as food safety. MNPs have a high surface-to-volume ratio, superparamagnetic properties, and are easily functionalized making them useful in a wide range of applications (116–118). However, current research uses MNPs against specific targets without understanding the full spectrum range of microorganisms the functionalizations can capture (93, 136, 197). This limits their application in broad-spectrum detection scenarios, such as for prevention or detecting an unknown organism.

The chitosan-functionalized MNPs (F#1 MNPs) developed by the Alocilja Nano-Biosensors Laboratory at Michigan State University represent an approach to broad-spectrum microbial capture. Previous studies by the Nano-Biosensors Lab combined with the data presented in chapters 2 and 3 show the F#1 MNPs capture a wide range of microbes (99, 123, 124, 126, 127). The chitosan component is hypothesized to electrostatically bind to the net negative bacterial membrane charge and surface receptors on bacteria and parasites, viral capsid proteins on viruses, and negatively charged phospholipids of the fungal plasma membrane (99, 102, 103, 105–107, 112, 113, 115, 125–127, 198–203). This non-selective binding mechanism suggests the F#1 MNPs can be used as a comprehensive approach to microbial capture in complex food matrices.

There remains a need for non-selective, broad-spectrum methods capable of capturing the diverse microbial taxa in complex matrices responsible for foodborne outbreaks. This study aims to evaluate the broad-spectrum capture capabilities of F#1 MNPs across multiple taxa in romaine lettuce samples, a common vehicle for foodborne pathogens with a highly diverse microbiome (63, 204–206). The study used 3 Gb shallow shotgun metagenomic sequencing to characterize the organisms F#1 MNPs can capture both in the presence and absence of spiked *Salmonella* ser. Newport and *Listeria monocytogenes*.

The nonselective nature of F#1 MNPs has the potential to significantly impact food safety by providing a versatile pre-analytical sample processing technique. By combining broad-spectrum capture with specific detection assays, F#1 MNPs could offer a comprehensive approach to foodborne pathogen detection and outbreak prevention.

Materials and Methods

<u>Inoculum Preparation</u>

The inoculum was prepared as in chapter 2. The average inoculums were 3.61 ± 0.04 $\log_{10}$ CFU/sample for *L. monocytogenes* and 3.46 ± 0.07 $\log_{10}$ CFU/sample for *Salmonella* ser. Newport. The inoculations for each batch are provided in Table 3.1.

<u>Romaine Lettuce Sample Preparation</u>

Three batches of romaine lettuce were purchased from local supermarkets. Each batch consisted of three samples (25 ± 1 g); one with 100 μL of PBS added (Group 1 – G1), one with 100 μL of ~4.61 $\log_{10}$ CFU/mL of *Listeria monocytogenes* added (Group 2 – G2), and one with 100 μL of ~4.46 $\log_{10}$ CFU/mL of *Salmonella* ser. Newport added (Group 3 – G3). Samples were then refrigerated (4 ± 2°C) for 24 ± 1 hours. Batches were screened for the pathogen of interest using the FDA Bacteriological Analytical Manual (BAM) protocol. Two batches of lettuce screened presumptive positive for

Salmonella spp. and are described further in the results section. Batches A and C were chopped, whereas Batch B was shredded (150).

FDA Bacteriological Analytical Manual (BAM) Media Preparation

All media were prepared as in chapter 2 with the following exceptions: the source of Xylose Lysine Deoxycholate (XLD) was Neogen Corps (Lansing, MI) and Bismuth Sulphite (BS) was not used in the negative control testing.

Chitosan-functionalized Magnetic Nanoparticles (F#1 MNPs)

The F#1 MNPs were resuspended as in chapter 2 except the source of the molecular grade water was Sigma Life Science, Switzerland.

F#1 MNP Extraction Protocol

The same optimized MNP extraction protocol from chapter 2 was used with a single exception. An incubation time of 10 min, as opposed to 15 min, was used for *Salmonella* ser. Newport to maintain consistency with the negative control incubation time of 10 min.

Aerobic Plate Count (APC) of F#1 MNP Capture

Samples were prepared as in chapter 2 except only 100 mL of PBS was used. Two batches of chopped lettuce (independent of those used for sequencing) were tested in duplicate. Samples underwent MNP extraction as described above. The MNPs were resuspended with 1mL of PBS. Ten-fold serial dilutions of the MNP and supernatant were prepared using PBS, spread onto TSA, and incubated at 35 ± 2°C for 48 ± 2 hours for manual aerobic plate count. Results were analyzed with a two-sample *t*-test with significance ≤ 0.05.

DNA Extraction

After MNP extraction, the MNPs were resuspended in 1 mL of PBS (VWR Life Science; Solon, OH) and centrifuged. The supernatant was decanted and 1.5mL of PBS added and vortexed. The sample was centrifuged again, supernatant decanted and then re-centrifuged to remove the remaining supernatant. Next 180 μL of ATL (Qiagen) was added to each sample and vortexed. All centrifuge steps were performed at 13,000 g for 1 min and all vortex steps were performed using maximum speed for 5 seconds.

The sample was then transferred to a 2 mL bead lysis tube containing 180 ± 10 mg of 0.1 mm Zirconia beads and lysed at 4 m/s for 30 seconds, paused for 30 seconds, then homogenized again at 4 m/s for 30 seconds using a FisherBrand Bead Mill 24. The remaining steps were done according to the Qiagen DNeasy® Blood & Tissue Handbook (06/2023) beginning with step 4 on page 55, except the sample was incubated for 60 (vs 30) minutes and vortexed every 15 minutes. The sample was removed from the bead lysis tube following centrifugation at the conclusion of all heating steps. The Zymo Research Genomic DNA Clean & Concentrator®-10 kit was followed as directed. The concentration and quality of DNA was measured on a Qubit® and NanoDrop, respectively.

Shotgun Metagenomic Sequencing and Data Analysis

Novogene (Sacramento, CA) performed the library construction, sequencing, and bioinformatics analysis at 3 Gb of depth using their standard protocol. Briefly, for library construction, a Covaris ultrasonic disruptor was used to randomly fragment DNA segments into ~350bp sequences, the ends were repaired, A-tails added, and sequencing adapters ligated prior to purification. Next, samples were sequenced using a NovaSeq X Plus with paired-end 150 bp sequencing. Low quality reads and adaptors were trimmed using fastp. Romaine lettuce (*Lactuca sativa*) DNA reads were aligned using Bowtie2 then removed. Next, sequences were compared using Kraken2 and species annotation results refined with Bracken.

Results

Two batches (Batches B and C) screened presumptive positive for *Salmonella* spp.; however, these colonies predominately grew on Hektoen Enteric (HE) agar with minimal growth on XLD. On both HE and XLD, the colonies were yellow with black centers. This is in contrast to the appearance of *Salmonella* ser. Newport which is blue-green with black centers on HE and red with black centers on XLD. Further testing on lysine iron agar or triple sugar iron was not conducted.

Comparison of aerobic plates counts (APC) between the MNP capture and remaining supernatant showed the average APC for the MNPs was 4.71 ± 0.44 $\log_{10}$ CFU/mL whereas the supernatant was 3.33 ± 0.40 $\log_{10}$ CFU/mL (p-value: 0.0012). The log reduction between the MNP capture and supernatant per mL was 1.38 ± 0.42.

The abundance clustering heatmap and summary table shows the broad-spectrum capture capabilities of F#1 MNPs (Figure 3.1 and Table 3.2). The MNPs extracted gram-positive, gram-negative, and cell wall-less bacteria, as well as archaea. Among eukaryotes, only fungi are represented. The MNPs also showed versatility in virus capture, binding to a range of viral types including enveloped RNA and DNA viruses, non-enveloped DNA viruses, and bacteriophages. Figure 3.2 shows the relative abundance of phyla and genera in the samples. The phyla Pseudomonadota followed by Bacillota were the most prevalent across all groups. Within these phyla, *Pseudomonas* and *Bacillus* were the predominant genera represented, respectively.

The presence of *Salmonella* ser. Newport (SSN) or *L. monocytogenes* (*Lm*) did not significantly change the species captured by F#1 MNP. The analysis by Novogene returned 3301 distinct operational taxonomic units (OTUs). *Salmonella enterica* was identified in all samples except lettuce sample A spiked with *Salmonella* ser. Newport and lettuce sample A spiked with *L. monocytogenes. L. monocytogenes* was only identified in all three lettuce C samples regardless of spike status (Table 3.3).

Based on taxa abundance, there was no significant difference using analysis of similarities (ANOSIM) at any taxonomic level between any group combinations (G1 – spiked with PBS, G2 – spiked with *L. monocytogenes*, G3 – spiked with *Salmonella* ser. Newport) (Table 3.4). The metagenomeSeq analysis showed significant differences only at the species level for *Megavirus chilense* and *Tepidibacter hydrothermalis*, both of which were significantly more abundant in G1 compared to G2 (Figure S3.1). There was no significant result in the Kraken-LEfSe analysis.

While batch-to-batch variation was not statistically compared, the composition of microorganisms F#1 MNPs captured from Batch A appears to differ from Batches B and C (Figure 3.3). Batch A consisted of conventional chopped lettuce sourced from one geographic region of the US, while Batches B and C were both organic lettuce from the same location – Batch B was shredded and Batch C was chopped. Batches B and C originated from a different, yet geographically proximate region of the U.S. to Batch A. All batches were processed in the same growing season.

Discussion

Preventing and detecting foodborne outbreaks depends on the ability to detect a broad range of microorganisms in complex food matrices. This study highlights the potential of chitosan-functionalized magnetic nanoparticles (F#1 MNPs) as a broad-spectrum approach to microbial capture. This is especially useful in food safety when pathogen-agnostic and multi-organism screening/testing is warranted. This was demonstrated by the representation of gram-positive, gram-negative, cell wall-less bacteria, fungi, archaea, and viruses in the shotgun metagenomic sequencing and analysis. This range of microorganisms is consistent with the hypothesized interaction of chitosan with these taxa. Additionally, the MNPs effectively concentrated bacteria, yielding a significantly higher APC of 4.71 ± 0.44 $\log_{10}$ CFU/mL compared to 3.33 ± 0.40 $\log_{10}$ CFU/mL in the supernatant (p-value: 0.0012). This represents a 1.38 ± 0.42 $\log_{10}$ increase in bacterial concentration per mL, which equates to 24.0 ± 6.3 times concentration for the MNP-captured samples compared to the supernatant, demonstrating the ability of the MNPs to capture and concentrate microorganisms.

The analysis did not detect the presence of parasite DNA extracted with the MNPs; however, it remains unknown whether parasites were present but not captured by the MNPs or if none or only a small quantity were present. The parasite *Toxoplasma gondii* is recognized as one of the top five foodborne pathogens leading to hospitalization and death in the U.S. (1, 2). A review by Cheraghipour et al. compiled several studies demonstrating the antiparasitic effects of chitosan (203). However, neither the review nor the associated literature provides a definitive binding mechanism of action for chitosan to *T. gondii*. *Giardia duodenalis* (formerly *G. lamblia* or *G.*

intestinalis) is the most prevalent foodborne parasite (1). Yarahmadi et al. demonstrated that chitosan exhibits antigiardial properties, though the exact mechanism of action remains unknown. Shapiro et al. reported the presence of a negative charge present on *T. gondii* oocysts, while González-Robles et al. demonstrated the associated negative charge of *Giardia lamblia* trophozoites (207, 208). These studies further support the potential for chitosan's positive charge to bind to the negatively charged surfaces of foodborne parasites, similar to its proposed binding mechanism in bacteria. Based on these properties, it is hypothesized that the F#1 MNPs have the potential to bind and extract parasites. To initially test this hypothesis, parasitic oocysts can be placed in a buffered solution, such as PBS, followed by applying the MNP capture protocol. Transmission electron microscopy can be used to visualize binding. If binding occurs, then the next step would involve testing in food matrices to determine the value of F#1 MNPs as a preanalytical processing tool for detecting foodborne parasites.

The five most common foodborne viruses (Norovirus, Hepatitis A, Astrovirus, Rotavirus, and Sapovirus) are all non-enveloped RNA viruses. While sequencing revealed both DNA and RNA and enveloped and non-enveloped viruses, no non-enveloped RNA viruses were sequenced. Similarly to enhancing the understanding of F#1 MNPs as a preanalytical processing tool for detection of foodborne parasites, similar studies are needed for foodborne viruses.

Previous microbiome studies of romaine lettuce show bacteria are predominantly present with fungi, viruses, and archaea present at lower levels. The predominant phyla on the plant phyllosphere are typically Pseudomonoadota (or Proteobacteria), Bacillota (or Firmicutes), and Actinomycetota (or Actinobacteria) (204, 209, 210). This is in agreement with the microorganisms extracted and sequenced in this study with the three dominant phyla being Pseudomonadota followed by Bacillota and Actinomycetota. One limitation of this study was the lack of sequencing of the lettuce microbiome as a comparison to determine whether the F#1 MNPs captured a representative sample of the microbiome.

Previous studies show microbiome changes based on the organisms present, geography, season, and processing (82, 206, 211, 212). However, the only significant difference detected between groups was at the species level for *Megavirus chilense* and *Tepidibacter hydrothermalis*. This stability suggests the presence of pathogens at low levels does not significantly affect the overall capture ability of F#1 MNPs. This could be due to the pathogens of interest being present at relatively lower abundances, Batch A being distinct from Batches B and C masking significance, or an insufficient incubation time to observe a resultant change. Gu et al. showed *Lm* inoculated on lettuce influenced the bacterial communities based on the inoculum amount and storage temperature and time (206). This study also showed wide variation in samples taken from different retail bags of the same production batch. This means Batch A may not be significantly different from Batches B and C; therefore, increasing the sample size may further identify differences between batches. Exploring this information further may determine whether the presence of pathogens at higher levels effects the capture ability of F#1 MNPs. However, the aim of this study was to characterize the ability of the F#1 MNPs to capture a diverse range of microorganisms.

Sequencing data showed false-negative and false-positive results for the targets of interest in both the spiked and non-spiked samples. Limitations of current bioinformatic analysis pipelines for metagenomic sequencing can lead to these discrepancies. Novogene uses Kraken2 combined with Bracken; however, a limitation of this pipeline is its potential for misclassification at the species level when genomes from different species or genera are highly conserved (213). Furthermore, the F#1 MNPs are capable of capturing a variety of microbes in addition to the targets, as shown by the abundance clustering heatmap and phylogenetic analysis. Although the target pathogens were spiked at ~3.5 $\log_{10}$ CFU, the relative abundance for the positive samples was consistently 10^{-4} and 10^{-6} for *S. enterica* and *L. monocytogenes*, respectively. This suggests that the initial spiking levels accounted for only a small fraction of the total microbial community; therefore, increasing the sequencing depth would improve coverage. The false-positive results could be due to the presence of DNA without culturable bacteria. Or, in the case of the *Salmonella* samples that were screened as presumptive positives (Batches B and C), the presence of *S. enterica* could represent an atypical strain. This further demonstrates the need to combine the F#1 MNP extracts with selective methods to amplify target pathogens to detectable limits.

Conclusion

This study, using laboratory-based spike-and-recovery protocols, demonstrates the potential applicability of F#1 MNPs in preanalytical sample processing for food safety testing. The MNPs captured bacteria, archaea, fungi, and viruses, highlighting their applicability in pathogen-agnostic and multi-pathogen detection methods, which are critical in food safety.

Tables

Batch	*L. monocytogenes*	*Salmonella* ser. Newport
A	3.59 ± 0.08	3.54 ± 0.04
B	3.66 ± 0.07	3.40 ± 0.06
C	3.59 ± 0.06	3.45 ± 0.11
Average	3.61 ± 0.04	3.46 ± 0.07

Table 3.1: Average inoculation amounts ($\log_{10}$ CFU/sample) for *L. monocytogenes* and *Salmonella* ser. Newport on romaine lettuce for metagenomic study. The average inoculums per batch ± standard deviation are presented by pathogen.

Domain/Entity	OTUs - Phylum	OTUs - Genus
Bacteria	30	1081
Archaea	4	37
Eukarya	3	55
Virus	6	41
Total	43	1214

Table 3.2: Number of distinct operational taxonomic units (OTUs) at the phylum and genus level. At both levels, Bacteria, Archaea, Eukarya, and Viruses were present. For the domain Eukarya, only fungi were identified.

Sample Identification	OTUs	Rank of *S. enterica*	Relative Abundance of *S. enterica*	Rank of *L. monocytogenes*	Relative Abundance of *L. monocytogenes*
Lettuce A	594	341	1.31×10^{-4}	NS	NS
Lettuce B	1085	162	2.23×10^{-4}	NS	NS
Lettuce C	2325	297	2.06×10^{-4}	1836	3.25×10^{-6}
Lettuce spiked with *Lm* A	316	NS	NS	NS	NS
Lettuce spiked with *Lm* B	858	120	4.43×10^{-4}	NS	NS
Lettuce spiked with *Lm* C	2489	338	1.50×10^{-4}	1692	3.09×10^{-6}
Lettuce spiked with SSN A	286	NS	NS	NS	NS
Lettuce spiked with SSN B	1283	92	8.28×10^{-4}	NS	NS
Lettuce spiked with SSN C	1932	241	2.38×10^{-4}	1491	3.34×10^{-6}

Table 3.3: Sequencing of target species by sample. There was a total of 3301 distinct operational taxonomic units (OTUs). The number of OTUs per sample are represented along with the rank and relative abundance of the target species. Samples were not spiked, spiked with *L. monocytogenes* (*Lm*), or spiked with *Salmonella* ser. Newport (SSN). NS: Not sequenced.

	G1-G2		G1-G3		G2-G3	
	R-value	P-value	R-value	P-value	R-value	P-value
Kingdom	-0.22222	1	-0.25926	1	-0.22222	1
Phylum	-0.22222	1	-0.25926	1	-0.18519	0.8
Class	-0.25926	1	-0.25926	1	-0.25926	1
Order	-0.2963	1	-0.37037	1	-0.25926	1
Family	-0.2963	1	-0.33333	1	-0.25926	1
Genus	-0.25926	1	-0.33333	1	-0.25926	1
Species	-0.33333	1	-0.2963	0.8	-0.2963	0.8

Table 3.4: Analysis of similarities. Sample G1 (negative control) was compared to sample G2 (spiked with *L. monocytogenes*) and G3 (spiked with *Salmonella* ser. Newport) at all taxonomic levels. Sample G2 was also compared to sample G3. There were no significant differences between any groups at any level. A p-value ≤ 0.05 is statistically significant.

Figures

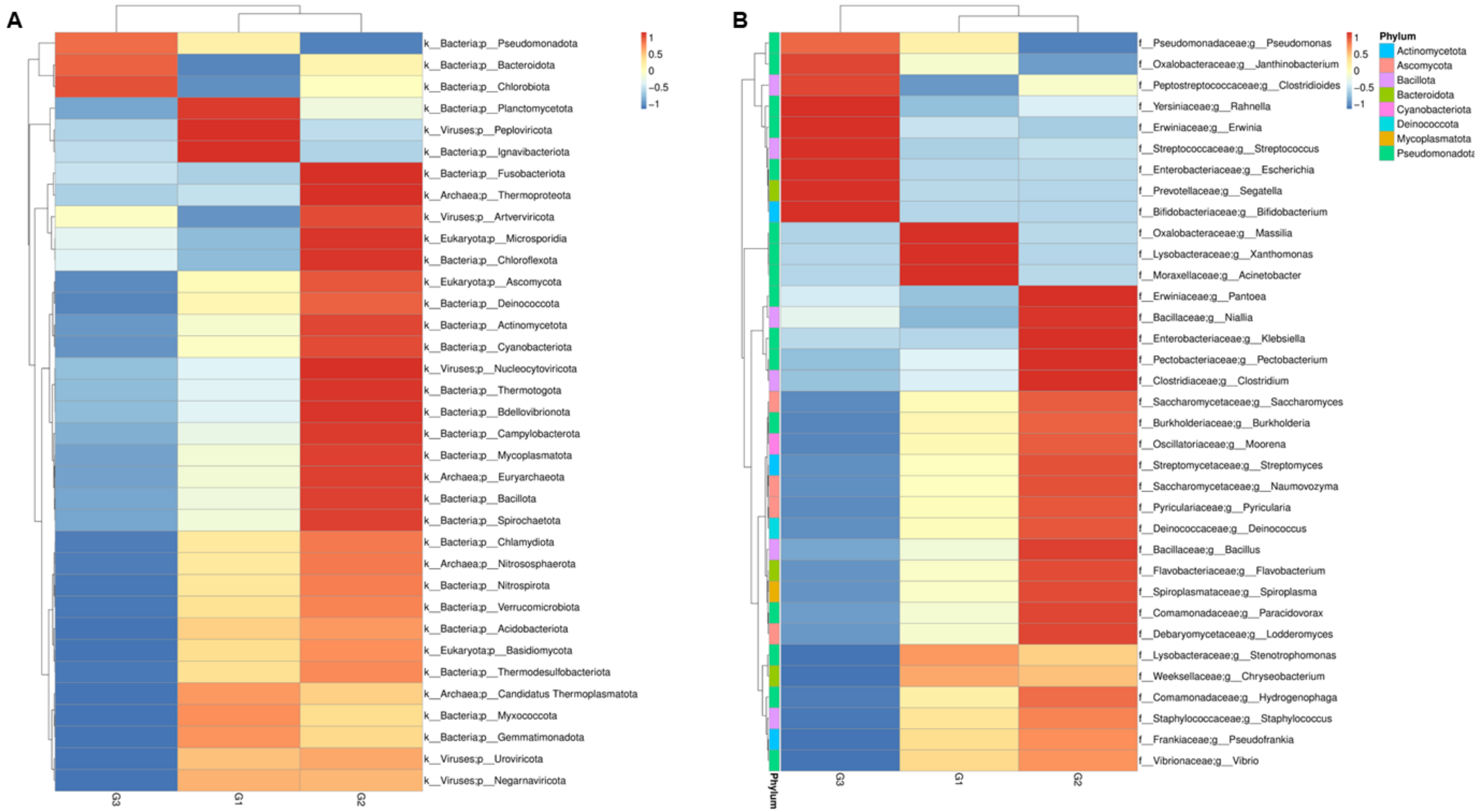

Figure 3.1: Abundance clustering heat map showing the distribution of the top 35 dominant (A) phyla and (B) genera of groups G1 (F#1 MNP captured without added pathogen), G2 (F#1 MNP captured in the presence of *L. monocytogenes*), and G3 (F#1 MNP captured in the presence of *Salmonella* ser. Newport).

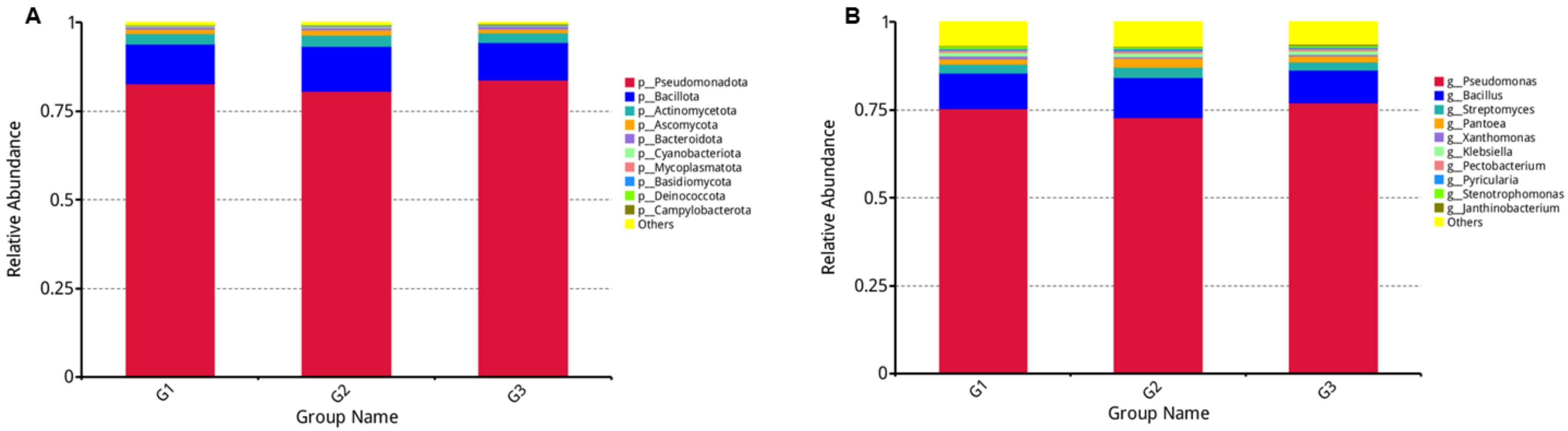

Figure 3.2: Relative abundance of top 10 (A) phyla and (B) genera captured by chitosan-functionalized magnetic nanoparticles. G1 (F#1 MNP captured without added pathogen), G2 (F#1 MNP captured in the presence of *L. monocytogenes*), and G3 (F#1 MNP captured in the presence of *Salmonella* ser. Newport).

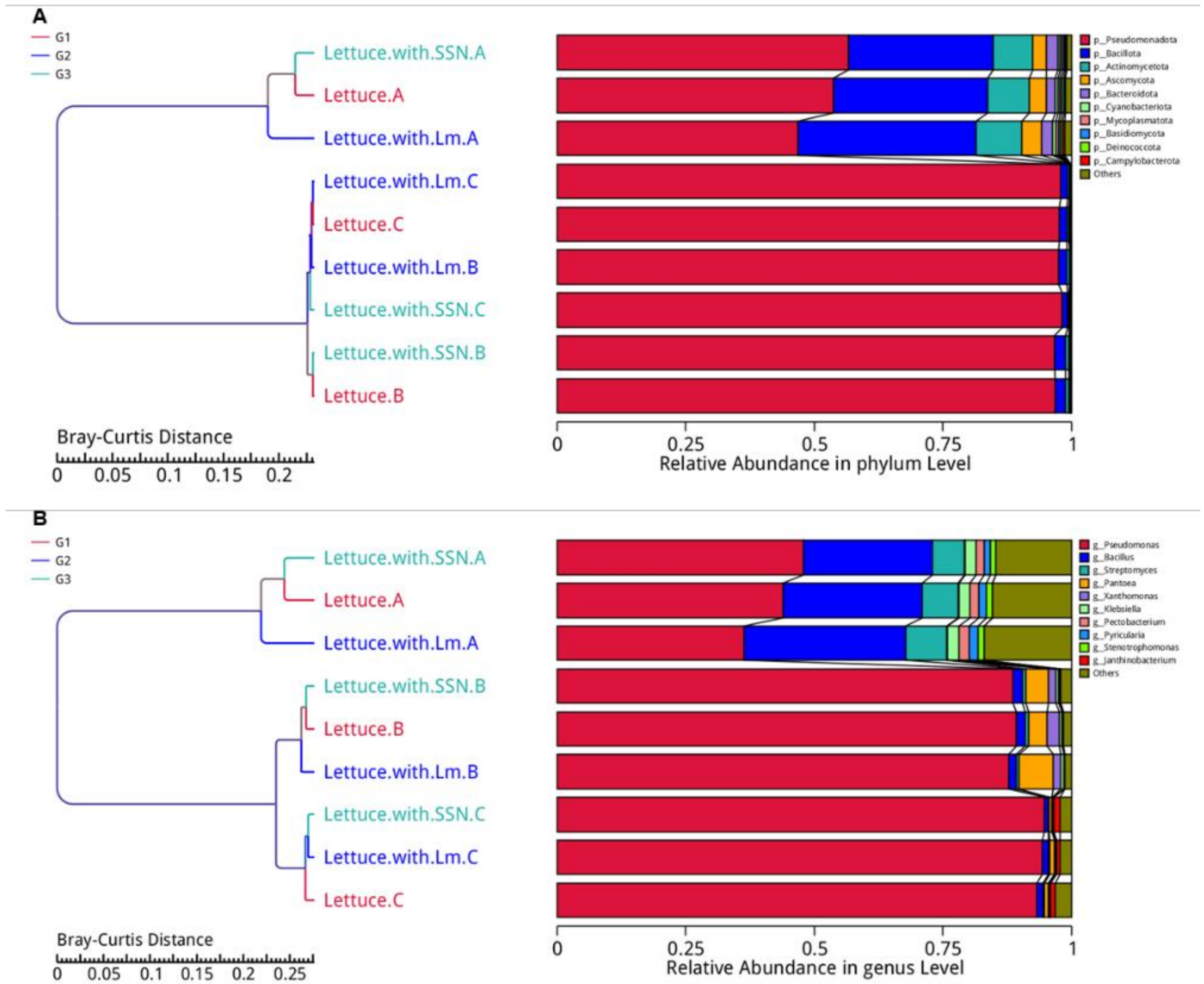

Figure 3.3: Bray-Curtis distance clustering tree (left) and relative abundance distribution of each sample (right) at the phylum (A) and genus (B) levels. Samples were not spiked (G1), spiked with *L. monocytogenes* (*Lm*) (G2), or spiked with *Salmonella* ser. Newport (SSN) (G3).

CHAPTER 5: CONCLUSIONS AND FUTURE RESEARCH

Conclusions

The purpose of this dissertation was to evaluate and optimize the use of chitosan-functionalized magnetic nanoparticles (F#1 MNPs) as a preanalytical sampling processing tool for the detection of foodborne pathogens in complex and diverse food matrices. This research contributed to an expanded body of knowledge regarding methods to improve the speed of low-level foodborne pathogen isolation and detection under laboratory conditions. This is especially important because current advancements in the rapid detection of foodborne pathogens focus almost exclusively on improving the downstream detection assay with little to no regard for sample preparation (84–86).

Two foodborne pathogens were used, one gram-positive (*Listeria monocytogenes*) and one gram-negative (*Salmonella* ser. Newport) bacterium, which contribute significantly to the number of foodborne associated illnesses and deaths in the U.S. (1, 2). The bacteria were cold-stressed (refrigerated) to simulate food storage conditions (70, 139, 141). This was especially important because while it is hypothesized that the F#1 MNPs bind to microbes similarly to other particles functionalized by chitosan, this has yet to be proven. Therefore, the physiological state of the microbe that likely exists in naturally contaminated samples was considered.

This proof-of-concept study used statistical design of experiments (DOE) – specifically, the definitive screening design (DSD) and central composite design (CCD) - to rapidly optimize the extraction protocol for low bacterial contamination on various complex food matrices. This study builds on earlier work, advancing the field by rapidly optimizing pathogen extraction and concentration across a diverse range of food matrices. Unlike traditional methods that rely on matrix-specific validation through extensive iterations of variable combinations, this research shows the F#1 MNPs can consistently capture target pathogens across diverse food matrices with only minor protocol modifications, which can be quickly determined by using a CCD for optimization. For example, all the pathogen-matrix combinations used the same extraction protocol except for incubation time, which was 10 or 15 minutes. Alternatively, a standard protocol can be developed and used to determine the lower limit of capture to assess whether further refinements are needed to meet regulatory requirements, similar to the testing of *Salmonella* ser. Newport in romaine lettuce.

Salmonella ser. Newport had a lower limit of capture in strawberries compared to romaine lettuce, which is likely attributed to attachment properties of *Salmonella* to these matrices and competing microorganisms. Similarly, differences in the lower limit of capture for *L. monocytogenes* was observed in romaine lettuce compared to cotto salami. Despite these variations, this study demonstrated the lower limit of capture can be reduced to ≤ 3 CFU/g with minimal modifications. As public health officials continue to refine risk-based approaches to food safety, further optimizations can be made to simplify sample preparation protocols.

The second part of the study highlighted the integration of the F#1 MNPs into existing enrichment protocols without inhibiting the growth of the target pathogen. Additional modifications led to a reduction to 4-12 hours of enrichment needed to isolate the target organism on selective agar. The results provided in chapters 2 and 3 can be integrated to further optimize the extraction of pathogens from food matrices and testing it against various broth and/or incubation modifications to further increase the sensitivity of assays and accelerate the time to detection.

Furthermore, the final part of the study, which used shotgun metagenomic sequencing analysis, expanded the understanding of the broad-spectrum capture capabilities and lack of pathogen specificity of F#1 MNPs. This highlights their potential application across a variety of microbes beyond bacterial foodborne pathogens, extending into additional fields such as using fungi as environmental bioindicators or quality control purposes. However, these applications must be confirmed and validated in naturally contaminated samples from diverse sources. This study also underscores F#1 MNPs as a potential tool for multi-organism detection, aligning with efforts to develop multi-organism and multi-pathogen enrichment broths and multiplex assays. These capabilities are especially important to pathogen-agnostic testing and identification of pathogens in novel food vehicles (35). However, additional studies are needed to fully explore these possibilities.

Previous studies using MNPs showed their integration with a wide range of detection assays such as polymerase chain reaction (PCR), loop-mediated isothermal amplification (LAMP), and cyclic voltammetry (93, 136). This study demonstrated their integration into enrichment protocols. Incorporating F#1 MNPs into existing food safety testing protocols offers the advantage of easier and quicker integration into regulatory standards, as these modifications build upon already approved workflows (141). The F#1 MNPs are a promising tool for pathogen extraction, concentration, isolation, and detection in food safety. The broad-spectrum capture capability combined with their compatibility with existing detection protocols is promising in improving the speed of pathogen detection and their applicability in agnostic, multi-pathogen detection methods. With further validation and continued optimization, F#1 MNPs can significantly improve foodborne pathogen detection, surveillance, and outbreak prevention.

Limitations

While the individual study limitations were discussed throughout the dissertation, the overarching limitations were the proof-of-concept study design and use of artificially inoculated samples. The research used only one strain of each of the two pathogens, with each pathogen artificially inoculated on two food matrices. Therefore, the generalizability of this study to other pathogens, strains, and foods is limited. Additionally, the studies were constrained to artificially inoculated, spiked samples due to the inability to acquire naturally contaminated samples. Despite the use of established protocols to simulate natural contamination, the cumulative effects of stresses encountered by pathogens during processing likely does not fully represent their physiological state, especially as it pertains to binding sites for the F#1 MNP.

Future Research

Chapter 2 established a framework for optimizing pathogen extraction using F#1 MNPs in various food matrices. However, this proof-of-concept study was conducted on a single serotype and strain of *Salmonella enterica* and *Listeria monocytogenes* in laboratory-based spike-and-recovery tests. To enable broader application of this technology, additional validation using diverse strains and a broader range and combinations of pathogens in diverse food matrices is needed. Further, these assays would have to be replicated on naturally contaminated sample matrices. Testing on naturally contaminated samples, though challenging to obtain, would significantly enhance the validity and applicability of F#1 MNPs in foodborne outbreaks.

As previously discussed, the exact binding mechanisms of the F#1 MNPs remain undefined but are hypothesized to resemble how other chitosan-functionalized particles and materials bind to microorganisms. Further investigation into these mechanisms could enable refinements to the specificity of the capture protocol. Comprehension of the binding interactions as related to cell physiology may facilitate improvements in growth media formulations, potentially decreasing lag-phases and doubling times, leading to faster recovery of single-colony isolates.

An important yet unexplored application of this technology is using F#1 MNPs for pathogen capture in large sample volumes (e.g., 375 g of food), for high-throughput water testing, or indicator organism detection. Leveraging F#1 MNPs in these applications can improve the sensitivity of detecting low level pathogen contamination, which is a well-documented challenge posed by the uneven distribution and low prevalence of foodborne pathogens in complex food matrices. By effectively concentrating pathogens into smaller, more manageable volumes, F#1 MNPs could reduce the space and resources required for high volume/high throughput testing, offering a promising solution for highly efficient detection workflows.

DISCLAIMER

The views and information presented are those of the author and do not represent the official position of the U.S. Army Medical Center of Excellence, the U.S. Army Training and Doctrine Command, or the Department of the Army, Department of Defense, or U.S. Government.

BIBLIOGRAPHY

1. Scallan E, Hoekstra RM, Angulo FJ, Tauxe R V., Widdowson M-A, Roy SL, Jones JL, Griffin PM. 2011. Foodborne Illness Acquired in the United States—Major Pathogens. Emerg Infect Dis 17:7–15.

2. Centers for Disease Control and Prevention. 2024. Burden of Foodborne Illnesses in the United States. https://www.cdc.gov/foodborneburden/burden/index.html. Retrieved 26 January 2025.

3. Shah HJ, Jervis RH, Wymore K, Rissman T, LaClair B, Boyle MM, Smith K, Lathrop S, McGuire S, Trevejo R, McMillian M, Harris S, Zablotsky Kufel J, Houck K, Lau CE, Devine CJ, Boxrud D, Weller DL. 2024. Reported Incidence of Infections Caused by Pathogens Transmitted Commonly Through Food: Impact of Increased Use of Culture-Independent Diagnostic Tests — Foodborne Diseases Active Surveillance Network, 1996–2023. MMWR Morb Mortal Wkly Rep 73:584–593.

4. Lund BM, O’Brien SJ. 2011. The Occurrence and Prevention of Foodborne Disease in Vulnerable People. Foodborne Pathog Dis 8:961–973.

5. Tserenpuntsag B, Chang H-G, Smith PF, Morse DL. 2005. Hemolytic Uremic Syndrome Risk and *Escherichia coli* O157:H7. Emerg Infect Dis 11:1955–1957.

6. Hunt JM. 2010. Shiga Toxin–Producing Escherichia coli (STEC). Clin Lab Med 30:21–45.

7. Nachamkin I, Allos BM, Ho T. 1998. *Campylobacter* Species and Guillain-Barré Syndrome. Clin Microbiol Rev 11:555–567.

8. Poropatich KO, Fischer Walker CL, Black RE. 2010. Quantifying the Association between *Campylobacter* Infection and Guillain-Barré Syndrome: A Systematic Review. J Health Popul Nutr 28:545–52.

9. Orsi RH, Wiedmann M. 2016. Characteristics and distribution of *Listeria* spp., including *Listeria* species newly described since 2009. Appl Microbiol Biotechnol 100:5273–5287.

10. Swaminathan B, Gerner-Smidt P. 2007. The epidemiology of human listeriosis. Microbes Infect 9:1236–1243.

11. Batz M, Hoffmann S, Morris JG. 2014. Disease-Outcome Trees, EQ-5D Scores, and Estimated Annual Losses of Quality-Adjusted Life Years (QALYs) for 14 Foodborne Pathogens in the United States. Foodborne Pathog Dis 11:395–402.

12. Hoffmann S, Maculloch B, Batz M. 2015. Economic Burden of Major Foodborne Illnesses Acquired in the United States. EIB-140.

13. Huang C, Lu T-L, Yang Y. 2023. Mortality risk factors related to listeriosis — A meta-analysis. J Infect Public Health 16:771–783.

14. Pouillot R, Kiermeier A, Guillier L, Cadavez V, Sanaa M. 2024. Updated Parameters for *Listeria monocytogenes* Dose–Response Model Considering Pathogen Virulence and Age and Sex of Consumer. Foods 13:751.

15. Maury MM, Tsai Y-H, Charlier C, Touchon M, Chenal-Francisque V, Leclercq A, Criscuolo A, Gaultier C, Roussel S, Brisabois A, Disson O, Rocha EPC, Brisse S, Lecuit M. 2016. Uncovering *Listeria monocytogenes* hypervirulence by harnessing its biodiversity. Nat Genet 48:308–313.

16. Fritsch L, Guillier L, Augustin J-C. 2018. Next generation quantitative microbiological risk assessment: Refinement of the cold smoked salmon-related listeriosis risk model by integrating genomic data. Microb Risk Anal 10:20–27.

17. United States Department of Agriculture - Food Safety and Inspection Service. 2010. FSIS Comparative Risk Assessment for *Listeria monocytogenes* in Ready-to-eat Meat and Poultry Deli Meats Report.

18. Pouillot R, Klontz KC, Chen Y, Burall LS, Macarisin D, Doyle M, Bally KM, Strain E, Datta AR, Hammack TS, Van Doren JM. 2016. Infectious Dose of *Listeria monocytogenes* in Outbreak Linked to Ice Cream, United States, 2015. Emerg Infect Dis 22:2113–2119.

19. World Health Organization - Food Safety Department. 2004. Risk assessment of *Listeria monocytogenes* in ready-to-eat foods 4.

20. Koopmans MM, Brouwer MC, Vázquez-Boland JA, van de Beek D. 2023. Human Listeriosis. Clin Microbiol Rev 36.

21. Radoshevich L, Cossart P. 2018. *Listeria monocytogenes*: towards a complete picture of its physiology and pathogenesis. Nat Rev Microbiol 16:32–46.

22. Welshimer HJ, Donker-Voet J. 1971. *Listeria monocytogenes* in Nature. Appl Microbiol 21:516–519.

23. Mcclure PJ, Roberts TA, Oguru PO. 1989. Comparison of the effects of sodium chloride, pH and temperature on the growth of *Listeria monocytogenes* on gradient plates and in liquid medium. Lett Appl Microbiol 9:95–99.

24. Petran RL, Zottola EA. 1989. A Study of Factors Affecting Growth and Recovery of *Listeria monocytogenes* Scott A. J Food Sci 54:458–460.

25. Malley TJV, Butts J, Wiedmann M. 2015. Seek and Destroy Process: *Listeria monocytogenes* Process Controls in the Ready-to-Eat Meat and Poultry Industry. J Food Prot 78:436–445.

26. Foodborne Illness Source Attribution Estimates – United States 2022. Foodborne Illness Source Attribution Estimates – United States, 2022.

27. Centers for Disease Control and Prevention. 2024. Investigation Update: *Listeria* outbreak, Leafy Greens - February 2023. https://www.cdc.gov/listeria/outbreaks/details-monocytogenes-02-23.html#:~:text=of%20this%20outbreak.-,Epidemiologic%20Data,%2C%202023%20(see%20timeline). Retrieved 26 January 2025.

28. United States Department of Agriculture - Food Safety and Inspection Service. 2014. FSIS Compliance Guideline: Controlling *Listeria monocytogenes* in Post-lethality Exposed Ready-to-Eat Meat and Poultry Products.

29. Centers for Disease Control and Prevention. 2024. *Listeria* Outbreak Linked to Meats Sliced at Delis. https://www.cdc.gov/listeria/outbreaks/delimeats-7-24.html. Retrieved 26 January 2025.

30. Centers for Disease Control and Prevention. 2024. *Listeria* Outbreak Linked to Ready-to-Eat Meat and Poultry Products. https://www.cdc.gov/listeria/outbreaks/meat-and-poultry-products-11-24.html. Retrieved 26 January 2025.

31. Teunis PFM, Kasuga F, Fazil A, Ogden ID, Rotariu O, Strachan NJC. 2010. Dose–response modeling of *Salmonella* using outbreak data. Int J Food Microbiol 144:243–249.

32. D’Aoust J-Y. 1994. *Salmonella* and the international food trade. Int J Food Microbiol 24:11–31.

33. Godínez-Oviedo A, Tamplin ML, Bowman JP, Hernández-Iturriaga M. 2024. Effects of intrinsic characteristics of *Salmonella enterica* strains isolated from foods and humans, and their interaction with food matrices during simulated gastric conditions. Int J Food Microbiol 413:110584.

34. Teunis PFM. 2022. Dose response for *Salmonella* Typhimurium and Enteritidis and other nontyphoid enteric salmonellae. Epidemics 41:100653.

35. Cheng RA, Eade CR, Wiedmann M. 2019. Embracing Diversity: Differences in Virulence Mechanisms, Disease Severity, and Host Adaptations Contribute to the Success of Nontyphoidal *Salmonella* as a Foodborne Pathogen. Front Microbiol 10.

36. Pogreba-Brown K, Austhof E, Tang X, Trejo MJ, Owusu-Dommey A, Boyd K, Armstrong A, Schaefer K, Bazaco MC, Batz M, Riddle M, Porter C. 2021. Enteric Pathogens and Reactive Arthritis: Systematic Review and Meta-Analyses of Pathogen-Associated Reactive Arthritis. Foodborne Pathog Dis 18:627–639.

37. Dworkin MS, Shoemaker PC, Goldoft MJ, Kobayashi JM. 2001. Reactive Arthritis and Reiter's Syndrome Following an Outbreak of Gastroenteritis Caused by *Salmonella enteritidis*. Clinical Infectious Diseases 33:1010–1014.

38. Fang FC, Fierer J. 1991. Human Infection with *Salmonella dublin*. Medicine 70:198–207.

39. Chiu C-H, Su L-H, Chu C. 2004. *Salmonella enterica* Serotype Choleraesuis: Epidemiology, Pathogenesis, Clinical Disease, and Treatment. Clin Microbiol Rev 17:311–322.

40. Medalla F, Gu W, Friedman CR, Judd M, Folster J, Griffin PM, Hoekstra RM. 2021. Increased Incidence of Antimicrobial-Resistant Nontyphoidal *Salmonella* Infections, United States, 2004–2016. Emerg Infect Dis 27:1662–1672.

41. Collins JP, Shah HJ, Weller DL, Ray LC, Smith K, McGuire S, Trevejo RT, Jervis RH, Vugia DJ, Rissman T, Garman KN, Lathrop S, LaClair B, Boyle MM, Harris S, Kufel JZ, Tauxe R V., Bruce BB, Rose EB, Griffin PM, Payne DC. 2022. Preliminary Incidence and Trends of Infections Caused by Pathogens Transmitted Commonly Through Food — Foodborne Diseases Active Surveillance Network, 10 U.S. Sites, 2016–2021. MMWR Morb Mortal Wkly Rep 71:1260–1264.

42. Snyder TR, Boktor SW, M'ikanatha NM. 2019. Salmonellosis Outbreaks by Food Vehicle, Serotype, Season, and Geographical Location, United States, 1998 to 2015. J Food Prot 82:1191–1199.

43. National Advisory Committee on Microbiological Criteria in Foods (NACMCF). 2024. Response to Questions Posed by the Food Safety and Inspection Service: Enhancing *Salmonella* Control in Poultry Products. J Food Prot 87:100168.

44. Kim M, Barnett-Neefs C, Chavez RA, Kealey E, Wiedmann M, Stasiewicz MJ. 2024. Risk Assessment Predicts Most of the Salmonellosis Risk in Raw Chicken Parts is Concentrated in Those Few Products with High Levels of High-Virulence Serotypes of *Salmonella*. J Food Prot 87:100304.

45. Miller EA, Elnekave E, Flores-Figueroa C, Johnson A, Kearney A, Munoz-Aguayo J, Tagg KA, Tschetter L, Weber BP, Nadon CA, Boxrud D, Singer RS, Folster JP, Johnson TJ. 2020. Emergence of a Novel *Salmonella enterica* Serotype Reading Clonal Group Is Linked to Its Expansion in Commercial Turkey Production, Resulting in Unanticipated Human Illness in North America. mSphere 5.

46. Pshenichnaya N, Lizinfeld I, Umbetova K, Konnova Y, Gopatsa G, Kuandykova A, Omarova B. 2023. Salmonella Reading: A rare case of generalized salmonellosis in non-endemic region. IDCases 33:e01879.

47. Ivers C, Kaya EC, Yucel U, Boyle D, Trinetta V. 2024. Evaluation of *Salmonella* biofilm attachment and hydrophobicity characteristics on food contact surfaces. BMC Microbiol 24:387.

48. Brouard C, Espié E, Weill F-X, Kérouanton A, Brisabois A, Forgue A-M, Vaillant V, de Valk H. 2007. Two Consecutive Large Outbreaks of *Salmonella enterica* Serotype Agona Infections in Infants Linked to the Consumption of Powdered Infant Formula. Pediatr Infect Dis J 26:148–52.

49. Russo ET, Biggerstaff G, Hoekstra RM, Meyer S, Patel N, Miller B, Quick R. 2013. A Recurrent, Multistate Outbreak of *Salmonella* Serotype Agona Infections Associated with Dry, Unsweetened Cereal Consumption, United States, 2008. J Food Prot 76:227–230.

50. Cavallaro E, Date K, Medus C, Meyer S, Miller B, Kim C, Nowicki S, Cosgrove S, Sweat D, Phan Q, Flint J, Daly ER, Adams J, Hyytia-Trees E, Gerner-Smidt P, Hoekstra RM, Schwensohn C, Langer A, Sodha S V., Rogers MC, Angulo FJ, Tauxe R V., Williams IT, Behravesh CB. 2011. *Salmonella* Typhimurium Infections Associated with Peanut Products. New England Journal of Medicine 365:601–610.

51. Keaton AA, Schwensohn CA, Brandenburg JM, Pereira E, Adcock B, Tecle S, Hinnenkamp R, Havens J, Bailey K, Applegate B, Whitney P, Gibson D, Manion K, Griffin M, Ritter J, Biskupiak C, Ajileye K, Golwalkar M, Gosciminski M, Viveiros B, Caron G, McCullough L, Smith L, Vidyaprakash E, Doyle M, Hardy C, Elliot EL, Gieraltowski LB. 2022. Multistate outbreak of *Salmonella* Mbandaka infections linked to sweetened puffed wheat cereal – United States, 2018. Epidemiol Infect 150:e135.

52. Myoda SP, Gilbreth S, Akins-Lewenthal D, Davidson SK, Samadpour M. 2019. Occurrence and Levels of *Salmonella*, Enterohemorrhagic *Escherichia coli*, and *Listeria* in Raw Wheat. J Food Prot 82:1022–1027.

53. Food and Drug Administration. 2024. 21 CFR.

54. Department of Agriculture. 2024. 9 CFR.

55. Food and Drug Administration Food Safety Modernization Act. 2011. Pub. L. No. 111-353, 124 STat. 3885.

56. Williams MS, Ebel ED, Golden NJ, Saini G, Nyirabahizi E, Clinch N. 2022. Assessing the effectiveness of performance standards for *Salmonella* contamination of chicken parts. Int J Food Microbiol 378:109801.

57. Department of Agriculture. Salmonella Framework for Raw Poultry Products, 89 Fed Reg 64678-64748 (7 August 2024) (to be codified at 9 CFR pt 381).

58. Katz TS, Harhay DM, Schmidt JW, Wheeler TL. 2024. Identifying a list of *Salmonella* serotypes of concern to target for reducing risk of salmonellosis. Front Microbiol 15.

59. Food and Drug Administratoin. Standards for the Growing, Harvesting, Packing, and Holding of Produce for Human Consumption Relating to Agricultural Water, 89 Fed Reg 37448-37519 (6 May 2024) (to be codified at 21 CFR pt 112).

60. Food and Drug Administration. Bacteriological Analytical Manual (BAM). https://www.fda.gov/food/laboratory-methods-food/bacteriological-analytical-manual-bam. Retrieved 26 January 2025.

61. United States Department of Agriculture - Food Safety and Inspection Service. Microbiology Laboratory Guidebook (MLG). https://www.fsis.usda.gov/news-events/publications/microbiology-laboratory-guidebook. Retrieved 26 January 2025.

62. Brown E, Dessai U, McGarry S, Gerner-Smidt P. 2019. Use of Whole-Genome Sequencing for Food Safety and Public Health in the United States. Foodborne Pathog Dis 16:441–450.

63. Centers for Disease Control and Prevention. 2024. Summary of Possible Multistate Enteric (Intestinal) Disease Outbreaks in 2017–2020. https://www.cdc.gov/foodborne-outbreaks/php/data-research/summary-2017-2020.html. Retrieved 26 January 2025.

64. Richardson LC, Bazaco MC, Parker CC, Dewey-Mattia D, Golden N, Jones K, Klontz K, Travis C, Kufel JZ, Cole D. 2017. An Updated Scheme for Categorizing Foods Implicated in Foodborne Disease Outbreaks: A Tri-Agency Collaboration. Foodborne Pathog Dis 14:701–710.

65. Parada J, Aguilera JM. 2007. Food Microstructure Affects the Bioavailability of Several Nutrients. J Food Sci 72.

66. 2023. Food Structure and the Complexity of Food Matrices, p. 290–313. *In* Food Digestion and Absorption Its Role in Food Product Development. Royal Society of Chemistry.

67. Guan N, Liu L. 2020. Microbial response to acid stress: mechanisms and applications. Appl Microbiol Biotechnol 104:51–65.

68. Marmion M, Macori G, Ferone M, Whyte P, Scannell AGM. 2022. Survive and thrive: Control mechanisms that facilitate bacterial adaptation to survive manufacturing-related stress. Int J Food Microbiol 368:109612.

69. Wesche AM, Gurtler JB, Marks BP, Ryser ET. 2009. Stress, sublethal injury, resuscitation, and virulence of bacterial foodborne pathogens. J Food Prot 72:1121–38.

70. Wu V. 2008. A review of microbial injury and recovery methods in food. Food Microbiol 25:735–744.

71. Kallio H, Hakala M, Pelkkikangas A-M, Lapveteläinen A. 2000. Sugars and acids of strawberry varieties. European Food Research and Technology 212:81–85.

72. Hingston P, Chen J, Allen K, Truelstrup Hansen L, Wang S. 2017. Strand specific RNA-sequencing and membrane lipid profiling reveals growth phase-dependent cold stress response mechanisms in *Listeria monocytogenes*. PLoS One 12:e0180123.

73. Bessaiah H, Anamalé C, Sung J, Dozois CM. 2021. What Flips the Switch? Signals and Stress Regulating Extraintestinal Pathogenic Escherichia coli Type 1 Fimbriae (Pili). Microorganisms 10:5.

74. Frank JF. 2001. Microbial attachment to food and food contact surfaces. Adv Food Nutr Res 43:319–70.

75. Acuff J, Ponder M. 2020. Interactions of Foodborne Pathogens with the Food Matrix, p. 129–156. *In* Food Engineering Series. Springer.

76. Wilson IG. 1997. Inhibition and facilitation of nucleic acid amplification. Appl Environ Microbiol 63:3741–51.

77. Rossen L, Nørskov P, Holmstrøm K, Rasmussen OF. 1992. Inhibition of PCR by components of food samples, microbial diagnostic assays and DNA-extraction solutions. Int J Food Microbiol 17:37–45.

78. Cossu A, Levin RE. 2014. Rapid Conventional PCR and Real-Time-qPCR Detection of Low Numbers of *Salmonella enterica* from Ground Beef without Enrichment. Food Biotechnol 28:96–105.

79. Wang W, Zhou Y, Xiao X, Yang G, Wang Q, Wei W, Liu Y, Yang H. 2018. Behavior of *Salmonella* Typhimurium on Fresh Strawberries Under Different Storage Temperatures and Wash Treatments. Front Microbiol 9.

80. Basak JK, Madhavi BGK, Paudel B, Kim NE, Kim HT. 2022. Prediction of Total Soluble Solids and pH of Strawberry Fruits Using RGB, HSV and HSL Colour Spaces and Machine Learning Models. Foods 11:2086.

81. Montero TM, Mollá EM, Esteban RM, López-Andréu FJ. 1996. Quality attributes of strawberry during ripening. Sci Hortic 65:239–250.

82. Brandl MT, Mammel MK, Simko I, Richter TKS, Gebru ST, Leonard SR. 2023. Weather factors, soil microbiome, and bacteria-fungi interactions as drivers of the epiphytic phyllosphere communities of romaine lettuce. Food Microbiol 113:104260.

83. Ingham SC, Borneman DL, Ané C, Ingham BH. 2010. Predicting growth-no growth of *Listeria monocytogenes* on vacuum-packaged ready-to-eat meats. J Food Prot 73:708–14.

84. Baetsen-Young AM, Vasher M, Matta LL, Colgan P, Alocilja EC, Day B. 2018. Direct colorimetric detection of unamplified pathogen DNA by dextrin-capped gold nanoparticles. Biosens Bioelectron 101:29–36.

85. Wang Y, Alocilja EC. 2015. Gold nanoparticle-labeled biosensor for rapid and sensitive detection of bacterial pathogens. J Biol Eng 9:16.

86. Law JW-F, Ab Mutalib N-S, Chan K-G, Lee L-H. 2015. Rapid methods for the detection of foodborne bacterial pathogens: principles, applications, advantages and limitations. Front Microbiol 5.

87. Stevens KA, Jaykus L-A. 2004. Bacterial Separation and Concentration from Complex Sample Matrices: A Review. Crit Rev Microbiol 30:7–24.

88. Fan W, Gao X, Li H, Guo W, Li Y, Wang S. 2022. Rapid and simultaneous detection of *Salmonella* spp., *Escherichia coli* O157:H7, and *Listeria monocytogenes* in meat using multiplex immunomagnetic separation and multiplex real-time PCR. European Food Research and Technology 248:869–879.

89. Eser E, Felton VA, Drolia R, Bhunia AK. 2024. *Salmonella* Detection in Food Using a HEK-hTLR5 Reporter Cell-Based Sensor. Biosensors (Basel) 14:444.

90. Röthlisberger P, Hollenstein M. 2018. Aptamer chemistry. Adv Drug Deliv Rev 134:3–21.

91. Joshi R, Janagama H, Dwivedi HP, Senthil Kumar TMA, Jaykus L-A, Schefers J, Sreevatsan S. 2009. Selection, characterization, and application of DNA aptamers for the capture and detection of *Salmonella enterica* serovars. Mol Cell Probes 23:20–28.

92. Bayramoglu G, Ozalp VC, Arica MY. 2024. Aptamer-based magnetic isolation and specific detection system for *Listeria monocytogenes* from food samples. Microchemical Journal 203:110892.

93. Dester E, Alocilja E. 2022. Current Methods for Extraction and Concentration of Foodborne Bacteria with Glycan-Coated Magnetic Nanoparticles: A Review. Biosensors (Basel) 12:112.

94. Kveton F, Blsakova A, Kasak P, Tkac J. 2020. Glycan Nanobiosensors. Nanomaterials 10:1406.

95. Cho S-H, Park J, Kim C-H. 2022. Systemic Lectin-Glycan Interaction of Pathogenic Enteric Bacteria in the Gastrointestinal Tract. Int J Mol Sci 23:1451.

96. James AM. 1982. The electrical properties and topochemistry of bacterial cells. Adv Colloid Interface Sci 15:171–221.

97. Rijpens N, Herman L, Vereecken F, Jannes G, De Smedt J, De Zutter L. 1999. Rapid detection of stressed *Salmonella* spp. in dairy and egg products using immunomagnetic separation and PCR. Int J Food Microbiol 46:37–44.

98. Uyttendaele M, Van Hoorde I, Debevere J. 2000. The use of immuno-magnetic separation (IMS) as a tool in a sample preparation method for direct detection of *L. monocytogenes* in cheese. Int J Food Microbiol 54:205–12.

99. Matta LL, Alocilja EC. 2018. Carbohydrate Ligands on Magnetic Nanoparticles for Centrifuge-Free Extraction of Pathogenic Contaminants in Pasteurized Milk. J Food Prot 81:1941–1949.

100. Rodoplu Solovchuk D, Boyaci IH, Tamer U, Sahiner N, Cetin D. 2023. A simple gradient centrifugation method for bacteria detection in skim milk. Microchemical Journal 189:108479.

101. Bruno JG. 2022. Syringe filter-based DNA aptamer-enzyme-linked colorimetric assay of *Salmonella* on lettuce. J Microbiol Methods 193:106406.

102. Kaur S, Dhillon GS. 2014. The versatile biopolymer chitosan: potential sources, evaluation of extraction methods and applications. Crit Rev Microbiol 40:155–175.

103. Crini G, Badot P-M. 2008. Application of chitosan, a natural aminopolysaccharide, for dye removal from aqueous solutions by adsorption processes using batch studies: A review of recent literature. Prog Polym Sci 33:399–447.

104. Harish Prashanth KV, Tharanathan RN. 2007. Chitin/chitosan: modifications and their unlimited application potential—an overview. Trends Food Sci Technol 18:117–131.

105. Hosseinnejad M, Jafari SM. 2016. Evaluation of different factors affecting antimicrobial properties of chitosan. Int J Biol Macromol 85:467–475.

106. Meng X, Xing R, Liu S, Yu H, Li K, Qin Y, Li P. 2012. Molecular weight and pH effects of aminoethyl modified chitosan on antibacterial activity in vitro. Int J Biol Macromol 50:918–924.

107. Kumar MNVR, Muzzarelli RAA, Muzzarelli C, Sashiwa H, Domb AJ. 2004. Chitosan Chemistry and Pharmaceutical Perspectives. Chem Rev 104:6017–6084.

108. Peter MG. 1995. Applications and Environmental Aspects of Chitin and Chitosan. Journal of Macromolecular Science, Part A 32:629–640.

109. Helander IM, Nurmiaho-Lassila EL, Ahvenainen R, Rhoades J, Roller S. 2001. Chitosan disrupts the barrier properties of the outer membrane of gram-negative bacteria. Int J Food Microbiol 71:235–44.

110. Duan C, Meng X, Meng J, Khan MdIH, Dai L, Khan A, An X, Zhang J, Huq T, Ni Y. 2019. Chitosan as A Preservative for Fruits and Vegetables: A Review on Chemistry and Antimicrobial Properties. Journal of Bioresources and Bioproducts 4:11–21.

111. Kong M, Chen XG, Xing K, Park HJ. 2010. Antimicrobial properties of chitosan and mode of action: A state of the art review. Int J Food Microbiol 144:51–63.

112. Yu Y, Su Z, Peng Y, Zhong Y, Wang L, Xin M, Li M. 2025. Recent advances in modifications, biotechnology, and biomedical applications of chitosan-based materials: A review. Int J Biol Macromol 289:138772.

113. Chicea D, Nicolae-Maranciuc A. 2024. A Review of Chitosan-Based Materials for Biomedical, Food, and Water Treatment Applications. Materials 17:5770.

114. Flórez M, Guerra-Rodríguez E, Cazón P, Vázquez M. 2022. Chitosan for food packaging: Recent advances in active and intelligent films. Food Hydrocoll 124:107328.

115. Cheba B amar. 2020. Chitosan: Properties, Modifications and Food Nanobiotechnology. Procedia Manuf 46:652–658.

116. Akbarzadeh A, Samiei M, Davaran S. 2012. Magnetic nanoparticles: preparation, physical properties, and applications in biomedicine. Nanoscale Res Lett 7:144.

117. Socoliuc V, Peddis D, Petrenko VI, Avdeev M V., Susan-Resiga D, Szabó T, Turcu R, Tombácz E, Vékás L. 2020. Magnetic Nanoparticle Systems for Nanomedicine—A Materials Science Perspective. Magnetochemistry 6:2.

118. Hojnik Podrepšek G, Knez Ž, Leitgeb M. 2020. Development of Chitosan Functionalized Magnetic Nanoparticles with Bioactive Compounds. Nanomaterials 10:1913.

119. Gao P, Wang L, He Y, Wang Y, Yang X, Fu S, Qin X, Chen Q, Man C, Jiang Y. 2021. An Enhanced Lateral Flow Assay Based on Aptamer–Magnetic Separation and Multifold AuNPs for Ultrasensitive Detection of *Salmonella* Typhimurium in Milk. Foods 10:1605.

120. Jia F, Duan N, Wu S, Ma X, Xia Y, Wang Z, Wei X. 2014. Impedimetric aptasensor for *Staphylococcus aureus* based on nanocomposite prepared from reduced graphene oxide and gold nanoparticles. Microchimica Acta 181:967–974.

121. Wang D, Chen Q, Huo H, Bai S, Cai G, Lai W, Lin J. 2017. Efficient separation and quantitative detection of *Listeria monocytogenes* based on screen-printed interdigitated electrode, urease and magnetic nanoparticles. Food Control 73:555–561.

122. Li Y, Wu L, Wang Z, Tu K, Pan L, Chen Y. 2021. A magnetic relaxation DNA biosensor for rapid detection of *Listeria monocytogenes* using phosphatase-mediated Mn(VII)/Mn(II) conversion. Food Control 125:107959.

123. Boodoo C, Dester E, David J, Patel V, KC R, Alocilja EC. 2023. Multi-Probe Nano-Genomic Biosensor to Detect *S. aureus* from Magnetically-Extracted Food Samples. Biosensors (Basel) 13:608.

124. Matta LL. 2018. Biosensing Total Bacterial Load In Liquid Matrices To Improve Food Supply Chain Safety Using Carbohydrate-Functionalized Magnetic Nanoparticles For Cell Capture And Gold Nanoparticles For Signaling. PhD Dissertation. Michigan State University, East Lansing, MI.

125. Matta LL, Harrison J, Deol GS, Alocilja EC. 2018. Carbohydrate-Functionalized Nanobiosensor for Rapid Extraction of Pathogenic Bacteria Directly From Complex Liquids With Quick Detection Using Cyclic Voltammetry. IEEE Trans Nanotechnol 17:1006–1013.

126. Dester E, Kao K, Alocilja EC. 2022. Detection of Unamplified *E. coli* O157 DNA Extracted from Large Food Samples Using a Gold Nanoparticle Colorimetric Biosensor. Biosensors (Basel) 12:274.

127. Boodoo C, Dester E, Asadullah Sharief S, Alocilja EC. 2023. Influence of Biological and Environmental Factors in the Extraction and Concentration of Foodborne Pathogens using Glycan-Coated Magnetic Nanoparticles. J Food Prot 86:100066.

128. Mun S, Choi S-J. 2015. Detection of *Salmonella typhimurium* by antibody/enzyme-conjugated magnetic nanoparticles. Biochip J 9:10–15.

129. Hepel M. 2020. Magnetic Nanoparticles for Nanomedicine. Magnetochemistry 6:3.

130. Bruschi ML, de Toledo L de AS. 2019. Pharmaceutical Applications of Iron-Oxide Magnetic Nanoparticles. Magnetochemistry 5:50.

131. Zhao Y, Li Y, Jiang K, Wang J, White WL, Yang S, Lu J. 2017. Rapid detection of *Listeria monocytogenes* in food by biofunctionalized magnetic nanoparticle based on nuclear magnetic resonance. Food Control 71:110–116.

132. Shim W-B, Lee C-W, Kim M-G, Chung D-H. 2014. An antibody–magnetic nanoparticle conjugate-based selective filtration method for the rapid colorimetric detection of *Listeria monocytogenes*. Anal Methods 6:9129–9135.

133. Alocilja E. June 2021. Functionalized Magnetic Particle Compositions and Related Methods. U.S. Patent 2021/0164970 A1. United States.

134. Bhusal N, Shrestha S, Pote N, Alocilja EC. 2018. Nanoparticle-Based Biosensing of Tuberculosis, an Affordable and Practical Alternative to Current Methods. Biosensors (Basel) 9:1.

135. Hoffmann S, White AE, McQueen RB, Ahn J-W, Gunn-Sandell LB, Scallan Walter EJ. 2024. Economic Burden of Foodborne Illnesses Acquired in the United States. Foodborne Pathog Dis.

136. Xiao F, Li W, Xu H. 2022. Advances in magnetic nanoparticles for the separation of foodborne pathogens: Recognition, separation strategy, and application. Compr Rev Food Sci Food Saf 21:4478–4504.

137. Mao Y, Huang X, Xiong S, Xu H, Aguilar ZP, Xiong Y. 2016. Large-volume immunomagnetic separation combined with multiplex PCR assay for simultaneous detection of *Listeria monocytogenes* and *Listeria ivanovii* in lettuce. Food Control 59:601–608.

138. Huang C, Mahboubat BY, Ding Y, Yang Q, Wang J, Zhou M, Wang X. 2021. Development of a rapid *Salmonella* detection method via phage-conjugated magnetic bead separation coupled with real-time PCR quantification. LWT 142:111075.

139. National Advisory Committee on Microbiological Criteria for Foods. 2010. Parameters for determining inoculated pack/challenge study protocols. J Food Prot 73:140–202.

140. International Organization for Standardization. 2016. ISO 16140-2:2016(E) Microbiology of food and animal feed—Method validation—Part 2: protocol for the validation of alternative (proprietary) methods against a reference method, First Edition.

141. Food and Drug Administration. 2019. Guidelines for the Validation of Microbiological Methods for the FDA Foods Program, 3rd Edition.

142. Schlech WF, Lavigne PM, Bortolussi RA, Allen AC, Haldane E V, Wort AJ, Hightower AW, Johnson SE, King SH, Nicholls ES, Broome C V. 1983. Epidemic listeriosis--evidence for transmission by food. N Engl J Med 308:203–6.

143. Greene SK, Daly ER, Talbot EA, Demma LJ, Holzbauer S, Patel NJ, Hill TA, Walderhaug MO, Hoekstra RM, Lynch MF, Painter JA. 2008. Recurrent multistate outbreak of *Salmonella* Newport associated with tomatoes from contaminated fields, 2005. Epidemiol Infect 136:157–65.

144. Food and Drug Administration. 2001. Evaluation and Definition of Potentially Hazardous Foods A Report of the Institute of Food Technologists for the Food and Drug Administration of the United States Department of Health and Human Services.

145. United States Department of Agriculture - Food Safety and Inspection Service. 2010. FSIS Guidance for Test Kit Manufacturers, Laboratories: Evaluating the Performance of Pathogen Test Kit Methods.

146. United States Department of Agriculture - Agricultural Marketing Service. 2006. Fruit and Vegetable Programs Fresh Products Branch United States Standards for Grades of Strawberries.

147. Food and Drug Administration. 2024. Bacteriological Analytical Manual (BAM) Chapter 5: *Salmonella* - May 2024 Edition.

148. Food and Drug Administration. 2022. Bacteriological Analytical Manual (BAM) - Chapter 10: Detection of *Listeria monocytogenes* in Foods and Environmental Samples, and Enumeration of *Listeria monocytogenes* in Foods - April 2022 Edition.

149. United States Department of Agriculture - Food Safety and Inspection Service. 2024. MLG 8.14 Revision: 14 Isolation and Identification of *Listeria monocytogenes* from Ready-to-Eat Meat, Poultry, Siluriformes (Fish), Egg Products, and Environmental Samples.

150. United States Department of Agriculture - Agricultural Marketing Service. 2023. Commercial Item Description: Leafy Greens, Pre-Cut, Ready-to-Eat, or Ready-to-Use.

151. United States Department of Agriculture - Food Safety and Inspection Service. 2024. MLG 1.03 Revision: .03 FSIS Laboratory System Introduction, Method Performance Expectations, and Sample Handling for Microbiology.

152. El-Shaarawi AH, Esterby SR, Dutka BJ. 1981. Bacterial density in water determined by poisson or negative binomial distributions. Appl Environ Microbiol 41:107–16.

153. Koyama K, Hokunan H, Hasegawa M, Kawamura S, Koseki S. 2016. Do bacterial cell numbers follow a theoretical Poisson distribution? Comparison of experimentally obtained numbers of single cells with random number generation via computer simulation. Food Microbiol 60:49–53.

154. Erickson MC. 2012. Internalization of Fresh Produce by Foodborne Pathogens. Annu Rev Food Sci Technol 3:283–310.

155. Kim J, Park S, Lee J, Lee S. 2023. Internalization of *Salmonella* in Leafy Vegetables during Postharvest Conditions. Foods 12:3106.

156. Grivokostopoulos NC, Makariti IP, Hilaj N, Apostolidou Z, Skandamis PN. 2022. Internalization of *Salmonella* in Leafy Greens and Impact on Acid Tolerance. Appl Environ Microbiol 88:e0224921.

157. Reid AN, Conklin C, Beaton K, Donahue N, Jackson E, Locascio B, Marsocci C, Szemreylo E, Szemreylo K. 2021. Inoculum Preparation Conditions Influence Adherence of *Salmonella enterica* Serovars to Red Leaf Lettuce (*Lactuca sativa*). J Food Prot 84:857–868.

158. Hill WM, Reaume J, Wilcox JC. 1976. Total Plate Count and Sensory Evaluation as Measures of Luncheon Meat Shelf Life. Journal of Milk and Food Technology 39:759–762.

159. Fruin JT, Foster JF, Fowler JL. 1978. Survey of the Bacterial Populations of Bologna Products. J Food Prot 41:692–695.

160. Paradis DC, Stiles ME. 1978. A Study of Microbial Quality of Vacuum Packaged, Sliced Bologna. J Food Prot 41:811–815.

161. Hassenberg K, Geyer M, Herppich WB. 2010. Effect of Acetic Acid Vapour on the Natural Microflora and *Botrytis cinerea* of Strawberries. Eur J Hortic Sci 75:141–146.

162. Ortiz-Solà J, Viñas I, Colás-Medà P, Anguera M, Abadias M. 2020. Occurrence of selected viral and bacterial pathogens and microbiological quality of fresh and frozen strawberries sold in Spain. Int J Food Microbiol 314:108392.

163. Liao C, Wang L. 2022. The Microbial Quality of Commercial Chopped Romaine Lettuce Before and After the “Use By” Date. Front Microbiol 13.

164. Patel J, Sharma M. 2010. Differences in attachment of *Salmonella enterica* serovars to cabbage and lettuce leaves. Int J Food Microbiol 139:41–7.

165. Takeuchi K, Matute CM, Hassan AN, Frank JF. 2000. Comparison of the Attachment of *Escherichia coli* O157:H7, *Listeria monocytogenes*, *Salmonella* Typhimurium, and *Pseudomonas fluorescens* to Lettuce Leaves. J Food Prot 63:1433–1437.

166. Pérez-Lavalle L, Valero A, Cejudo-Gómez M, Carrasco E. 2023. Fate and biofilm formation of *Salmonella enterica subsp. enterica* serovar Thompson on fresh strawberries stored under refrigeration and room temperatures. Food Control 153:109906.

167. Yin H-B, Chen C-H, Colorado-Suarez S, Patel J. 2022. Biocontrol of *Listeria monocytogenes* and *Salmonella enterica* on Fresh Strawberries with Lactic Acid Bacteria During Refrigerated Storage. Foodborne Pathog Dis 19:324–331.

168. Dickson JS, Koohmaraie M. 1989. Cell surface charge characteristics and their relationship to bacterial attachment to meat surfaces. Appl Environ Microbiol 55:832–6.

169. Foong SCC, Dickson JS. 2004. Attachment of *Listeria monocytogenes* on ready-to-eat meats. J Food Prot 67:456–62.

170. Grau FH, Vanderlinde PB. 1990. Growth of *Listeria monocytogenes* on Vacuum-packaged Beef. J Food Prot 53:739–741.

171. Chung K-T, Dickson JS, Grouse JD. 1989. Attachment and Proliferation of Bacteria on Meat. J Food Prot 52:173–177.

172. Ells TC, Truelstrup Hansen L. 2006. Strain and growth temperature influence *Listeria* spp. attachment to intact and cut cabbage. Int J Food Microbiol 111:34–42.

173. Daiquigan N, Grim CJ, White JR, Hanes DE, Jarvis KG. 2016. Early Recovery of *Salmonella* from Food Using a 6-Hour Non-selective Pre-enrichment and Reformulation of Tetrathionate Broth. Front Microbiol 7.

174. Silk TM, Roth TMT, Donnelly CW. 2002. Comparison of growth kinetics for healthy and heat-injured *Listeria monocytogenes* in eight enrichment broths. J Food Prot 65:1333–7.

175. Hammack TS, Amaguaña RM, June GA, Sherrod PS, Andrews WH. 1999. Relative effectiveness of selenite cystine broth, tetrathionate broth, and Rappaport-Vassiliadis medium for the recovery of *Salmonella* spp. from foods with a low microbial load. J Food Prot 62:16–21.

176. June GA, Sherrod PS, Hammack TS, Amaguana RM, Andrews WH. 1995. Relative effectiveness of selenite cystine broth, tetrathionate broth, and Rappaport-Vassiliadis medium for the recovery of *Salmonella* from raw flesh and other highly contaminated foods: precollaborative study. J AOAC Int 78:375–80.

177. Badieyan S, Dilmaghani-Marand A, Hajipour MJ, Ameri A, Razzaghi MR, Rafii-Tabar H, Mahmoudi M, Sasanpour P. 2018. Detection and Discrimination of Bacterial Colonies with Mueller Matrix Imaging. Sci Rep 8:10815.

178. Jung JH, Lee JE. 2016. Real-time bacterial microcolony counting using on-chip microscopy. Sci Rep 6:21473.

179. Naghili H, Tajik H, Mardani K, Razavi Rouhani SM, Ehsani A, Zare P. 2013. Validation of drop plate technique for bacterial enumeration by parametric and nonparametric tests. Veterinary Research Forum 4:179–83.

180. Herigstad B, Hamilton M, Heersink J. 2001. How to optimize the drop plate method for enumerating bacteria. J Microbiol Methods 44:121–9.

181. Samadpour M. December 2004. Enrichment Methods for the Detection of Pathogens and Other Microbes. U.S. Patent 2004/0241644 A1. United States.

182. Bosilevac JM, Koohmaraie M. 2008. Effects of using reduced volumes of nonselective enrichment medium in methods for the detection of *Escherichia coli* O157:H7 from raw beef. J Food Prot 71:1768–73.

183. Sheth I, Li F, Hur M, Laasri A, De Jesus AJ, Kwon HJ, Macarisin D, Hammack TS, Jinneman K, Chen Y. 2018. Comparison of three enrichment schemes for the detection of low levels of desiccation-stressed *Listeria* spp. from select environmental surfaces. Food Control 84:493–498.

184. Ryser ET, Arimi SM, Bunduki MM, Donnelly CW. 1996. Recovery of different *Listeria* ribotypes from naturally contaminated, raw refrigerated meat and poultry products with two primary enrichment media. Appl Environ Microbiol 62:1781–1787.

185. Wagner E, Fagerlund A, Langsrud S, Møretrø T, Jensen MR, Moen B. 2021. Surveillance of *Listeria monocytogenes*: Early Detection, Population Dynamics, and Quasimetagenomic Sequencing during Selective Enrichment. Appl Environ Microbiol 87:e0177421.

186. Ottesen A, Ramachandran P, Reed E, White JR, Hasan N, Subramanian P, Ryan G, Jarvis K, Grim C, Daquiqan N, Hanes D, Allard M, Colwell R, Brown E, Chen Y. 2016. Enrichment dynamics of *Listeria monocytogenes* and the associated microbiome from naturally contaminated ice cream linked to a listeriosis outbreak. BMC Microbiol 16:275.

187. Zheng J, Reed E, Maounounen-Laasri A, Deng X, Wang SS, Ramachandran P, Ferreira C, Bell R, Brown EW, Hammack TS, Wang H. 2024. Evaluation of universal preenrichment broth and comparison of rapid molecular methods for the detection of *Salmonella* from spent sprout irrigation water (SSIW). Int J Food Microbiol 411:110527.

188. Kumar R, Surendran PK, Thampuran N. 2010. Evaluation of culture media for selective enrichment and isolation of *Salmonella* in seafood. J AOAC Int 93:1468–71.

189. Sherrod PS, Amaguana RM, Andrews WH, June GA, Hammack TS. 1995. Relative effectiveness of selective plating agars for recovery of *Salmonella* species from selected high-moisture foods. J AOAC Int 78:679–90.

190. Vassiliadis P. 1983. The Rappaport—Vassiliadis (RV) enrichment medium for the isolation of salmonellas: An overview. Journal of Applied Bacteriology 54:69–76.

191. Li X, Zeng D, He Z, Ke P, Tian Y, Wang G. 2022. Magnetic chitosan microspheres: An efficient and recyclable adsorbent for the removal of iodide from simulated nuclear wastewater. Carbohydr Polym 276:118729.

192. Zhang W, Li Q, Mao Q, He G. 2019. Cross-linked chitosan microspheres: An efficient and eco-friendly adsorbent for iodide removal from waste water. Carbohydr Polym 209:215–222.

193. Wang G, Qafoku NP, Szecsody JE, Strickland CE, Brown CF, Freedman VL. 2019. Time-Dependent Iodate and Iodide Adsorption to Fe Oxides. ACS Earth Space Chem 3:2415–2420.

194. Couture RA, Seitz MG. 1983. Sorption of anions of iodine by iron oxides and kaolinite. Nuclear and Chemical Waste Management 4:301–306.

195. Rhodes P, Quesnel LB. 1986. Comparison of Muller-Kauffmann tetrathionate broth with Rappaport-Vassiliadis (RV) medium for the isolation of salmonellas from sewage sludge. Journal of Applied Bacteriology 60:161–167.

196. Busse M. 1995. Media for *Salmonella*. Int J Food Microbiol 26:117–31.

197. Han H, Sohn B, Choi J, Jeon S. 2021. Recent advances in magnetic nanoparticle-based microfluidic devices for the pretreatment of pathogenic bacteria. Biomed Eng Lett 11:297–307.

198. Poznanski P, Hameed A, Orczyk W. 2023. Chitosan and Chitosan Nanoparticles: Parameters Enhancing Antifungal Activity. Molecules 28:2996.

199. Boroumand H, Badie F, Mazaheri S, Seyedi ZS, Nahand JS, Nejati M, Baghi HB, Abbasi-Kolli M, Badehnoosh B, Ghandali M, Hamblin MR, Mirzaei H. 2021. Chitosan-Based Nanoparticles Against Viral Infections. Front Cell Infect Microbiol 11.

200. Yilmaz Atay H. 2019. Antibacterial Activity of Chitosan-Based Systems, p. 457–489. *In* Functional Chitosan. Springer Singapore, Singapore.

201. Allan CR, Hadwiger LA. 1979. The fungicidal effect of chitosan on fungi of varying cell wall composition. Exp Mycol 3:285–287.

202. Meng D, Garba B, Ren Y, Yao M, Xia X, Li M, Wang Y. 2020. Antifungal activity of chitosan against *Aspergillus ochraceus* and its possible mechanisms of action. Int J Biol Macromol 158:1063–1070.

203. Cheraghipour K, Masoori L, Ezzatkhah F, Salimikia I, Amiri S, Makenali AS, Taherpour F, Mahmoudvand H. 2020. Effect of chitosan on *Toxoplasma gondii* infection: A systematic review. Parasite Epidemiol Control 11:e00189.

204. Williams TR, Marco ML. 2014. Phyllosphere Microbiota Composition and Microbial Community Transplantation on Lettuce Plants Grown Indoors. mBio 5.

205. Erlacher A, Cardinale M, Grosch R, Grube M, Berg G. 2014. The impact of the pathogen *Rhizoctonia solani* and its beneficial counterpart *Bacillus amyloliquefaciens* on the indigenous lettuce microbiome. Front Microbiol 5.

206. Gu G, Kroft B, Lichtenwald M, Luo Y, Millner P, Patel J, Nou X. 2022. Dynamics of *Listeria monocytogenes* and the microbiome on fresh-cut cantaloupe and romaine lettuce during storage at refrigerated and abusive temperatures. Int J Food Microbiol 364:109531.

207. Shapiro K, Largier J, Mazet JAK, Bernt W, Ell JR, Melli AC, Conrad PA. 2009. Surface properties of *Toxoplasma gondii* oocysts and surrogate microspheres. Appl Environ Microbiol 75:1185–91.

208. González-Robles A, Argüello C, Chávez B, Cedillo-Rivera R, Ortega-Pierres G, Martínez-Palomo A. 1989. Giardia lamblia: surface charge of human isolates in culture. Trans R Soc Trop Med Hyg 83:642–3.

209. Rastogi G, Sbodio A, Tech JJ, Suslow T V, Coaker GL, Leveau JHJ. 2012. Leaf microbiota in an agroecosystem: spatiotemporal variation in bacterial community composition on field-grown lettuce. ISME J 6:1812–1822.

210. Williams TR, Moyne A-L, Harris LJ, Marco ML. 2013. Season, Irrigation, Leaf Age, and *Escherichia coli* Inoculation Influence the Bacterial Diversity in the Lettuce Phyllosphere. PLoS One 8:e68642.

211. Leonard SR, Simko I, Mammel MK, Richter TKS, Brandl MT. 2021. Seasonality, shelf life and storage atmosphere are main drivers of the microbiome and *E. coli* O157:H7 colonization of post-harvest lettuce cultivated in a major production area in California. Environ Microbiome 16:25.

212. Olimi E, Kusstatscher P, Wicaksono WA, Abdelfattah A, Cernava T, Berg G. 2022. Insights into the microbiome assembly during different growth stages and storage of strawberry plants. Environ Microbiome 17:21.

213. Wood DE, Lu J, Langmead B. 2019. Improved metagenomic analysis with Kraken 2. Genome Biol 20:257.

APPENDIX

Supplementary Tables:

DSD: PBS - SSN									
Run Order	Block	Bacterial Concentration (log_{10} CFU/sample)	PBS Volume (mL)	PBS pH	Sample Preparation Time (min)	MNP Final Concentration (mg/mL)	MNP Incubation Time (min)	Magnet Separation Time (min)	Capture Efficiency
1	1	2	25	7.4	5	0.025	20	20	0.0769
2		2	25	7.4	5	0.25	10.5	5	0.3397
3		6	225	7.4	1	0.025	10.5	20	0.6731
4		4	125	7.4	3	0.1375	10.5	12.5	0.5695
5		2	225	7.4	3	0.025	1	20	0.0000
6		6	25	7.4	3	0.25	20	5	0.8113
7		4	25	7.4	1	0.025	1	5	0.3476
8		6	225	7.4	1	0.25	1	5	0.6735
9		4	225	7.4	5	0.25	20	20	0.6476
10	2	6	225	7.4	5	0.025	20	5	0.5731
11		6	125	7.4	5	0.25	1	20	0.7430
12		6	25	7.4	5	0.025	1	12.5	0.5409
13		2	25	7.4	1	0.25	1	20	0.4895
14		2	225	7.4	1	0.25	20	12.5	0.4296
15		6	25	7.4	1	0.1375	20	20	0.7596
16		4	125	7.4	3	0.1375	10.5	12.5	0.6604
17		2	125	7.4	1	0.025	20	5	0.2097
18		2	225	7.4	5	0.1375	1	5	0.0000

Table S1.1: Design matrix and input for definitive screening design (DSD) for *Salmonella* ser. Newport (SSN) in PBS.

DSD: Strawberry - SSN									
Run Order	Block	Bacterial Concentration (log_{10} CFU/sample)	PBS Volume (mL)	PBS pH	Sample Preparation Time (min)	MNP Final Concentration (mg/mL)	MNP Incubation Time (min)	Magnet Separation Time (min)	Capture Efficiency
1	1	4	225	8	5	0.25	10	20	0.8069
2		4	25	3.5	1	0.025	1	5	0.5111
3		2	225	3.5	1	0.1375	10	20	0.4700
4		6	225	8	1	0.025	10	5	0.6798
5		6	225	3.5	5	0.025	10	12.5	0.7032
6		4	125	5.75	3	0.1375	5.5	12.5	0.6711
7		2	25	3.5	5	0.25	1	20	0.2437
8		2	25	8	1	0.25	1	12.5	0.4215
9		6	25	8	5	0.1375	1	5	0.7838
10		6	25	5.75	1	0.25	10	5	0.7145
11		2	225	5.75	5	0.025	1	20	0.2437
12	2	2	225	3.5	1	0.25	5.5	5	0.4515
13		6	25	8	5	0.025	5.5	20	0.7724
14		4	125	5.75	3	0.1375	5.5	12.5	0.6553
15		6	125	3.5	1	0.025	1	20	0.8030
16		2	25	3.5	5	0.025	10	5	0.5735
17		2	25	8	1	0.025	10	20	0.2647
18		2	225	8	3	0.025	1	5	0.1220
19		6	225	3.5	5	0.25	1	5	0.7235
20		6	25	3.5	3	0.25	10	20	0.8142
21		6	225	8	1	0.25	1	20	0.7279
22		2	125	8	5	0.25	10	5	0.3547

Table S1.2: Design matrix and input for definitive screening design (DSD) for *Salmonella* ser. Newport (SSN) in strawberries.

DSD: Romaine Lettuce - SSN									
Run Order	Block	Bacterial Concentration (log_{10} CFU/sample)	PBS Volume (mL)	PBS pH	Sample Preparation Time (min)	MNP Final Concentration (mg/mL)	MNP Incubation Time (min)	Magnet Separation Time (min)	Capture Efficiency
1	1	6	25	5.75	1	0.25	10	5	0.5680
2		4	225	8	5	0.25	10	20	0.5145
3		4	125	5.75	3	0.1375	5.5	12.5	0.4274
4		6	225	3.5	5	0.025	10	12.5	0.6133
5		2	25	3.5	5	0.25	1	20	0.0000
6		2	25	8	1	0.25	1	12.5	0.1462
7		2	225	3.5	1	0.1375	10	20	0.0000
8		4	25	3.5	1	0.025	1	5	0.3169
9		6	225	8	1	0.025	10	5	0.5473
10		6	25	8	5	0.1375	1	5	0.6947
11		2	225	5.75	5	0.025	1	20	0.0855
12	2	2	225	8	3	0.025	1	5	0.3783
13		6	25	8	5	0.025	5.5	20	0.6207
14		6	125	3.5	1	0.025	1	20	0.6353
15		6	25	3.5	3	0.25	10	20	0.6407
16		6	225	3.5	5	0.25	1	5	0.7085
17		2	25	8	1	0.025	10	20	0.0856
18		4	125	5.75	3	0.1375	5.5	12.5	0.3931
19		2	225	3.5	1	0.25	5.5	5	0.0000
20		2	25	3.5	5	0.025	10	5	0.0856
21		2	125	8	5	0.25	10	5	0.0000
22		6	225	8	1	0.25	1	20	0.6800

Table S1.3: Design matrix and input for definitive screening design (DSD) for *Salmonella* ser. Newport (SSN) in romaine lettuce.

CCD: PBS - SSN				
Run Order	Block	MNP Final Concentration (mg/mL)	MNP Incubation Time (min)	Capture Efficiency
1	1	0.1375	10.5	0.2000
2		0.1375	10.5	0.4000
3		0.1375	1	1.0000
4		0.025	20	0.0000
5		0.25	1	0.8333
6		0.1375	10.5	0.6000
7		0.25	20	0.6250
8		0.1375	10.5	0.6250
9		0.025	1	0.5000
10		0.1375	20	0.5000
11		0.25	10.5	0.6667
12		0.025	10.5	0.1250
13	2	0.1375	10.5	0.3333
14		0.1375	10.5	*
15		0.1375	1	1.0000
16		0.025	20	0.0000
17		0.25	1	0.0000
18		0.1375	10.5	0.0000
19		0.25	20	0.7500
20		0.1375	10.5	0.5000
21		0.025	1	*
22		0.1375	20	0.8000
23		0.25	10.5	0.3333
24		0.025	10.5	0.0000
25		0.1375	10.5	0.6667
26		0.1375	10.5	0.2500
27		0.1375	1	0.2000
28		0.025	20	0.0000
29		0.25	1	1.0000
30		0.1375	10.5	0.5000

Table S1.4: Design matrix and input for central composite design (CCD) for *Salmonella* ser. Newport (SSN) in PBS. *Denotes no CFUs in the MNP extract or supernatant.

Table S1.4 (cont'd)

Run Order	Block	MNP Final Concentration (mg/mL)	MNP Incubation Time (min)	Capture Efficiency
31		0.25	20	1.0000
32		0.1375	10.5	0.5000
33		0.025	1	1.0000
34		0.1375	20	1.0000
35		0.25	10.5	1.0000
36		0.025	10.5	0.2500

CCD: PBS - *Lm*				
Run Order	Block	MNP Final Concentration (mg/mL)	MNP Incubation Time (min)	Capture Efficiency
1	1	0.1375	10.5	1.000
2		0.025	1	0.200
3		0.25	1	1.000
4		0.25	20	0.846
5		0.1375	10.5	1.000
6		0.1375	1	0.600
7		0.025	10.5	0.875
8		0.1375	10.5	0.933
9		0.1375	10.5	0.714
10		0.1375	10.5	0.875
11		0.25	20	1.000
12		0.025	1	0.000
13		0.1375	20	0.900
14		0.025	20	0.500
15		0.1375	20	1.000
16		0.025	10.5	0.500
17		0.25	10.5	0.571
18		0.025	20	1.000
19		0.1375	1	1.000
20		0.1375	10.5	1.000
21		0.25	10.5	1.000
22		0.25	1	0.667

Table S1.5: Design matrix and input for central composite design (CCD) for *L. monocytogenes* (*Lm*) in PBS.

CCD: Strawberry - SSN					
Run Order	Block	PBS pH	MNP Final Concentration (mg/mL)	MNP Incubation Time (min)	Presence (1)/ Absence (0)
1	1	5.75	0.025	10.5	0
2		5.75	0.25	10.5	1
3		8	0.1375	10.5	1
4		3.5	0.25	20	1
5		3.5	0.1375	10.5	0
6		8	0.025	1	1
7		5.75	0.1375	10.5	1
8		3.5	0.025	1	1
9		3.5	0.25	1	1
10		3.5	0.025	20	1
11		8	0.25	20	1
12		8	0.25	1	0
13		5.75	0.1375	1	0
14		5.75	0.1375	20	1
15		8	0.025	20	0
16		5.75	0.1375	10.5	1
17	2	N/A	0.1375	1	0
18			0.1375	10.5	1
19			0.1375	10.5	0
20			0.025	1	0
21			0.025	10.5	1
22			0.25	10.5	1
23			0.1375	20	1
24			0.1375	10.5	1
25			0.25	1	1
26			0.025	20	0
27			0.1375	10.5	1
28			0.25	20	1

Table S1.6: Design matrix and input for central composite design (CCD) for *Salmonella* ser. Newport (SSN) in strawberries.

CCD: Romaine Lettuce - SSN				
Run Order	Block	MNP Final Concentration (mg/mL)	MNP Incubation Time (min)	Presence (1)/ Absence (0)
1	1	0.1375	20	0
2		0.1375	1	1
3		0.025	10.5	0
4		0.25	10.5	0
5		0.25	20	0
6		0.025	20	0
7		0.1375	10.5	0
8		0.1375	10.5	1
9		0.025	1	1
10		0.25	1	0
11	2	0.1375	20	1
12		0.1375	1	0
13		0.025	10.5	0
14		0.25	10.5	0
15		0.25	20	0
16		0.025	20	0
17		0.1375	10.5	0
18		0.1375	10.5	0
19		0.025	1	0
20		0.25	1	0

Table S1.7: Design matrix and input for central composite design (CCD) for *Salmonella* ser. Newport (SSN) in romaine lettuce.

CCD: Romaine Lettuce - *Lm*				
Run Order	Block	MNP Final Concentration (mg/mL)	MNP Incubation Time (min)	Presence (1)/ Absence (0)
1	1	0.1375	20	0
2		0.025	10.5	1
3		0.1375	10.5	1
4		0.025	1	0
5		0.025	20	1
6		0.25	10.5	1
7		0.25	1	1
8		0.25	20	0
9		0.1375	10.5	1
10		0.1375	1	0
11	2	0.1375	20	0
12		0.025	10.5	0
13		0.1375	10.5	1
14		0.025	1	0
15		0.025	20	1
16		0.25	10.5	1
17		0.25	1	1
18		0.25	20	1
19		0.1375	10.5	1
20		0.1375	1	1

Table S1.8: Design matrix and input for central composite design (CCD) for *L. monocytogenes* (*Lm*) in romaine lettuce.

CCD: Cotto Salami - *Lm*				
Run Order	Block	MNP Final Concentration (mg/mL)	MNP Incubation Time (min)	Presence (1)/ Absence (0)
1	1	0.025	20	1
2		0.25	1	1
3		0.1375	20	1
4		0.025	1	0
5		0.1375	10.5	1
6		0.25	20	1
7		0.1375	10.5	0
8		0.1375	1	1
9		0.025	10.5	0
10		0.25	10.5	0
11	2	0.025	20	0
12		0.25	1	1
13		0.1375	20	1
14		0.025	1	0
15		0.1375	10.5	1
16		0.25	20	1
17		0.1375	10.5	1
18		0.1375	1	1
19		0.025	10.5	0
20		0.25	10.5	1

Table S1.9: Design matrix and input for central composite design (CCD) for *L. monocytogenes* (*Lm*) in cotto salami.

Supplementary Figures:

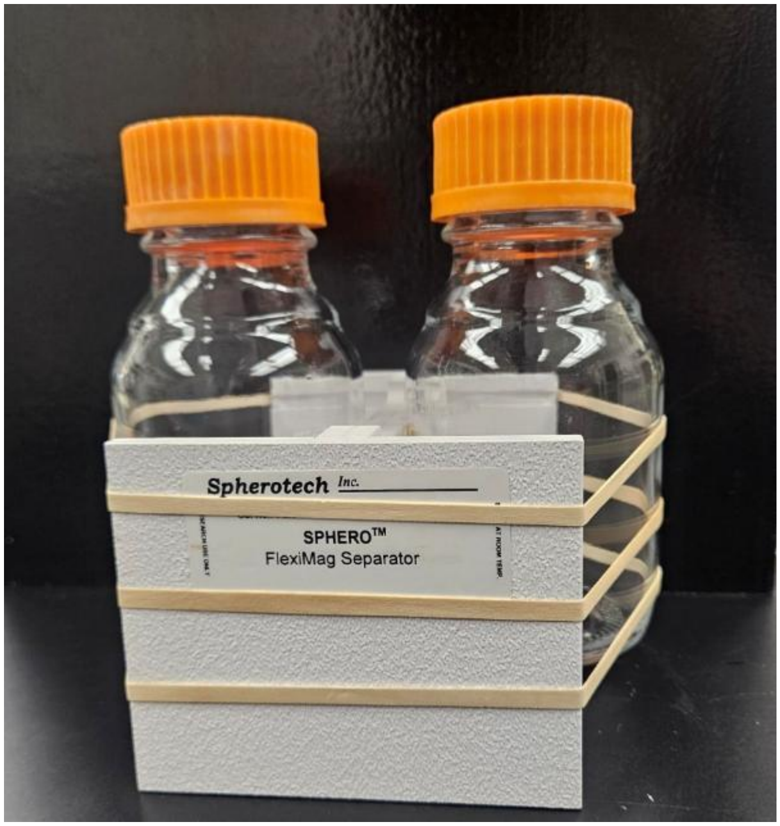

Figure S1.1: Representation of rubber bands used to secure 250 mL reagent bottles to the Spherotech FlexiMag Separator Magnet.

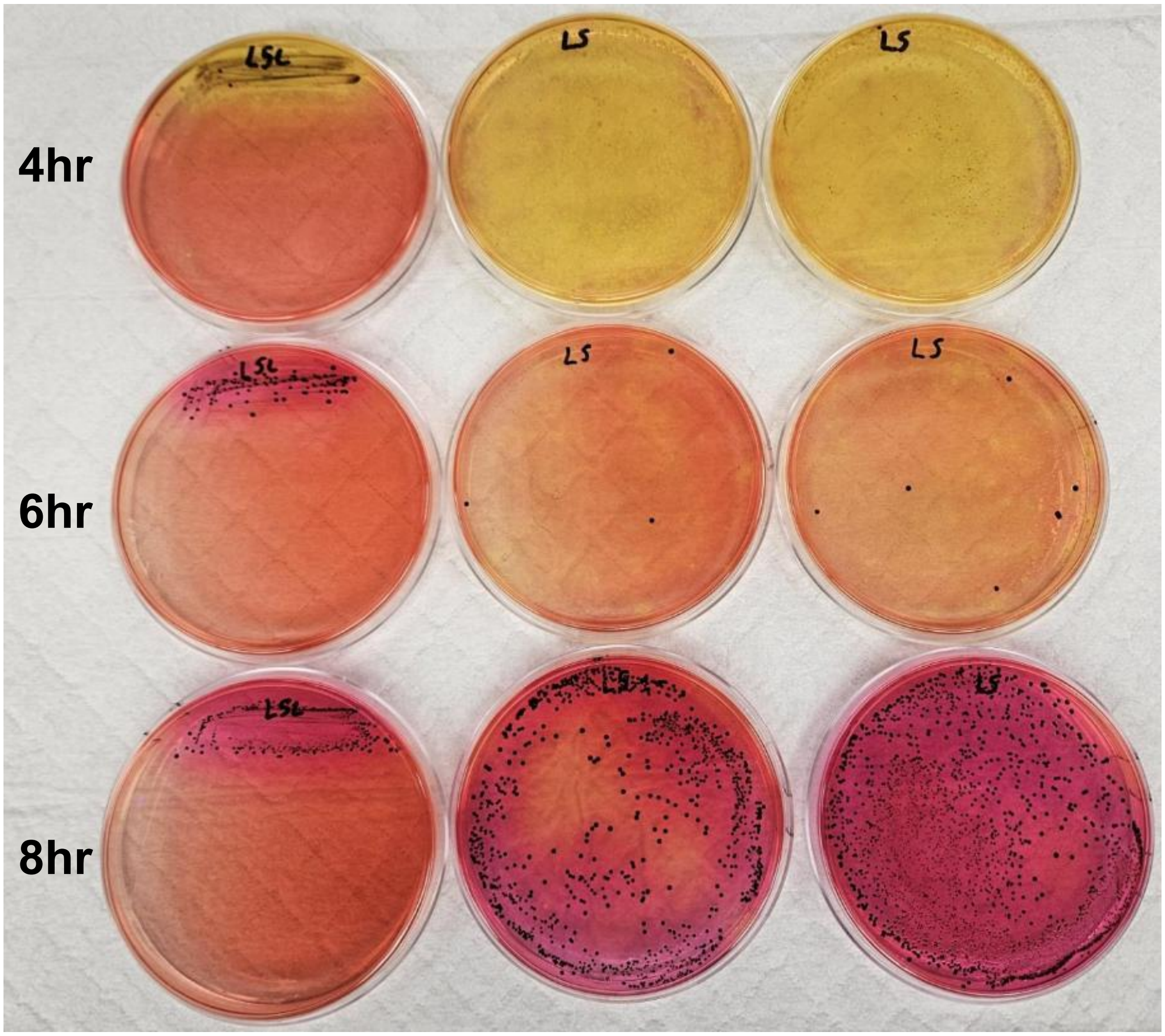

Figure S2.1: FDA Bacteriological Analytical Manual (BAM) protocol modification testing enrichment dynamics of *Salmonella* ser. Newport in romaine lettuce on xylose lysine deoxycholate (XLD) agar. Column 1 are streak plates whereas columns 2 and 3 are spread plates. Row 1 is 4 hours total incubation time, row 2 is 6 hours, and row 3 is 8 hours.

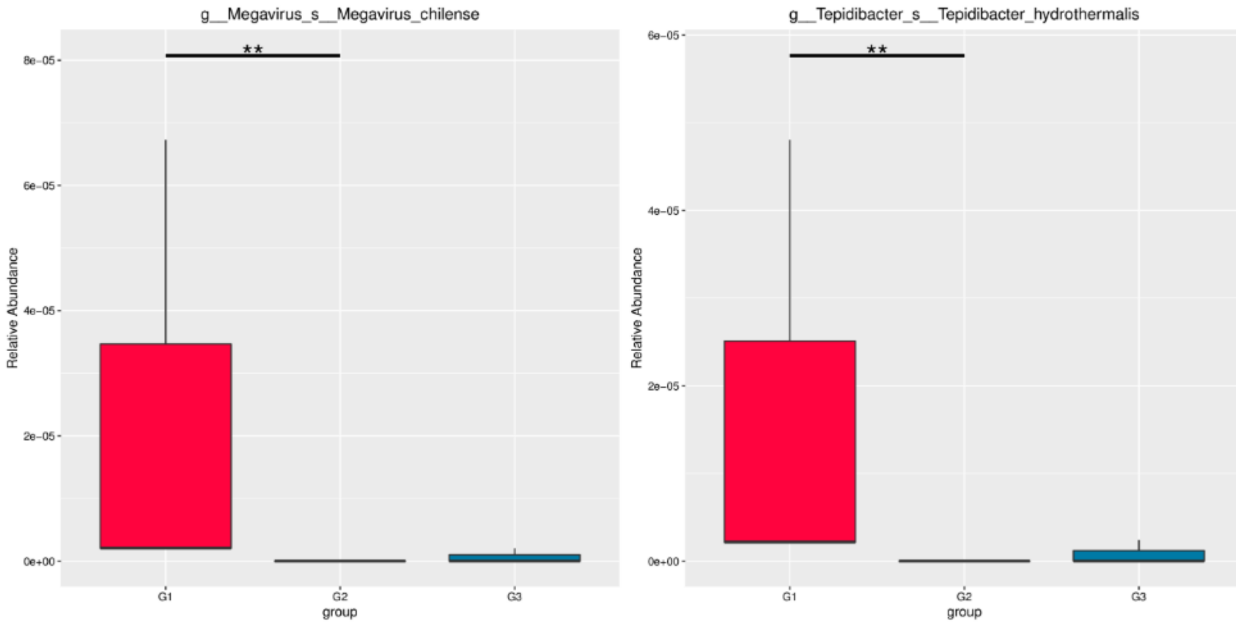

Figure S3.1: Relative abundance comparison of *Megavirus chilense* (A) and *Tepidibacter hydrothermalis* (B) between groups G1 (not spiked), G2 (spiked with *L. monocytogenes*) and G3 (spiked with *Salmonella* ser. Newport). **p < 0.0001